



UNIVERSITA' DEGLI STUDI DI VERONA

*DEPARTMENT OF*

*Diagnostic and Public Health, Microbiology Section*

*GRADUATE SCHOOL OF*

*Life and Health sciences*

*DOCTORAL PROGRAM IN*

*Applied Life and Health Sciences*

*Microbiology and Infectious Diseases*

XXX Cycle      Year 2014

**ANTIMICROBIAL AND ANTIBIOFILM ACTIVITIES OF BIOGENIC  
SELENIUM NANOPARTICLES: A CONTRIBUTION TO THE  
DEVELOPMENT OF AN ALTERNATIVE STRATEGY AGAINST THE  
ANTIBIOTIC RESISTANCE CONCERN**




S.S.D. MED/07

Coordinator: Prof. Giovanni Malerba

Tutor: Prof.ssa Maria del Mar Lleo

Doctoral Student: Dott.ssa Eleonora Cremonini

Quest'opera è stata rilasciata con licenza Creative Commons Attribuzione – non commerciale  
Non opere derivate 3.0 Italia . Per leggere una copia della licenza visita il sito web:  
<http://creativecommons.org/licenses/by-nc-nd/3.0/it/>

-  **Attribuzione** Devi riconoscere una menzione di paternità adeguata, fornire un link alla licenza e indicare se sono state effettuate delle modifiche. Puoi fare ciò in qualsiasi maniera ragionevole possibile, ma non con modalità tali da suggerire che il licenziante avalli te o il tuo utilizzo del materiale.
-  **NonCommerciale** Non puoi usare il materiale per scopi commerciali.
-  **Non opere derivate** —Se remixi, trasformi il materiale o ti basi su di esso, non puoi distribuire il materiale così modificato.

Antimicrobial and antibiofilm activities of biogenic  
selenium nanoparticles: a contribution to the development of an alternative strategy against the antibiotic resistance concern  
Eleonora Cremonini  
Tesi di Dottorato  
Verona, 15 Gennaio 2018

## SOMMARIO

---

Il biofilm batterico è una comunità strutturata di cellule racchiuse in una matrice polimerica autoprodotta, composta principalmente da esopolisaccaridi, acidi nucleici, lipopolisaccaridi e proteine (Costerton, 1999) capace di proteggere i batteri dai meccanismi di difesa dell'ospite e dagli antibiotici favorendo la persistenza dell'infezione. Inoltre la vicinanza tra le cellule batteriche all'interno della comunità favorisce lo scambio "orizzontale" di materiale genetico compresi i geni dell'antibiotico resistenza (Flemming, 2007). In campo medico le infezioni biofilm-correlate possono portare al diffondersi di infezioni persistenti e difficili da eradicare (Bjarnsholt, 2013).

Recenti sviluppi nel campo delle nanotecnologie hanno suggerito come nanoparticelle (NPs) di origine biogenica, potrebbero essere d'aiuto nel trattamento di infezioni biofilm-correlate (Kostakioti, 2013).

Obiettivo di questa tesi di dottorato è stato analizzare l'azione antibatterica e antibiofilm di nanoparticelle di selenio (SeNPs) bio-sintetizzate da due ceppi batterici di origine ambientale (*Bacillus Mycooides* SeITE01 e *Stenotrophomonas maltophilia* SeITE02). Le SeNPs sono state caratterizzate per le loro proprietà chimico-fisiche, la loro attività antibatterica e antibiofilm e confrontate con NPs di selenio prodotte chimicamente. L'attività antibatterica e antibiofilm dei tre tipi di SeNPs è stata valutata nei confronti di una serie di isolati clinici e ceppi di riferimento di *Pseudomonas aeruginosa*. Le NPs prodotte da *S. maltophilia* (Sm-SeNPs(-)) si sono dimostrate le più attive con valori di MIC, molto bassi per alcuni dei ceppi testati, e una rilevante attività inibente la formazione e disgregante il biofilm.

SeNPs con caratteristiche simili ma diversa origine hanno mostrato una diversa attività antibatterica. Questo, unitamente al diverso meccanismo di bio-sintesi, induce ad ipotizzare che la superficie delle NPs sia ricoperta da diverse biomolecole (*coating*), importanti per la loro attività e interazione con le cellule batteriche.

Abbiamo poi indagato il ruolo del *coating* nell'azione delle NPs sottoponendo le Sm-SeNPs(-) a diversi trattamenti denaturanti (10%SDS, 10%SDS+10'bollitura,

10%SDS+30'bollitura) e confrontando l'attività antibatterica ed antibiofilm delle NPs ottenute con SeNPs non trattate. L'attività antibatterica diminuiva progressivamente alla perdita del *coating* superficiale, mostrando un progressivo aumento del valore di MIC in corrispondenza del'impoverimento, nella percentuale di proteine e carboidrati. L'attività antibiofilm (effetto sulla biomassa, sulla vitalità cellulare e microscopia a fluorescenza) ha confermato l'azione antibatterica mostrata in precedenza. In accordo con i dati presenti in letteratura (Tran, 2009) abbiamo poi evidenziato come il trattamento con Sm-SeNPs(-) induca produzione di ROS.

Successivamente si è valutata la possibile attività antibatterica sinergica tra SeNPs e alcuni antibiotici. La combinazione di NPs e antibatterici non ha portato ad un incremento rilevante dell'attività antibiofilm, avendo le SeNPs di per sé una sostanziale azione. Solo in un caso (un isolato clinico multi-resistente), l'abbinamento di Sm-SeNPs(-) e antibiotici ha mostrato sinergismo.

Infine, l'attività antibiofilm delle Sm-SeNPs(-) è stata saggiata in una serie di modelli complessi *in vitro* (ferita cronica e *flow cells*) e *in vivo* (*Caenorhabditis elegans* e modello murino). Il modello di ferita è un derma artificiale formato da diversi strati di collagene, che ricrea le condizioni di ferite croniche e da ustione. In questo caso le NPs non hanno mostrato una buona attività contro i biofilm di *P. aeruginosa* e *S. aureus* testati.

Nelle *flow cells* vengono ricreate le condizioni di un flusso costante di nutrienti che si possono ritrovare in situazioni reali come cateteri vescicali o venosi. L'attività delle NPs è stata valutata monitorando la riduzione delle cellule vitali presenti nel biofilm durante il trattamento con un flusso costante di 128µg/ml di Sm-SeNPs(-), e al termine di quest'ultimo.

Nel nematode *C. elegans* le SeNPs hanno mostrato una tossicità dipendente dalla concentrazione, mentre nel più complesso modello di topo (*wild type* e affetto da Fibrosi Cistica), l'instillazione tracheale di NPs non ha dato tossicità sistemica. In ultimo, sono state utilizzate linee cellulari umane (cellule dendritiche e fibroblasti).

Complessivamente i dati raccolti al termine di questa tesi di dottorato evidenziano come nanoparticelle di selenio bio-sintetizzate da batteri possano costituire *in*

*vitro* una valida alternativa all'utilizzo della convenzionale terapia antibatterica ed in alcuni casi siano addirittura più efficaci. Inoltre non si sono dimostrate tossiche nel modello murino né in linee cellulari umane.

## ABSTRACT

---

Bacterial biofilms are microbial communities embedded in a highly hydrated exopolymer (EPS) matrix and can exist on different biotic and abiotic surfaces. The presence of these protective EPS matrix allows biofilms to survive in harsh environmental conditions and to resist to antibiotic action, representing a challenge for the common antimicrobial therapy. Recently, a wide range of nanoparticles (i.e. silver, gold, iron oxide) have been intensively studied as antimicrobial agents including their use against multidrug-resistant (MDR) bacteria.

We evaluated the physicochemical characteristics and biological activity of biogenic selenium nanoparticle (SeNPs) produced by exploiting the selenite reduction capability of two bacterial environmental isolate (*Bacillus mycooides* SeITE01 (Bm) and *Stenotrophomonas maltophilia* SeITE02 (Sm)) and compared to the one of chemically synthesized SeNPs (Ch-SeNPs).

The ability of Bm-SeNPs(+) and Sm-SeNPs(-) to inhibit bacterial growth was initially tested against different clinical isolates from *Pseudomonas aeruginosa* species. Sm-SeNPs(-) showed the greatest antibacterial activity, with low MIC values against some of the strains tested, and a relevant antibiofilm activity, both in inhibiting the formation and disaggregating the mature EPS matrix.

NPs with similar dimension and characteristics but originating from taxonomically different bacterial species, showed a different antimicrobial and antibiofilm activity. Due to the SeNPs mechanism of secretion, the NPs are characterized by having an organic layer coating their surface that seems to be involved in the nanoparticle mechanism of action.

We demonstrated that the progressive coating denaturation cause an increasing loss of NPs antimicrobial activity. Sm-SeNPs(-) were subjected to different denaturing treatments (10%SDS, 10%SDS+10'boiling, 10%SDS+30'boiling) able to disaggregate the biogenic coating layer on their surface, and the antimicrobial and antibiofilm activity of the obtained NPs was tested against a large panel of Gram-negative and Gram-positive species. The results showed an increasing MIC value corresponding to a progressively strongest denaturing treatment. The

antibiofilm activity of the SeNPs was greater when the complete coating was present on their surface. Moreover, despite the poor knowledge about the mechanism of action of these nanomaterials, according to literature, we demonstrated that during the treatment with SeNPs, the planktonic form of the strains tested produced a large amount of ROS.

The possible synergic activity of Sm-SeNPs in association with antibiotics was evaluated focusing on MDR clinical isolates of *P. aeruginosa* and *S. aureus*. In general, the SeNPs showed a greater activity than the antibiotics alone, only for the MDR *P. aeruginosa* INT strain the combination of biogenic SeNPs and antibacterial drugs evidenced a synergistic activity.

Finally, the antibiofilm activity of Sm-SeNPs(-) was tested on different complex *in vitro* and *in vivo* models, confirming the potent antibacterial activity of the NPs tested and their inability to cause damage in human cell cultures and in the mouse model. Despite the poor knowledge about the mechanism of action of these nanomaterials, the results obtained provide interesting inputs to consider SeNPs as a novel and alternative antimicrobial strategy to treat challenging microbial infections such as biofilm-associated infections and those caused by MDR bacteria.

## TABLE OF CONTENTS

---

<b>1. ABBREVIATIONS.....</b>	<b>pag.18</b>
<b>2. RATIONAL AND OBJECTIVE OF THE STUDY.....</b>	<b>pag.19</b>
<b>3. INTRODUCTION.....</b>	<b>pag.20</b>
<b>3.1 Bacterial biofilms.....</b>	<b>pag.20</b>
The process of biofilm formation and its complex architecture.....	pag.21
The importance of biofilm related infections in the clinical practice..	pag.26
<b>3.2 Innovative anti-biofilm treatments and alternative approaches.....</b>	<b>pag.28</b>
Strategies for combating persisters.....	pag.28
Phage therapy.....	pag.29
Quorum Sensing inhibitors.....	pag.30
Nanotechnology.....	pag.32
<b>3.3 Selenium nanoparticles.....</b>	<b>pag.35</b>
Mechanisms of microbial SeNPs synthesis.....	pag.36
Antimicrobial and antibiofilm activities of Selenium nanoparticles...	pag.39
Coating medical devices with SeNPs to prevent bacterial colonisation and biofilm formation.....	pag.40
Cytotoxicity and other possible applications for SeNPs.....	pag.40
<b>4. MATERIALS AND METHODS.....</b>	<b>pag.42</b>
<b>4.1 Preparation and characterization of Selenium nanoparticles.....</b>	<b>pag.42</b>
Preparation of Biogenic Selenium Nanoparticles (SeNPs).....	pag.42
Cell free extracts and CFX-SeNPs preparation.....	pag.42
Scanning electron microscopy (SEM).....	pag.43
Dynamic Light Scattering (DLS) Analysis.....	pag.43
Quantification of proteins and carbohydrates still remaining on the NPs surface after different denaturing treatment.....	pag.44
<b>4.2 Antimicrobial and antibiofilm activity of Selenium nanoparticles.....</b>	<b>pag.44</b>
Growth conditions and Microbial strains.....	pag.44



Determination of the minimum inhibitory concentration (MIC) of biogenic NPs.....	pag.47
Biofilm formation assay.....	pag.47
Biofilm inhibition and disintegration assay for biogenic SeNPs.....	pag.48
Biofilm formation and treatment with different types of SeNPs.....	pag.48
Quantification of the biofilm biomass (Crystal Violet assay, CV assay).....	pag.48
Quantification of surviving cells.....	pag.49
Reactive Oxygen Species production assay (ROS assays).....	pag.49
<b>4.3 Evaluation of the synergic effect of biogenic SeNPs and antibiotics.....</b>	<b>pag.50</b>
Microbial strains and growth conditions.....	pag.50
Drugs and antibiotics used.....	pag.50
Determination of minimum inhibitory concentration and fractional inhibitory concentration (FIC).....	pag.50
Biofilm formation and treatment with combination of SeNPs and antibiotic.....	pag.51
Quantification of cells.....	pag.51
Quantification of the biofilm biomass (Crystal Violet assay, CV assay).....	pag.52
<b>4.4 Chronic <i>in vitro</i> wound model.....</b>	<b>pag.52</b>
Day 1 (first layer).....	pag.52
Day 2 (second layer).....	pag.52
Set up of the infection protocol.....	pag.53
Determination of the minimum inhibitory concentration (MIC) of biogenic NPs.....	pag.54
<b>4.5 Flow cells growth model.....</b>	<b>pag.54</b>
Quantification of cells in biofilms.....	pag.56
<b>4.6 <i>Caenorhabditis elegans</i>: a simple “in vivo” model.....</b>	<b>pag.56</b>
Preparation of Nematode Growth Medium (NGM) plates.....	pag.56
Preparation of bacterial food source ( <i>E. coli</i> OP50).....	pag.56

Transferring the worms (“chunking” technique).....	pag.57
Obtaining a synchronised <i>C. elegans</i> population (“bleaching”).....	pag.57
<i>C. elegans</i> infection assay.....	pag.57
<b>4.7 Fluorescence microscopy.....</b>	<b>pag.58</b>
<b>4.8. SeNPs toxicity in an <i>in vivo</i> mouse model.....</b>	<b>pag.58</b>
Intratracheal challenge of Sm-SeNPs(-).....	pag.58
<b>4.9 Evaluation of SeNPs cytotoxic effect in human cell cultures.....</b>	<b>pag.59</b>
Preparation and culture of dendritic cells and fibroblasts.....	pag.59
Quantification of cytokine production.....	pag.59
Cell viability evaluation.....	pag.60
<b>4.10 Statistical analysis.....</b>	<b>pag.60</b>
<b>5. RESULTS.....</b>	<b>pag.61</b>
<b>5.1 Biogenic selenium nanoparticles: characterization, antimicrobial and antibiofilm activity.....</b>	<b>pag.61</b>
Determination of Minimum Inhibitory Concentration (MIC) for SeNPs against <i>P. aeruginosa</i> PAO1.....	pag.63
Antimicrobial activity of SeNPs against clinical isolates of <i>P. aeruginosa</i> .....	pag.65
Inhibition of <i>P. aeruginosa</i> strains biofilm formation by SeNPs.....	pag.68
Degradation of <i>P. aeruginosa</i> biofilms by SeNPs.....	pag.68
Antimicrobial activity of SeNPs against clinical isolates of <i>Candida spp</i> .....	pag.71
Inhibition of the formation and degradation of <i>Candida</i> strains biofilm by SeNPs .....	pag.71
<b>5.2 Investigation of the biogenic coating as a possible modulator for the SeNPs antimicrobial and antibiofilm activity.....</b>	<b>pag.73</b>
Characterization of Sm-SeNPs(-) as biogenic products and after different treatments.....	pag.74

Characterization and antimicrobial activity for Sm-SeNPs(48).....	pag.77
Antimicrobial activity of the various kinds of Selenium NPs.....	pag.78
Anti-biofilm effect of native and treated Sm-SeNPs(-).....	pag.81
Fluorescence microscopy.....	pag.85
ROS production.....	pag.87
<b>5.3 Evaluation of the possible synergic effect of biogenic selenium nanoparticles and antibiotics.....</b>	<b>pag.87</b>
Antibiofilm activity of different combination of SeNPs and antibiotics.....	pag.89
<b>5.4 Evaluation of the antibiofilm activity of biogenic selps in complex “in vitro” and “in vivo” models.....</b>	<b>pag.92</b>
Chronic wound model.....	pag.92
Flow cells.....	pag.96
<i>Caenorhabditis elegans</i> .....	pag.99
Mouse model.....	pag.101
<b>5.5 Effects of biogenic selenium nanoparticles on human dendritic cells and fibroblasts.....</b>	<b>pag.102</b>
Evaluation of cell viability.....	pag.102
Quantification of cytokine production.....	pag.104
<b>6. DISCUSSION.....</b>	<b>pag.106</b>
<b>7. CONCLUSION AND PERSONAL CONSIDERATIONS.....</b>	<b>pag.115</b>
<b>8. ACKNOWLEDGMENTS.....</b>	<b>pag.117</b>
<b>9. BIBLIOGRAPHY.....</b>	<b>pag.118</b>
<b>10. SCIENTIFIC CONTRIBUTION FROM THE PhD THESIS.....</b>	<b>pag.127</b>

## 1. ABBREVIATIONS

---

AD, Artificial Dermis

Bm-SeNPs(+), Selenium nanoparticles produced by *Bacillus mycooides* SeITE01

BSA, Bovine Serum Albumin

Ch-NPs, chemical nanoparticles

CF, Cystic Fibrosis

CFU, Colony Forming Unit

CFX, Cell Free Extracts

CLA, Clarithromycin

CLSI, Clinical and Laboratory Standards Institute

CV, Crystal Violet staining

DCs, dendritic cells

DLS, Dynamic Light Scattering

EDAX, Energy Dispersive X-ray Analysis

FICI, Fractional Inhibitory Concentration Index

FTIR, Fourier Transform Infrared spectroscopy

GM-CSF, Granulocyte-Colony Stimulating Factor

HA, Hyaluronic Acid

H<sub>2</sub>DCF-DA, dichlorodihydrofluorescein diacetat

HMW, High-Molecular Weight

IL, interleukin

LEV, Levofloxacin

LPS, lipopolysaccharide

MDR, Multi Drug Resistant

MIC, Minimum Inhibitory concentration

MTP, microtiter plate

NGM, Nematode Growth Medium

NPs, nanoparticles

OD, Optical Density

O/N, overnight

PDI, Polydispersity Index

PS, Physiological Saline

ROS, Reactive Oxygen Species

SeNPs, selenium nanoparticles

Sm-SeNPs(-), Selenium nanoparticles produced by *Stenotrophomonas maltophilia* SeITE02

Sm-SeNPs(48), Selenium nanoparticles produced by *S. maltophilia* SeITE02 after 48 hours of incubation with sodium selenite.

SEM, Scanning Electron Microscopy

SEM, Standard Error Mean

SD, Standard Deviation

SDS, Sodium Dodecyl Sulfate

TRIM, Trimethoprim/Sulfamethoxazole

TSB, Tryptic Soy Broth

TSA, Tryptic Soy Agar

VAN, Vancomycin

WT, Wild Type

## 2. RATIONAL AND OBJECTIVE OF THE STUDY

---

Aim of this study was to evaluate the antimicrobial activity of biogenic produced Selenium nanoparticles in order to find a possible alternative strategy in the fighting against antibiotic resistance. Biofilm-forming pathogens have been shown to associate with a wide range of chronic human diseases and an important characteristic of these chronic biofilm-related infections is the extreme resistance to antibiotics. The emergence of nanotechnology led to new antimicrobial options, suggesting the use of nanomaterials as complementary agents to antibiotics.

This three years PhD project is the result of a multidisciplinary collaboration between different Department of the University of Verona and, some parts of the study, have seen the contribution of the Laboratory of Pharmaceutical Microbiology, led by Prof. *Tom Coenye*, at Ghent University, Belgium. The Selenium nanoparticles used, were produced by the research group of Prof. *Giovanni Vallini*, in the Environmental Microbiology Laboratory, Department of Biotechnology, University of Verona.

That to underline how important the collaborations with other research areas could be. In our case, microorganisms capable of transforming the toxic Selenium oxyanion into non-toxic elemental Selenium could be considered as biocatalysts for the production of nanomaterials (SeNPs), eventually exploitable in different biotechnological applications. Especially in the clinical practice, where the lack of new antimicrobial molecules and the increasing onset of drug-resistant bacterial strains, lead to the necessity of alternative therapeutic strategies. An environmental beneficially process turned out to be a biocompatible product that could be administered to inhibit the growth of pathogens, including those resistant to antibiotics.

### 3. INTRODUCTION

---

#### 3.1 BACTERIAL BIOFILMS

Marshall, in 1976, noted the involvement of “very fine extracellular polymer fibrils” that anchored bacteria to surfaces. However, the term “biofilm” was used for the first time by Costerton in 1981 to describe the way of growth of some bacterial aggregates and only in 1984 was cited the relationship between human infections and bacterial biofilms (Bjarnsholt, 2013). Before that, was Leeuwenhoek that examining the “animalcules” in the plaque on his own teeth in the late seventeenth century, for first introduced the general idea that the sessile bacterial cells differ profoundly from their planktonic floating counterparts (Donlan, 2002). The observation of natural aquatic ecosystems and the direct quantitative recovery techniques, showed then that more than 99.9% of the bacteria are able to grow in biofilms on a wide variety of surfaces (Costerton, 1995). The definition of the term “biofilm” has deeply evolved from the first observations to our days, to accommodate new knowledge. Starting from the already mentioned study of attached bacterial communities in aquatic systems encased in a “glycocalyx” matrix, that Costerton and collaborators hypothesized important for the bacterial adhesion (Costerton, 1978), going to the statement that biofilm consists of single cells and microcolonies, all embedded in a highly hydrated, predominantly anionic, exopolymer matrix (Costerton, 1995). In 1990 Characklis and Marshall defined other aspects of biofilm-way-of-growth, such as the typical spatial and temporal heterogeneity and the presence of inorganic or abiotic substances held together in the biofilm matrix. Moreover, Costerton et al., (1995) emphasized the characteristic of biofilms adhering to surfaces and interfaces, and to each other, including microbial aggregates such as floccules and adherent populations within pore spaces of porous media. Finally, by Costerton and Lappin-Scott, was introduced the concept that adhesion elicit expression of genes controlling the production of bacterial components, necessary for biofilm attachment and formation. Emphasizing in this way, that the process of biofilm formation was regulated by specific genes transcribed during initial cell attachment (Ciofu, 1994). Recently, has been hypothesized that biofilms can grow

without being attached to a surface and that part of the esopolysaccharide matrix could originate from the host (Bjarnsholt, 2013).

Because bacterial biofilms cause very serious problems in industrial water systems, this field have been the first where the researchers tried to develop methods and strategies to control their costly depredations (Costerton, 1987). In the medical field, most, if not all, relevant microorganisms, including Gram-positive and Gram-negative bacteria, both aerobic and anaerobic, mycobacteria and fungi can form and grow in biofilms (Cuellar-Cruz, 2012).

*The process of biofilm formation and its complex architecture*

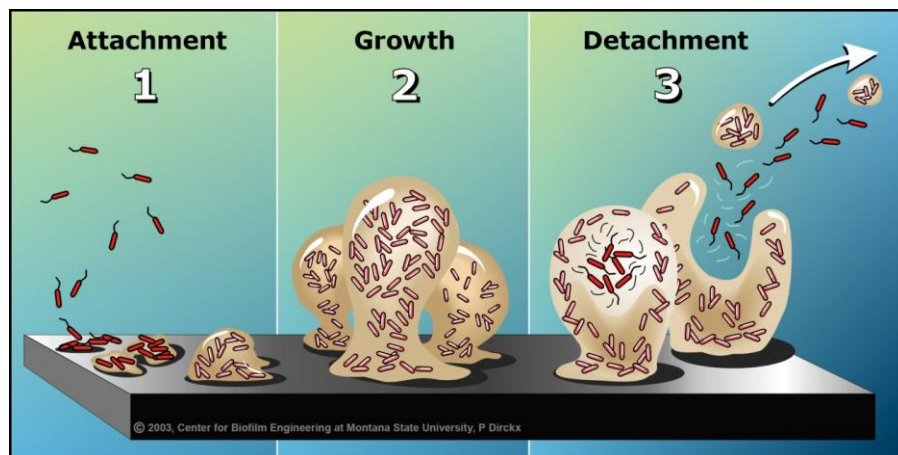


Figure 1. Different stages of biofilm formation (*Center for Biofilm Engineering, Montana State University*).

Usually, we can divide the process of biofilm formation in three different and subsequent steps. A single free-floating cell can adhere to a surface and start to replicate forming a microcolony (phase of attachment) that can grow and develop into an organized community (phase of growth). The possible transition from planktonic mode of growth to the biofilm one, seems to occur in response to environmental changes (Kostakioti, 2013). The initial attachment, mediated by pili, fimbers and adhesions, is a reversible and dynamic process that can follow different phases in which the bacterial cells can detach and rejoin the planktonic

form in response to different stimuli (e.g. repulsive forces, nutrient limitation) (Dunne, 2002). From the sessile mature form of the biofilms, non-sessile planktonic individuals bacteria, can disperse and rapidly multiply or colonize other surfaces (i.e. detachment).

Inside their niche, bacteria can encounter different attractive or repelling forces, depending on nutrient levels, pH, ionic strength, and temperature. Moreover, the properties of different types of medium, combined with the composition of bacterial cells surface, could affect the velocity and direction toward or away from the contact surface (Kostakioti, 2013). Motile bacteria seems to have a competitive advantage for the presence of flagella used to overcome hydrodynamic and repulsive forces. Indeed, for a number of pathogens as *Pseudomonas aeruginosa*, *Vibrio cholerae*, *Listeria monocytogenes*, and *Escherichia coli* as been reported the importance of flagellar motility for their initial attachment (Kostakioti, 2013). Schmit et al. (Schmit, 2011), demonstrated that also chemotaxis plays a relevant role in directing the microbial attachment in response to nutrient changes. In the case of *P. aeruginosa*, mutations in the CheR1 methyltransferase have been show to alter the aminoacid response with the result to impair cells attachment and biofilms maturation.

Bacteria can coordinate their growth within the biofilm structure using the complex communication system known as Quorum Sensing (QS), a cell-density-dependent gene expression mechanism regulated by the excretion of small signalling molecules (Brackman, 2015). When these released molecules reach a certain extracellular threshold concentration, they bind a receptor, activating the QS system. Both Gram-negative and Gram-positive bacteria have a typical QS system. The first consists in a system made by three fundamental components a synthase homolog (LuxI), an acyl-homoserinelactone (AHL) signalling molecules, and a LuxR receptor homolog (Fuqua, 2002). In *P. aeruginosa*, as an example, many genes are regulated and expressed by the QS system including those having a role in pathogenesis and encoding for alkaline protease, pyocyanin, pyoverdine, cyanide, lipase, twitching movement, alginate production, etc, ... (Al-Wrafy, 2017).



On the contrary, Gram-positive bacteria generally use small peptide signalling molecules, that when transported out of the cell, bind to a membrane-associated two-component receptor (Williams, 2007). This binding to the receptor, activates a signal transduction system leading to the transcription of QS-regulated genes. Moreover, there is a third QS system, used in both Gram-positive and Gram-negative bacteria, that include the use of an auto-inducer (AI-2) as signalling molecule and is considered to be responsible for interspecies communication (Xavier, 2003).

The Quorum Sensing system seems also to be responsible for the regulation of biofilm formation in several bacterial species. Different research project highlighted how the biofilm structure and the formation process by mutant forms of different Gram-negative bacterial species is drastically altered (Brackman, 2015). Similar results were observed when the same bacterial species (*Burkholderia multivorans*, *B. cenocepacia*, and *P. aeruginosa*) were treated with some QS inhibitors (QSI) (Brackman, 2009). As regard Gram-positive bacteria, there is the evidence that in *Staphylococcus aureus* biofilm formation, is enhanced by the *agr* QS system, while hamamelitannin, a non-peptide analog of the RNAIII inhibiting peptide, decreases *S. aureus* attachment both in *in vitro* and *in vivo* models (Brackman, 2016; Boles, 2008). For these reasons, QSI can be considered as promising antibiofilm agents that could be used as a novel alternative strategy in fighting biofilm-related infections. However, very little is known about the relationship between the antibiofilm effect of QSI and the susceptibility of biofilms to antibiotics (Brackman, 2015).

The self-produced viscoelastic exopolymeric matrix (EPS) that cover this complex bacterial community, constitute a protection to this mode of growth that allows the survival of the bacterial cells in hostile environments (Costerton, 1999). Typically, the matrix is composed for 90% of the dry mass of biofilms compared to just 10% for the bacteria (Kundukad, 2016). We could define the EPS as a cross-linked three-dimensional architecture made up of different polymers as polysaccharides, nucleic acids, proteins and other macromolecules that facilitate biofilm formation and maintenance. Furthermore inside the matrix

we could find adhesive fibers as pili and flagella, and extracellular DNA (eDNA), with the stabilising function for the three-dimensional biofilm structure (Kostakioti, 2013). Research has shown that eDNA, not only does have a significant role in stabilizing the structure of biofilms, but it also promotes tolerance to antimicrobial peptides and aminoglycosides by chelating cations and restricting diffusion of cationic antimicrobials (Cao, 2015).

Inside the matrix, a complex structure with channels that allow the circulation of nutrients, and different regions that could host different cells with various pattern of gene expression, define the physicochemical properties of biofilm structure as well as contribute to the key properties such as antibiotic resistance and processes including detachment. The heterogeneity within the biofilm structure mediates the penetration of the nutrient flow while protects the dormant persister cells against the activity of antibiotic (Thomsen, 2017). Indeed, EPS biopolymers are highly hydrated and the matrix formed is able to keep the biofilm cells together and retains water. Different studies have also shown that metabolically inactive and non dividing persister cells that we can found within biofilms, can be tolerant to a number of antibiotics despite the fact that they are genetically identical to the rest of the bacterial population (Lewis 2005, 2008). In this contest, is also facilitated the process of horizontal gene transfer, since the cells are maintained in close proximity to each other not fully immobilized, and can exchange genetic information (Flemming, 2007). Thus leading to an increase of the presence and exchange of genes related to antibiotic resistance.

The EPS matrix contributes to the protection of the cells from environmental stresses (Kundukad, 2016). On the other hand, has a key role also in facilitating the cell to cell interactions, including the communication between different bacterial species (Kostakioti, 2013).

In this contest, we have to mention dental plaque, one of the most clear example of mixed species biofilm community. The close relationship between different cells inside the plaque and the ability of these microorganisms to interact with neighbourhood build up a benefit for the community way of growth. As an example, oxygen consumers and oxygen sensitive microorganisms are closely

related: the first ones create conditions that are suitable for the proliferations of the others (Marsh, 2011). Moreover, mutualistic interactions were also detected in the catabolism of complex molecules (Bradshaw, 1994). In response to these complex metabolic processes, the spatial distribution and organisation of the interacting bacteria varies significantly in the various mouth districts emphasizing the role of the habitat properties in the biofilm community composition (Marsh, 2011). The presence of mixed biofilms of *Streptococcus mutans*, *Prevotella species* and *Fusobacterium species*, to list few microorganisms, and other bacteria can cause caries, periodontitis and severe gingivitis (Kuramitsu, 2011).

Another important structural component of the biofilm matrix, typical of Gram-negative bacteria is the lipopolysaccharide (LPS), a complex glycolipid that forms part of the outer membrane of the cell wall. This molecule plays a role in antigenicity, inflammatory response and in mediating interactions with antibiotics. LPS contributes to biofilm function, architecture and integrity by influencing bacterial cell-to-cell adhesion and viscoelastic properties of biofilms (Al-Wrafy, 2017).

The heterogeneity in metabolic and reproductive activity within a biofilm correlates with a non-uniform susceptibility and a nutrient limitation that represent one of the most important cause of starvation induced tolerance (Anutrakunchai, 2015). Nutritional starvation and high cell density, two key characteristics of biofilm physiology, are important factors in mediating the antimicrobial tolerance (Fux, 2005). Recently, Mlynarcik et al. (Mlynarcik, 2017), demonstrated that nutrient deprivation contribute to the increased tolerance of *P. aeruginosa* cells through the production of persisters cells. Moreover, starvation-induced growth arrest cause an inactivity of the antibiotics target (Nguyen, 2011).

The importance of biofilm related infections in the clinical practice

Infection or disease	Common biofilm bacterial species
Dental caries	Acidogenic Gram-positive cocci (e.g., <i>Streptococcus</i> )
Periodontitis	Gram-negative anaerobic oral bacteria
Otitis media	Nontypable strains of <i>Haemophilus influenzae</i>
Musculoskeletal infections	Gram-positive cocci (e.g., staphylococci)
Necrotizing fasciitis	Group A streptococci
Biliary tract infection	Enteric bacteria (e.g., <i>Escherichia coli</i> )
Osteomyelitis	Various bacterial and fungal species—often mixed
Bacterial prostatitis	<i>E. coli</i> and other Gram-negative bacteria
Native valve endocarditis	Viridans group streptococci
Cystic fibrosis pneumonia	<i>P. aeruginosa</i> and <i>Burkholderia cepacia</i>
Meloidosis	<i>Pseudomonas pseudomallei</i>
Nosocomial infections	
ICU pneumonia	Gram-negative rods
Sutures	<i>Staphylococcus epidermidis</i> and <i>S. aureus</i>
Exit sites	<i>S. epidermidis</i> and <i>S. aureus</i>
Arteriovenous shunts	<i>S. epidermidis</i> and <i>S. aureus</i>
Schleral buckles	Gram-positive cocci
Contact lens	<i>P. aeruginosa</i> and Gram-positive cocci
Urinary catheter cystitis	<i>E. coli</i> and other Gram-negative rods
Peritoneal dialysis (CAPD) peritonitis	A variety of bacteria and fungi
IUDs	<i>Actinomyces israelii</i> and many others
Endotracheal tubes	A variety of bacteria and fungi
Hickman catheters	<i>S. epidermidis</i> and <i>C. albicans</i>
Central venous catheters	<i>S. epidermidis</i> and others
Mechanical heart valves	<i>S. aureus</i> and <i>S. epidermidis</i>
Vascular grafts	Gram-positive cocci
Biliary stent blockage	A variety of enteric bacteria and fungi
Orthopedic devices	<i>S. aureus</i> and <i>S. epidermidis</i>
Penile prostheses	<i>S. aureus</i> and <i>S. epidermidis</i>

Figure 2. Partial list of human infections involving biofilms (Costerton, 1999).

Bacterial biofilms can form and grow on different biotic surfaces and, as already mentioned, are the main cause of different recalcitrant infections that could be difficult to treat, and affect various district of the human body. Gram-negative and Gram-positive oral bacterial species are the main cause of dental plaque and periodontitis, an infection of the gum. The biofilm-based infections recurrent in the lungs of patients affected by cystic fibrosis (CF), in otitis media or in chronic wounds are able to get the nutrients required for the microorganisms growth from the blood stream, the interstitial fluid in tissues or lungs (Bjarnsholt, 2013). Especially in CF patients, the presence of a “slime” in the sputum of affected people, allow the formation and the protection of bacterial aggregates able to colonize the lung of these patients. Recurrent in these cases are the infection of opportunistic pathogens as *P. aeruginosa* or *Burkholderia complex* species. The

presence of *P. aeruginosa* mucoid alginate producing strains, confer an enhanced resistance to antibiotics, phages, host immune system, and is detected in the majority of CF patients (O'Brien, 2017). Despite the aggressive treatment of the infections, that bacterial cells can persist in the CF lung causing a continuous degradation of the lung tissues. Consequently, the inflammatory process leads to a decline in lung function, the primary cause of death in CF patients (Bjarnsholt, 2013).

Different studies highlighted how the CF lung airways can be affected by a polymicrobial infections that vary in their composition and diversity throughout a patient's lifetime (Magalhães, 2016; Moran Losada, 2016, Paganin, 2015). Social interactions between the different bacterial species evidence that interactions within and among species can alter virulence properties of *P. aeruginosa* both in the short term in the evolution of this pathogen in the long term disease (O'Brien, 2017).

Different nosocomial infections are caused by a variety of microorganisms that can colonize various medical devices as endotracheal tubes, urinary or venous catheters, orthopaedic devices and joint prosthesis. The types of bacteria responsible for this unpleasant condition are *Streptococcus* species, *S. aureus*, *S. epidermidis*, and regarding the Gram-negative, *Pseudomonas*, *Enterococcus* and *Candida spp.* The origin of the infections may derive from the patient skin (Jamal, 2017). In these kind of infections, the “recalcitrance” of bacterial cells embedded in the biofilm matrix, is the main cause for the failure of antibiotic therapy and the infection recurrence. The recalcitrant biofilm cells, able to survive inside the host also in presence of high concentration of antibiotics, could spread in the human body and colonize other districts (Lebeaux, 2014).

Especially in immune-compromised patients, the manifestation of infections by opportunistic biofilm-forming pathogens can be a main concern, leading to devastating symptoms and, in last instances, death.

The tolerance of bacterial biofilms to antimicrobial compounds is based on a multifactorial physical, physiological and adaptive mechanisms that allows biofilm cells to sustain a long-term exposure to antimicrobial agents without loss

of viability. The physical tolerance is based on the complex tridimensional structure of the EPS matrix, widely described above. On the other hand, the physiological side of the biofilm tolerance is caused by the metabolic state of nutritional starvation. Finally, adaptive mechanisms of induced tolerance can be considered all the transient refractory subpopulations of bacterial cells in biofilm which appear in response to the presence of a specific antimicrobial agent.

We can generally assert that the tolerance of mature biofilms is often 1000 times higher against most antimicrobial agents, including antibiotics and detergents, if compared with their planktonic counterparts (Bjarnsholt, 2013).

### **3.2 INNOVATIVE ANTI-BIOFILM TREATMENTS AND ALTERNATIVE APPROACHES**

Conventionally used antibacterial drugs are active against the planktonic form of bacterial cells responsible for the acute phase of infection but they fail in the completely eradication of biofilms, leading to the persistence of the disease (Bjarnsholt, 2013). For that reasons there is an urgent need to develop novel antibiofilm strategies that can replace or potentiate conventional antimicrobial agents. The use of combined antibiotic therapy is a strategy often employed also in the treatment of multi drug resistance (MDR) infections. Bacterial strains resistant to the antibiotics now in use have become a serious public health problem that increases the need to develop of new bactericidal materials.

#### *Strategies for combating persisters*

Due to their structural composition, biofilms restrict the penetration of antibiotics forming a barrier that protect the cells from the environment. However, the presence of a biofilm-specific resistance mechanism, responsible for recalcitrant infectious diseases, has been hypothesized (Lewis, 2010). After a treatment with an antibiotic, able to kill the majority of the cells within the biofilm, a small fraction of cells, called “persisters”, is able to remain alive. This surviving population is now able to re-establish the biofilm community, causing a chronic

infection. Once awakened, the bacterial cells are again capable to initiate infection (Mina, 2016). Persister dormant bacterial cells are especially significant in those sites where the immune components are limited (e.g. in the nervous system) or are less effective as in immune-compromised patients (Lewis, 2012).

Different microbial biotechnological approaches have been developed to kill sleeping cells resistant to traditional antibiotics (e.g. fluoroquinolones, aminoglycosides and  $\beta$ -lactams). These kind of approaches could exploit the ability of certain compounds to enter the EPS matrix and consequently the bacterial cell, without the need of active transport, to finally kill the persister cells (Wood, 2017).

Another alternative approach could be the one to wake dormant cells and then treat them with traditional antibiotics adding sugars and glycolysis intermediates (e.g. mannitol, glucose, fructose, pyruvate) able to rapidly wake persisters (Allison, 2011). Similarly, *P. aeruginosa* persister cells may also be awakened with cis-2-decenoic acid, which causes a burst in protein synthesis, and then killed by ciprofloxacin (Marques, 2014). In the same way, *S. aureus* persister cells can be efficiently awakened using cis-2-decenoic acid, and, once in a non-dormant state, show a loss of tolerance to ciprofloxacin (Mina, 2016). Apply a treatment in order to avoid the production of reactive oxygen species, may help the antibiotic treatment against *Burkholderia cepacia* complex biofilms (Van Hacker, 2013). Mehemet and collaborators (Orman, 2016), demonstrated that the treatment with nitric oxide (NO) at the onset of stationary phase, significantly reduced *E.coli* persister cells formation through its ability to inhibit respiration.

Recently, some anticancer molecules have been suggested to be effective *in vitro* for eliminating recalcitrant, multidrug tolerant bacteria. Thus, due to the similarities between cancer cells and bacterial infections, 5-fluorouracil (5-FU), gallium (Ga) compounds and mitomycin C revealed some promising properties such as broad activity (all three compounds), dual antibiotic and antivirulence properties (5-FU), efficacy against multidrug resistant strains (Ga), and the ability to kill metabolically dormant persister cells which cause chronic infections (mitomycin C) (Soo, 2017).

### Phage therapy

The increasing need of novel and effective treatments to target the complex biofilm structures has led to a growing interest on bacteriophages (phages) as a strategy for biofilm control and prevention (Pires, 2017). The ability of lytic phages to target specifically bacteria and kill these cells embedded in the biofilm, with no effect on commensal flora, suggest the potentiality in the use of this strategy as well as against antibiotic resistant strains (Al-Wrafiy, 2017). However, there is still a limited knowledge about the phages mechanism of interaction with the population that compose the bacterial biofilm (Pires, 2017). Recently, relevant studies were conducted to evaluate the possible use of phage therapy in the treatment of chronic lung infections (Waters, 2017; Abedon, 2015), showing the possibility to use this innovative strategy as an alternative treatment against *P. aeruginosa* lung infections, in several cases associated with Cystic Fibrosis. Moreover, numerous in vitro experiments have demonstrated that genetically engineered phages are able to infect biofilm cells causing a production of depolymerases with the final advantage of penetrate the inner layers of the biofilm and degrading components of the EPS matrix (Azeredo, 2008). Evidence suggested also the use of phage therapy in the treatment of post-burn infections caused by opportunistic pathogens as *E. coli*, *P. aeruginosa*, *S. aureus* and *Klebsiella pneumoniae* (Ahmad, 2002).

Bacteriophages can be modified to have an extended host range or a longer viability in the mammalian bloodstream, enhancing their potential as an alternative to conventional antibiotic treatment. They can also be engineered to transfer various compounds applicable for drug or gene delivery or an insertion of an active depolymerase genes could enforce the biofilm disaggregation (Bàrdy, 2016). Although a bacterial resistance to phages is already well known, a use of phage cocktails could overcome this problem, especially in the treatment of wound infections (Chhibber, 2017; Chadha, 2016). The use of a such mixed therapy could be also more effective in reducing the frequency of bacterial mutation in multi-drug resistant infections (Gu, 2012).



### Quorum Sensing inhibitors

Suppressing the cell-to-cell Quorum Sensing communicating system within the bacterial biofilm, could be another promising antimicrobial strategy for the treatment of challenging infections and the prevention of biofilm formation. Different strategies have been proposed, here are reported some examples.

Efflux pumps play an important role in the exclusion or inclusion of quorum-sensing-biomolecules necessary for biofilm formation. Altering the functioning of these pumps may interrupt the molecular traffic inside and outside the bacterial cell. The application of metallic nanoparticles as efflux pump inhibitors could represent a potential candidate to reduce biofilm-forming capacity of microbes and could also help the bactericidal effect of conventional antibiotics (Gupta, 2017).

Hammamelitanin (HAM), was discovered for the first time in a virtual screening of a library of small molecules based on RNAIII inhibiting peptide (RIP). This small molecules demonstrated able to block the QS system in *S. aureus* and affect biofilm formation causing altered cell wall synthesis and extracellular DNA (eDNA) release. Moreover, HAM can increase the susceptibility of *S. aureus* biofilms towards different classes of antibiotics (Brackamn, 2016).

*Streptococcus mutans* quorum sensing pathway can be effectively inhibit, interfering with the peptidase (PEP) domain contained in the ATP-binding cassette transporter *ComA*. Via an high-throughput screening, Ishii and collaborators (Ishii, 2017), found potent small molecules able to attenuate *S. mutans* biofilm formation and development without inhibiting bacterial cell growth.

The autoinducer acyl-homoserine lactones (AHLs) signalling molecules can be inhibit by various glucosamine monomers. Some strains of *P. aeruginosa* and *E. coli* demonstrated to be particularly sensitive to this mechanism (Biswas, 2017).

Quorum sensing can be inhibit also altering the autoinducer-binding receptors as, LasR and RhlR. Flavonoids are able to prevent the binding of LasR/RhlR DNA in a non competitive way, resulting in a suppression of virulence factor production in *P. aeruginosa* strains (Paczkowski, 2017).

*Enterococcus faecalis* is an opportunistic pathogen, naturally present in the gastrointestinal tract of humans and animals, able to cause urinary tract infections, bacteraemia, prosthetic joint infection, abdominal-pelvic infections, and endocarditis.

*E. faecalis* quorum-sensing systems could be inhibited by focusing specifically on the autoinducers (GBAP and CylLS) and their receptors. Autoinducer-antagonists are able to interact with specific receptors and do not exert selective pressure like antibiotics, without interfering with the normal host flora (Ali, 2017).

Natural compounds as plant extract could also be considered an alternative to the usual clinical practice. Recently, Al-Haidari and collaborators (Al-Haidari, 2016), tested different plant extract of *Citrus sinensis*, *Laurus nobilis*, *Elettaria cardamomum*, *Allium cepa*, and *Coriandrum sativum* as quorum quenching inhibitors, demonstrating a potent effect. These extracts exhibited significant anti-QS activity, acting on pyocyanin formation, twitching and swimming motility, and biofilm development of *P. aeruginosa* PA14 strain.

### Nanotechnology

Novel antibiotic drug delivery system are gaining importance for the urgent need to develop new efficient strategies to target microbial biofilms and resistant bacteria. Recently, a wide range of nanoparticles (e.g. silver, gold, iron oxide) have been intensively studied as antimicrobial agents, including their use against multidrug-resistant bacteria (Wang, 2017; Taylor, 2011). Some authors reported the use of these nanomaterials as a delivering strategy to improve their therapeutic efficacy challenging the developing resistance of the pathogens (Shaker, 2017; Bagga, 2017). Conjugating nanoparticles with an unresponsive antibiotic could be a possible strategy to restore its efficacy against otherwise resistant microbes (Shaikh, 2017; Li, 2014). The combined therapy might fill the gap where common chemotherapy fail (Beyth, 2015). A such novel synergistic approach can be applied to treat biofilm infections facilitating the penetration of the conventional agents within the exopolysaccharide matrix and inducing the microbes into their planktonic status thus targeting bacterial growth (Kostakioti , 2013) or inducing biofilm dispersion (Shafiei, 2013).

The relevant characteristic about the possible use of these nanomaterials is related to combating antibiotic resistance mechanisms. Indeed, in contrast to traditional antibiotics, where the resistance paths are usually relatively simple, NPs could combat microbes via multiple mechanisms simultaneously active. The advantage of this line of action is that microorganisms are unlikely to have multiple related genes, consequently it is much more difficult to develop a resistance to nanoparticles (Wang, 2017). Peculiar features of the NPs that represent an advantage for their antibacterial activity are the size: ultra-small and controllable size of nanoparticles is suitable also for the treatment of intracellular bacterial infections (Ranghar, 2012). Current research has demonstrated that the size of metal NPs can greatly affect its antibacterial activity (Esfandiari, 2014).

The shape is another important factor related to nanoparticles antimicrobial activity. NPs with different shapes can cause varying damages in bacterial cells through interactions with periplasmic enzymes (Cha, 2015).

Finally, we have to mention the zeta potential, which has a strong influence on bacterial adhesion. Positively charged NPs, compared with negatively charged and neutral NPs counterparts, have been believed to enhance ROS production. Negatively charged NPs seem to not adhere to bacteria because of the negative potential on both sides. However, at high concentrations, negatively charged NPs have a certain level of antibacterial activity due to molecular crowding, which leads to interactions between the NPs and the bacterial surface (Arakha, 2015).

The use of NPs as carriers for drug delivery, can help in the increasing of drug levels in the serum, protecting the drug molecules from chemical reaction until they reach their action site. Another important characteristic in the possible use of NPs as alternative strategies is their security: nanocarriers can target directly the infection site minimizing systemic undesired effects. Moreover, a controllable release of antibiotic could be possible (Wang, 2017).

Nanomaterials are currently used as an antibacterial coating in different implantable devices, especially in dental implants, where nanoparticles can inhibit the adhesion and colonisation of different bacterial species (e.g.

*Streptococcus mutans*, *Streptococcus epidermidis* or *E. coli*). Partially implantable devices as catheters can be treated with nanomaterials to retard or prevent the formation of bacterial biofilms (Samuel, 2004).

The treatment of chronic wound is another challenging side of microbial infections. A cover called a “dressing”, on which nanomolecules, as silver, can be added, could help reducing the risk of chronicity of wound infections and promote the proliferation of epithelial cells and the formation of new tissues (Yu, 2014).

Although the antibacterial mechanism of these nanomaterials is not fully understood, different authors suggested some possible way of action. Currently, the most frequently proposed are oxidative stress, metal ion release and non-oxidative mechanisms.

The production of Reactive Oxygen Species (ROS) is an important antibacterial mechanism of NPs that leads to the induction of oxidative stress. Different types of NPs produce different types of ROS by reducing oxygen molecules. In normal conditions, the production and clearance of ROS in bacterial cells are balanced. When there is an excessive production of ROS, the redox balance of the cell favours oxidation, which produce a state of oxidative stress leading to the damage of bacterial cells (Wang, 2017).

Metal ions can be released by metal oxide and penetrate into the bacterial cell. Inside the cell, metal ions can interfere with different physiological processes and in the end, resulting in bacteria death (Yu, 2014). Regarding the non-oxidative mechanisms of action assigned to NPs, relevant are the interaction with the bacterial cell wall, an important defensive barrier that protect the cell from the external environment. The ability of NPs to penetrate, through different mechanism, the cell membrane. The inhibiting activity of the synthesis of bacterial proteins and DNA and finally, the ability of inhbiting the biofilm formation (Wang, 2017).

It has also been suggested that the EPS matrix enables sequestering of particles from the surrounding biofilm environment (Flemming, 2007), thus helping the NPs mechanism of action. Furthermore, the EPS has been described as a “honeycomb” like structure (Schaudinn, 2009) with pores of various sizes

potentially allowing preferential absorption of key nutrients and blocking penetration based on size, structure, or charges. While the mechanisms regulating particle uptake are not yet known, it has been shown that these mechanisms are strongly dependent on the surface nanoparticle ionization (Nevius, 2012).

However, NPs antibacterial effects are not fully understood and their potential toxicity towards human tissues requires further investigation. Another potential limitation affecting the clinical application of metal/metalloid nanoparticles is the ability of some nanostructured materials to stimulate the release, by dendritic cells (DCs) and other cells in the immune system, of reactive oxygen species or chemical mediators able to cause unwanted side-effects such as hypersensitivity reactions or inflammatory responses (Di Gioacchino, 2011). Particularly, oxygen free radicals can cause severe tissue damage, and may also release cytokines that play a key role in the induction of inflammatory and immune responses (Donini, 2007). Therefore, nanoparticle candidates suitable for clinical applications must not induce DC activation or have toxic effects against cells of the immune system and other tissues.

### **3.3 SELENIUM NANOPARTICLES**

The increasing request of alternative antibiotic strategies and the recent developments in nanotechnology occurred in the last years, allow the production and the improvement of tailored metal/metalloid nanoparticles with physicochemical properties that can inhibit via different mechanisms, microorganisms growth and biofilm formation (Cremonini, 2016). In this context, selenium nanoparticles (SeNPs) have shown to possess antibacterial, antiviral and antioxidant properties, suggesting they could be suitable as therapeutic candidates to combat infectious diseases. If compared to their counterparts, Selenite and Selenate, SeNPs are biocompatible and non-toxic and can be synthesized through different physical, chemical and biological methods (Wadhvani, 2016). In particular, nanostructured particles that can be synthesized using bacterial and fungal cells as biological catalysts, are gaining importance: biogenesis of

nanoparticles could be a non-toxic and eco-friendly process for the synthesis of novel antibacterial products (Zonaro, 2015).

Selenium is a natural non-metallic element, occurring in four oxidation states: Selenate ( $\text{Se}^{6+}$ ), Selenite ( $\text{Se}^{4+}$ ), Selenite ( $\text{Se}^{2-}$ ), and elemental Selenium ( $\text{Se}^0$ ). It is essential in trace amounts for humans and animals but toxic at concentrations higher than the dietary doses. It is a key component of a variety of functional seleno-proteins in all living organisms, with the exception of higher plants and yeasts (Lampis, 2016). Some kind of microorganisms play a major role in the biogeochemical cycle of this element being able to tolerate selenium oxyanions using a Selenite/Selenate reduction mechanism. Depending on the species, the microbial reduction can occur through different mechanisms and can be the result of detoxification mechanism, a maintenance of the redox potential, or part of the respiratory electron transfer chain (Lampis, 2016).

#### Mechanisms of microbial SeNPs synthesis

Several microbial strains can reduce the toxic Selenite oxyanion to the less toxic elemental Selenium through the formation of Selenium nanoparticles (SeNPs), with a typical spherical shape and a diameter of 50-400 nm (Lampis, 2014). By definition, we can call nanoparticles, that particles having one dimension up to 100 nm (Singh, 2015).

The biogenic synthesis of these SeNPs can be extracellular, intracellular or bounded to the cell membrane. In a recent review, Wadhawani and collaborators (Wadhawani, 2016) give a detailed list of the different microbial and fungal species for whom synthesis of SeNPs has been reported. Gram-negative bacterial species as *Pseudomonas spp.*, *Agrobacterium spp.* and *E. coli*, preferentially secrete the NPs via an extracellular mechanism. *Stenotrophomonas spp.*, however, are able to use both extracellular and intracellular mechanisms. Among the Gram-positive species, the synthesis of SeNPs has been reported for several *Bacillus*, and *Lactobacillus* species. Extracellular production of monodispersed SeNPs has been characterized in fungal strains of *Aspergillus* and plants (Wadhawani, 2016; Li, 2017). Recent studies showed the ability of *Burkholderia fungorum* strains to secrete Selenium nanoparticles, under aerobic conditions, as a consequence of an

intracellular reduction mechanism followed by a secretory process through cell lysis (Khoei, 2016).

Due to the secretion process, the surface of biogenic SeNPs is surrounded by different chemical products, especially proteins, strongly related to NPs formation or metal reduction (Dobias, 2011). These proteins seems to be primarily implicated in the cell metabolism of fatty acid and carbohydrates. The binding ability of the proteins is also related to the spatial configuration and can control the size of the secreted NPs (Dobias, 2011). The “capping” agents are also important for their role in affecting the surface charge and NPs stability (Jain, 2015).

For both the two bacterial strains, *Bacillus mycooides* SeITE01 and *Stenotrophomonas maltophilia* SeITE02, used in this study and capable of producing SeNPs using an efficient Selenite reduction mechanism, a putative method for the biosynthesis of NPs has been addressed.

The bacterial strain SeITE01 was firstly isolated from the rhizosphere of the Selenium hyperaccumulator legume *Astragalus bisulcatus* grown in Selenium contaminated soil. Its ability to induce the formation of amorphous  $\text{Se}^0$  nanoparticles under aerobic conditions as a consequence of the reduction of Selenite was characterized, and the product of this reduction lead to an extracellular accumulation of Selenium nanoparticles. The size of SeNPs is directly dependent on the incubation times: when the time of incubation is increased also the NPs size resulted increased. In Fig.3 is reported a tentative explanation for the process of SeNPs formation given by Lampis and collaborators (Lampis, 2014).  $\text{SeO}_3^{2-}$  ions could be reduced into  $\text{Se}^0$  by the simultaneous activity of enzymatic proteins, released by the bacterium, and sulfhydryl groups on thiols of peptides released by *Bacillus* cells. Also the membrane reductases may play a significant role in  $\text{SeO}_3^{2-}$  reduction. Once reduced, Selenite ions are able to form Se nuclei which, subsequently, grow into the large SeNPs by further reductions and aggregation of these Se atoms; small SeNPs could stick together forming larger ones. As mentioned previously, SeITE01 cultures grown in the presence of Selenite, demonstrated the presence of spherical intracellular deposits of SeNPs by TEM analysis. The presence of a

bacillithiol reductase (BSH) system seems also to have a significant role the cytosolic thiol redox in *Bacillus spp*, concomitantly with the functions of other pathways (Fig.3B).

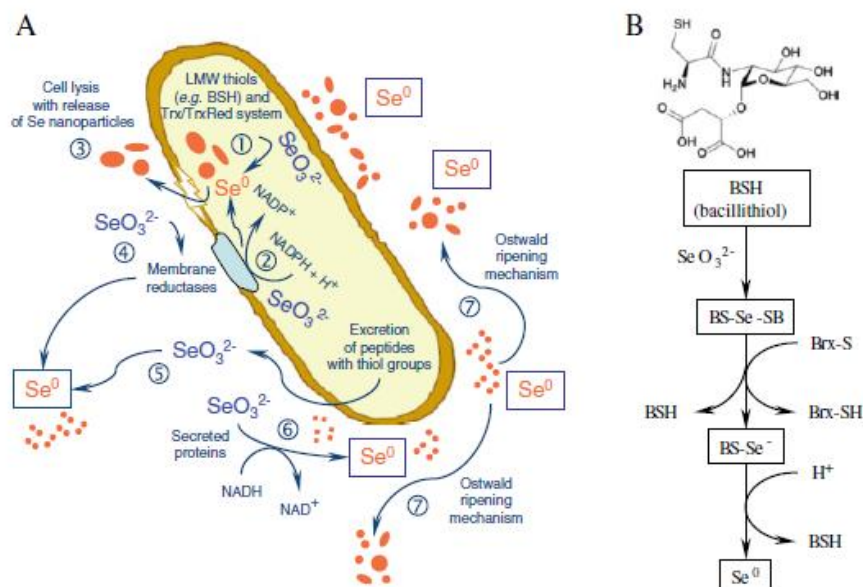


Figure 3. Hypothesis of SeNPs formation in *Bacillus mycoides* SeITE01 has described by Lampis et al. (2014).

The strain *S. maltophilia* SeITE02, as well, was isolated for the first time from the rhizosphere of *Astragalus bisulcatus* plant grown on polluted soil. This strain was proven to be highly resistant to  $\text{SeO}_3^{2-}$  and capable of reducing it to elemental selenium under aerobic growth conditions with the consequent production of SeNPs (Lampis, 2016).

The authors suggested that spherically shaped SeNPs could be observed mainly in the extracellular space, already after 13 h of incubation. In the same way of the strain *B. mycoides* SeITE01, the size of the secreted NPs is dependent on the time of incubation. It is worth noting that SeNPs of the same age displayed irregular dimensions. Observation using TEM analysis suggested that a releasing mechanism takes place in *S. maltophilia* SeITE02 after the initial formation of small nanoparticles within the cell. After the release of SeNPs, bacterial cells appeared damaged in their cell walls and empty ghost cells were abundant and evident once the stationary phase was reached.



Through proteomic analysis, an alcohol dehydrogenase (AdH) homologue, was clearly identified and possibly associated with the biogenic synthesis of SeNPs. This result was confirmed by the identification of the gene encoding for alcohol dehydrogenase in the draft genome sequence of *S. maltophilia* SeITE02 (Bertolini, 2014). This enzyme showed oxido-reductase activity and is involved in the metabolism of alcohols, it can work using both NADH and NADPH as electron donors and usually requires metallic cofactors. Basing on these results, a putative mechanism for Selenite biotransformation into SeNPs by *S. maltophilia* SeITE02, has been suggested. Inside the cells, a reduction of Selenite to elemental Selenium through reactions with thiol-containing molecules and/or peptides/proteins is carried out. Once formed, Se<sup>0</sup> seeds are released to the extracellular space possibly by an already unknown export system, until they grow to form detectable SeNPs. An alcohol dehydrogenase homologue, was also identified and the authors concluded that this protein may play a role in SeNP synthesis and stabilization (Lampis, 2016).

#### Antimicrobial and antibiofilm activities of Selenium nanoparticles

Selenium-based nanomaterials have revealed interesting antimicrobial potential against a broad range of pathogenic strains, belonging both to Gram-positive and Gram-negative bacterial species. Tran et al., demonstrated that SeNPs produced using a simple colloidal synthesis method, are able to inhibit *S. aureus* growth already after 5 h of treatment and are also able to prevent *S. aureus* biofilm formation (Tran, 2011). In addition, SeNPs demonstrated a potent inhibiting activity against the growth of particularly challenging *S. aureus* methicillin-resistant (MRSA) strains (Chihalova, 2015).

Recent studies on biogenic SeNPs, demonstrated that these particle are effective against biofilms formed by different clinical bacterial isolates belonging to *P. aeruginosa*, *S. aureus* and *Proteus mirabilis* species (Shakibaie, 2014). A collection of more than 30 species isolated from different hospitalized patients was tested for the susceptibility to SeNPs biogenically produced by a *Bacillus* sp. strain. The results of this study showed that the NPs tested were good anti-biofilm

agents against the clinical isolates considered. Moreover, the study showed that different selenium oxidation states exhibits different effects on biofilms.

Furthermore, biogenic SeNPs proved also capable of inhibit the proliferation of the promastigote and amastigote forms of *Leishmania spp.*, in a dose dependant manner, and limit the localized cutaneous exacerbations in the animal model (Mahmoudvand, 2014; Beheshti, 2013).

The antimicrobial activity of SeNPs against different yeast ad fungal strains (Shakibaie, 2015) has also been detected. Pathogenic fungi, as *Asperigllus* or *Candida*, are important human opportunistic pathogens, causing a spectrum of various lung infections, especially in immuno-compromised patients. In the last years, with the raise of resistant strains to current antifungal agents, the development of novel antimicrobial formulations is critical.

#### Coating medical devices with SeNPs to prevent bacterial colonisation and biofilm formation

Bacterial colonization and biofilm formation on medical devices is the primary cause for the spread of nosocomial infections, which primarily affects critically immuno-compromised patients. Try to prevent bacterial colonization on these devices by coating with a non toxic antimicrobial agent or bacterial adherence inhibitor, could be a possible alternative strategy.

Different surfaces can be functionalized with Selenium NPs in order to prevent biofilm formation, as reported by Wang (Wang, 2012). Selenium-coated polycarbonate medical devices inhibit the growth of *S. aureus* biofilms on their surface if compared to non-coated devices. Biogenically synthesized SeNPs can inhibit *S. aureus* adherence and micro-colony formation on polystyrene, glass, and catheter coated-surface (Sonkusre, 2015). Moreover, paper towels covered with Selenium nanoparticles showed an high effectiveness against *S. aureus*, *P. aeruginosa*, *E. coli*, and *S. epidermidis* (Wang, 2015).

#### Cytotoxicity and other possible applications for SeNPs

Selenium nanoparticles have gained a great attention also as potential cancer therapeutic agents and drugs carriers, as well as they have shown excellent

antioxidant activity and disease prevention effects (Huang, 2013). He and collaborators (He, 2014) demonstrated that SeNPs are not toxic at supra-nutritional levels in Sprague–Dawley rats and may be suitable as cancer chemoprevention agents. Different are the evidences that Selenium plays also a role in mammalian development, male reproduction, and immune function (He, 2014). SeNPs can be internalized selectively by cancer cells through endocytosis and induce cell apoptosis by triggering apoptotic signal transduction pathways (Zhang, 2013). A variety of toxicology studies have been done to assess the SeNPs exposure effects on health. Toxic changes have been observed in fish and embryos exposed to nanoparticles, including oxidative stress-related changes such as lipid oxidation, apoptosis, changes in gene expression and non-specific oxidative stress (Chen, 2006; Nel, 2006).

SeNPs demonstrated also able to reduce cell viability in human tumour lines as HeLa cells, in a dose-dependent manner (Ren, 2012).

In this study we demonstrated how microorganisms capable of transforming the toxic Selenium oxyanion into non-toxic elemental Selenium could be considered as biocatalysts for the production of nanomaterials (SeNPs), eventually exploitable in different biotechnological applications. In such a context, an environmental beneficially process turned out to be a biocompatible product that efficiently inhibit the growth of pathogens, including those resistant to antibacterial drugs.

## 4. MATERIALS AND METHODS

---

### 4.1 PREPARATION AND CHARACTERIZATION OF SELENIUM NANOPARTICLES

#### Preparation of Biogenic Selenium Nanoparticles (SeNPs)

Biogenic SeNPs were produced by exploiting the selenite reduction capability of two different environmental bacterial isolates. *Stenotrophomonas maltophilia* SeITE02 and *Bacillus mycooides* SeITE01 were used to produce respectively Sm-SeNPs(-) and Bm-SeNPs(+) (Lampis, 2014; Santi, 2013; Di Gregorio, 2005). Sterile nutrient broth supplemented with 2 mM Na<sub>2</sub>SeO<sub>3</sub> was inoculated to achieve final concentrations of 10<sup>5</sup> and 10<sup>7</sup> CFU/ml for *B. mycooides* SeITE01 and *S. maltophilia* SeITE02 respectively. The cultures were incubated aerobically at 27°C in a rotary shaker (150 rpm) for 6 h (*B. mycooides* SeITE01) or 24 h (*S. maltophilia* SeITE02). Bacterial cells and nanoparticles were removed from the culture medium by centrifugation at 10000 g for 10 min. The pellets were washed twice with 0.9% NaCl, suspended in Tris/HCl buffer (pH 8.2) and the cells were disrupted by ultrasonication at 100 W for 5 min. The suspension was then centrifuged at 10000 g for 30 min to separate disrupted cells (pellet) from nanoparticles (supernatant). The nanoparticles were recovered after centrifugation at 40000 g for 30 min, washed twice and suspended in deionized sterile water. Ch-SeNPs were produced as described by Lin (Lin, 2005).

#### Cell free extracts and CFX-SeNPs preparation

*Stenotrophomonas maltophilia* SeITE02 and *B. mycooides* SeITE01 cells were grown for 24 h until stationary phase. They were then centrifuged at 3000 g for 15 min and washed twice with phosphate buffer saline. The pellet was resuspended in 100 mM Tris–HCl pH 7.4 and sonicated at 100 W five times for 5 min. Finally, unbroken cells were separated by centrifugation at 16000 g for 30 min and the supernatant was recovered. CFX-SeNPs were then prepared by exposing Ch-SeNPs to CFX of *S. maltophilia* SeITE02 or *B. mycooides* SeITE01 overnight in agitation. CFX-SeNPs were recovered through centrifugation and washed twice

with 100 mM Tris-HCl pH 7.4, as described by Dobias and coworkers (Dobias, 2011).

#### Scanning electron microscopy (SEM)

Both the biogenic and synthetic SeNPs were analysed by Scanning Electron Microscopy (SEM). The nanoparticles were fixed, dehydrated through an increasing ethanol concentration series and dried in liquid CO<sub>2</sub> using the critical point method. The particles were mounted on metallic specimen stubs and directly observed using an XL30 ESEM (FEI, Hillsboro, OR, USA) equipped with an EDAX micro-analytical system, which was used to determine the elemental composition of the analysed nanoparticles.

#### Dynamic Light Scattering (DLS) Analysis

Measurements of Dynamic Light Scattering (DLS) from dispersed nanoparticles were made in Nanoscience Lab at University of Calgary (Canada). Data were measured using a Zeta sizer Nano-ZS by Malvern instrument with He-Ne laser at the wave length of 633 nm and a power of 4.0m was a light source collecting data at a fixed scattering angle of 173°. 300µL of the sample was applied to a quartz cell with a 10mm path length and data collected at 25°C. From the auto correlation function, the relaxation rate,  $\hat{W}$ , is determined allowing for the translational diffusion coefficient, D, to be calculated using  $D = \hat{W}/Q^2$ , where Q is the magnitude of the scattering vector [ $Q = (4\pi n/l) \sin \theta$ ; n is the refractive index of the solution, l the wave length of the scattered light, and  $\theta$  the scattering angle]. The viscosity of the water was taken as  $8.9 \times 10^{-4}$  Pas and its refractive index as 1.33 at 25°C. The diffusion coefficient so f the dispersed particles can be determined from the intensity of the autocorrelation function. Hydrodynamic diameter, Dh, can then be calculated from the diffusion coefficients, D, by using the Stokes-Einstein relation [ $Dh = (KBT)/3p\eta D$ ; where KBT is thermal energy and  $\eta$  is the viscosity of the dispersion medium]. Our analysis used a cumulant fit to the correlation function and gives the averaged weighted diameter and a polydispersity index (PDI). A regularized fit to the DLS data gives more details on

the size distribution of the dispersed nanoparticles. All the values were obtained using the software provided by the Malvern with the instrument.

#### Quantification of proteins and carbohydrates still remaining on the NPs surface after different denaturing treatment

Biogenic SeNPs were collected through centrifugation at 16000 rpm and subsequently exposed to three different treatments: (1) 10% SDS; (2) 10% SDS and boiling for 10 min; (3) 10% SDS and boiling for 30 min (Dobias, 2011). SeNPs were then centrifuged at 16000 rpm and the supernatants was separated in order to quantify proteins and carbohydrates content obtained after different treatments.

Protein concentration was determined using the method of Lowry et al. (Lowry, 1951) using bovine serum albumin (BSA) as standard; carbohydrates were measured using the anthrone method (Roe, 1955) using glucose as standard.

SeNPs obtained after different treatments were characterized using Dynamic Light Scattering (DLS) analysis. DLS was carried out using a Zen 3600 Zetasizer Nano ZS (Malvern Instruments, Malvern, UK) equipped with a 633 nm helium-neon laser light source (4.0 mW), detecting scattering information at a fixed angle of 173°. SeNPs samples (300 µl) were transferred to a quartz cuvette (10 mm path length), and the mean size distribution and zeta potential were recorded at 25°C using the software provided by Malvern Instruments.

## **4.2 ANTIMICROBIAL AND ANTIBIOFILM ACTIVITY OF SELENIUM NANOPARTICLES**

### Growth conditions and Microbial strains

Tryptic Soy Broth (TSB, Oxoid, Basingstoke, England), a highly nutritious general medium was used for the growth of bacteria.

<b>Formula</b>	<b>gm/liter</b>
Pancreatic digest of casein	17.0
Enzymatic digest of soya bean	3.0
Sodium chloride	5.0
Dipotassium hydrogen phosphate	2.5
Glucose	2.5

Sabouraud Liquid Medium (*Oxoid*), a liquid medium recommended for sterility testing, for non-sterile testing and for the determination of the fungistatic activity of pharmaceutical products was used for the growth of fungal strains.

<b>Formula</b>	<b>gm/liter</b>
Pancreatic digest of casein	17.0
Enzymatic digest of soya bean	3.0
Sodium chloride	5.0
Dipotassium hydrogen phosphate	2.5
Glucose	2.5

Different bacterial strains belonging to different bacterial species representative of both Gram-negative and Gram-positive were considered in this study (Tab.1).

Table 1. List of the different bacterial strains considered in the study and their origin.

<b>Bacterial species</b>	<b>Strain Name</b>	<b>Origin</b>
<i>Pseudomonas aeruginosa</i>	PAO1	Ref strain
<i>P. aeruginosa</i>	ATCC27853	Ref strain
<i>P. aeruginosa</i>	INT	Urine sample (MDR)
<i>P. aeruginosa</i>	BR1	Broncoalveolar lavage
<i>P. aeruginosa</i>	BR2	CF patient sputum
<i>P. aeruginosa</i>	CFC20	CF patient sputum
<i>P. aeruginosa</i>	CFC21	CF patient sputum
<i>P. aeruginosa</i>	CFCA	CF patient sputum
<i>P. aeruginosa</i>	CFCB	CF patient sputum
<i>P. aeruginosa</i>	FUS1	Burn wound
<i>P. aeruginosa</i>	TN1	Nasal swab
<i>Stenotrophomonas maltophilia</i>	VR10	Broncoalveolar lavage
<i>S. maltophilia</i>	VR20	Broncoalveolar lavage
<i>Achromobacter xylosoxidans</i>	C	CF patient sputum
<i>Burkholderia cenocepacia</i>	LMG16656	CF patient sputum
<i>Acinetobacter baumannii</i>	LMG 10531	wound infection
<i>Staphylococcus aureus</i>	Mu50	Ref strain (MDR)
<i>S. aureus</i>	UR1	Urine sample
<i>S. haemolyticus</i>	UST1	Burn wound
<i>S. epidermidis</i>	ET024	Endotracheal tube
<i>Propionibacterium acnes</i>	LMG 16711	Human facial acne
<i>Candida albicans</i>	CVr-21	Vaginal swab
<i>C. albicans</i>	SC5314	Reference strain
<i>C. parapsilosis</i>	CP-Vr5	Vaginal swab



#### Determination of the minimum inhibitory concentration (MIC) of biogenic NPs

The susceptibility of each strain to different types of SeNPs were determined in triplicate according to the Clinical and Laboratory Standard Institute (CLSI, 2016) protocol using broth microdilution method in flat-bottom 96 well microtiter plates. The microbial inoculum was standardized to approximately  $10^5$  CFU/ml. Plates were incubated at 37°C for 24 h and the optical density (O.D.) at 590 nm was determined using a multilabel microtiter plate reader (*Envision, Perkin-Elmer* LAS, Waltham, MA). The MIC was recorded as the lowest SeNPs concentration at which no significant O.D. increase was observed.

#### Biofilm formation assay

Bacterial cells were grown at 37 °C in TSB-1% glucose and yeast cells were grown in *Sabouraud* medium until they reached the exponentially growing phase ( $OD_{650nm}=0.4$ ). Exponentially growing cells were then diluted in culture medium to reach approximately  $10^6$  CFU/ml. Two hundred microliter of each cell suspension were used to inoculate sterile flat-bottomed polystyrene 96-well microtiter plates (MTP) (*CytoOne, Starlab*). As a negative control, 200 µl of the medium without any bacterium were added to the related well and plates were incubated aerobically at 37°C without agitation for 24 h to allow biofilm formation. After incubation, the planktonic cells were aseptically aspirated and washed with sterile physiological saline solution (PS). The biofilm formed was quantified adding 100 µl of 1% methylene blue staining to each well for 15 minutes at room temperature. Each well was then slowly washed once with sterile water and dried at 37 °C. The methylene blue bound to the biofilm was extract using 100 µl of 70% ethanol and the absorbance measured at 570 nm using “A3 Plate Reader” microplate reader (*DAS srl, Italy*). All experiments were performed in triplicate. Optical densities greater than 2, between 1 and 2 or between 0.5 and 1 optical units were considered to correspond to strong (S), medium (M) or low (L) biofilm production respectively.

#### Biofilm inhibition and disintegration assay for biogenic SeNPs.

In order to evaluate the anti-biofilm effect of SeNPs the bacterial strains were separately inoculated into 96-well microplates as previously described. SeNPs were diluted in TSB-1% glucose or *Sabouraud* medium to reach the concentration of 50-500 µg/mL and added to the wells. After 24 h incubation at 37 °C, the biofilm formation was quantified with methylene blue and the absorbance measured at 570 nm, as previously described.

In order to evaluate the biofilm disaggregating effect of SeNPs the bacterial strains were plated into 96-well MTPs and incubated for 24 h at 37 °C to allow biofilm formation. After incubation the medium was aseptically aspirated. SeNPs were diluted in medium to reach the concentration of 50-500 µg/mL and added to the wells. The microplates were then incubated for additionally 24 h at 37 °C and the amount of biofilm was quantified as previously described. All the mentioned experiment were performed in triplicate.

#### Biofilm formation and treatment with different types of SeNPs

A series of polystyrene round-bottomed 96-well microtiter plates were inoculated with 100 µl of a bacterial culture containing approximately  $5 \times 10^7$  CFU/ml and incubated at 37°C for 4 h. The biofilms formed were rinsed once with 100 µl of physiological saline solution (PS) to remove all non-adherent cells and subsequently treated with 128 µg/ml of the four different kinds of SeNPs diluted in PS. For every strain, untreated biofilms were included as control. Then, 100 µl of fresh medium was added to each well and the plates were incubated for additional 20 hours at 37°C.

#### Quantification of the biofilm biomass (Crystal Violet assay, CV assay)

The biofilms obtained after treatment, were rinsed with 100 µl PS and were fixed to plates by addition of 100 µl 99% methanol. After an incubation of 15 min at room temperature, the supernatant was removed and the plates were air dried. Then, 100 µl of a 0.1% CV solution was added to each well (20 min incubation at room temperature). The excess of CV was removed by washing the plates under running tap water. Finally, 150 µl of 33% acetic acid was added in order to release

the CV bounded to the biofilms and the plate was put on a vortex for at least 20 minutes (800 rpm). The absorbance was then measured at 590 nm. The experiments were performed in triplicate (Peeters, 2007).

#### Quantification of surviving cells

After biofilm formation and treatment as reported above, bacteria included in the biofilm were collected by two cycles of sonication and vortexing. The cell pellet obtained after centrifugation (5 min at 13000 rpm) was resuspended in 1 ml of PS and the number of colony forming units (CFU) was determined by plating on TSA Tryptone Soy Agar, *Oxoid*). Three biological replicates were included (Peeters, 2007).

#### Reactive Oxygen Species production assay (ROS assays)

ROS production by bacterial cultures after treatment with biogenic nanoparticles was investigated. The concentration of NPs used was corresponding to the MIC for all strains considered, except for *S. aureus* Mu50 (the concentration of NPs applied was corresponding to 50% of growth inhibition). Overnight cultures of every strain were dispensed in four tubes and 2'-7'- dichlorodihydrofluorescein diacetat ( $H_2DCF-DA$ , *Sigma-Aldrich*, Bornem, Belgium) was added to a couple of tubes at a final concentration of 10  $\mu M$ . All tubes were incubated for 1 hour at 37°C and then centrifuged for 5 min at 13000 rpm. Biogenic NPs was added to two aliquot of cells (one with  $H_2DCF-DA$  and one without). Appropriate controls to which an equal volume of PS was added instead of NPs were also included. All cell suspensions were transferred to a black microtiter plate. Six wells were filled per condition. The fluorescence ( $\lambda_{ex}= 485$  nm and  $\lambda_{em}=535$  nm) was measured every 30 min for approximately 24 hours with microtiter plate reader (*Perkin-Elmer* LAS). The net fluorescence emission by the NPs-treated and the untreated cells (control) was calculated and a corresponding graph was constructed. The results are only comparable within a plate and not between different plates (Wang, 1999). All experiments were repeated at least three times.

### 4.3 EVALUATION OF THE SYNERGIC EFFECT OF BIOGENIC SeNPs AND ANTIBIOTICS

#### Microbial strains and growth conditions

Experiments were conducted using representative of both reference strains and clinical isolates. Specifically, we analyzed two strains of *Pseudomonas aeruginosa*, namely *P. aeruginosa* PAO1 (reference strain), INT (MDR clinical isolate) and two clinical strains of *Staphylococcus aureus*: Mu50 strain (reference strain, methicillin resistant and intermediate vancomycin resistant) and a clinical strain isolated from an urine sample (*S. aureus* UR1). All bacterial strains were grown in TSB medium at 37°C.

#### Drugs and antibiotics used

Clarithromycin (*Klacid*) (Abbott, BGP Products S.r.l. Roma, Italy)

Levofloxacin (*Glaxo Wellcome* S.p.A., Verona, Italy)

Oxacillin (*Sigma-Aldrich*, St. Louis, USA)

Trimethoprim/Sulfamethoxazole (*Bactrim*) (*Roche*, Basel, Switzerland)

Tobramycin (*Sigma-Aldrich*, St. Louis, USA)

Vancomycin (*Abbott*, BGP Products S.r.l. Roma, Italy)

#### Determination of minimum inhibitory concentration and fractional inhibitory concentration (FIC)

To evaluate the antibacterial activity of SeNPs in combination with antibiotics, a two-dimensional microdilution assay was used (Wan, 2016). Assays were carried out in TSB growth medium. Minimum inhibitory concentration (MIC) for each of the antibiotics (*Clarithromycin*, *Levofloxacin*, *Oxacillin*, *Trimethoprim/Sulfamethoxazole*, *Tobramycin* and *Vancomycin*) and nanoparticles was first estimated according to the Clinical and Laboratory Standard Institute (CLSI, 2016) protocol using the broth microdilution method in flat-bottom 96 well MTP. The fractional inhibitory concentration index (FICI) of a combination of antibiotics and SeNPs was subsequently determined by the checkerboard method. The antibiotic of the combination was serially diluted along the abscissa, while the SeNPs were diluted along the ordinata. An inoculum of approximately  $10^5$

CFU/ml was prepared from each strain. Each MTP well was inoculated with 100  $\mu$ l of the bacterial suspension, and the plates incubated at 37°C for 24 h under aerobic conditions. The results were assayed by measuring the optical density (OD)<sub>600</sub>. The combined antimicrobial effect of agents A and B (where A is one of the antibiotics and B SeNPs) was calculated as follows:

$$FICI = \frac{\text{MIC (A in combination with B)}}{\text{MIC (A alone)}} + \frac{\text{MIC (B in combination with A)}}{\text{MIC (B alone)}}$$

The combination is considered synergistic when the FICI is  $\leq 0.5$ , partially synergistic when the FICI is  $> 0.5$  to  $\leq 1$ , additive when the FICI is  $> 1$  to  $< 4$ , and antagonistic when the FICI is  $> 4$  (Odds, 2003).

#### Biofilm formation and treatment with combination of SeNPs and antibiotic

A series of polystyrene round-bottomed 96-well microtiter plates were inoculated with 100  $\mu$ l of a bacterial culture containing approximately  $5 \times 10^7$  CFU/ml and incubated at 37°C for 4 h. The biofilms formed were rinsed once with 100  $\mu$ l of physiological saline solution (PS) to remove all non-adherent cells. 100  $\mu$ l of fresh TSB medium were added to each well and the plates were incubated for further 24h. After incubation at 37°C, mature biofilms were treated with different concentration of SeNPs alone or in combination with the different antibiotics, diluted in PS. For every strain, no treated biofilms (six wells) will be included as a control.

#### Quantification of cells

After incubation at 37°C for 24 hours, the biofilms were rinsed with PS to remove sessile cells. The number of CFU/ml still present in biofilms were determined by conventional plating as previously described.

#### Quantification of the biofilm biomass (Crystal Violet assay, CV assay)

After 24 hours of incubation, the biofilms were rinsed with 100 µl PS and fixed to the bottom of the well by addition of 100 µl 99% methanol. Biofilms biomass after treatment was determined by CV staining as previously described and the results compared to a non treated control.

#### **4.4 CHRONIC IN VITRO WOUND MODEL**

Artificial dermis (AD) were prepared as described by Backman et al 2016. The protocol is composed of different subsequent steps with the final aim to form an artificial substrate composed of an upper layer and a lower layer able to recreate the real conditions that can be found in chronic wound and soft tissue infections having a surface consisting of hyaluronic acid and collagen.

##### Day 1 (first layer)

The upper layer is a chemically cross-linked hyaluronic acid (HA) spongy sheet. An high-molecular weight (HMW) solution of sodium hyaluronate powder (1.20–1.80 MDA; *Lifecore Biomedical*, MN, US) was prepared in sterile distilled water (DW) (1.5%, pH 6.8). Then the HMW-HA solution was adjusted to pH 3.5 adding some drops of a HCl solution. As a cross-linking agent for HA molecules, was used ethylene glycol diglycidyl ether (EX810; *Sigma-Aldrich*, Bornem, Belgium): an aqueous solution of EX810 with a weight ratio HA:EX810 of 5:1, was added to the HMW-HA solution with vigorous stirring. One ml of this mixed solution was finally poured into a freeze-drying container, stored at 4 °C overnight followed by freezing at -80°C and then an overnight freeze-drying.

##### Day 2 (second layer)

The lower layer is a spongy sheet composed of HA and collagen (Col). HA powder was dissolved in DW to have a 1% HMW-HA solution (pH 6.8). Separately, a second HA 1% solution was autoclaved at 120 °C for 30 min to obtain a partially hydrolyzed low-molecular-weight HA (LMW-HA) solution. A 0.1% collagen solution was warmed at 50 °C for 10 min to obtain a heat-denaturated collagen solution. The three above-mentioned solutions were then

mixed together and adjusted to pH 7.5 with NaOH. One milliliter of this final solution was poured into the freeze-drying container into which the first spongy sheet layer was prepared. The combined product was stored at 4 °C overnight followed by freezing at -80 °C and then freeze-drying to obtain a two-layered spongy sheet.

Finally, the artificial dermis (AD) obtained were taken off by the container by breaking the glass. Both sides were irradiated with a UV lamp for 20 min to cross-link the collagen molecules. This spongy sheet was then sterilized in an oven at 110 °C for 1 h to obtain a sterile AD of approximately 1 cm × 1 cm (height × width).

Set up of the infection protocol

To evaluate the inhibiting and eradicating activity of SeNPs, biofilms were grown on AD as previously described by Brackman et al (Brackman, 2011). The medium used for the experiments was prepared dissolving fresh plasma in sterile Bolton Broth (*Sigma-Aldrich*) and adding freeze-thaw laked horse blood at a final concentration of 5%.

<b>Formula</b>	<b>gm/liter</b>
Enzymatic digest of animal tissues	10.0
$\alpha$ -ketoglutaric acid	1.0
Lactalbumin hydrolysates	5.0
Sodium carbonate	0.6
Sodium Chloride	5.0

The ADs were placed in 24-well microtiter plate (TPP) and 500  $\mu$ l of the medium were added, and was entirely taken up by the sponge layer. Five hundred microliters of the medium were then added around the AD to avoid dehydration during the experiment. An overnight culture of the strains to test was resuspended in physiological saline and diluted to 10<sup>6</sup> CFU/mL. Each AD was inoculated with 10  $\mu$ l of the cell suspension. To evaluate inhibition of biofilm formation, 100  $\mu$ l of

SeNPs were spread on the surface of each AD immediately after inoculation. Sterile PS was added to the controls. After 24 h at 37°C biofilms were rinsed once with PS and the number of culturable cells (CFU) present in the biofilms were collected by placing the AD into tubes containing 10 mL PS. After three cycles of vortexing (30 s) and sonication (30 s; Branson 3510; Branson Ultrasonics Corp., Danbury, CT) the resulting suspension was serially diluted and plated in TSA medium.

To determine the biofilm eradicating activity, the plate with the ADs was incubated for 24 h at 37 °C to allow biofilm formation. After incubation, the medium was removed, the biofilms were washed with PS, fresh medium was added and 100 µl of SeNPs were dropped on top of the biofilm. Plates were incubated at 37 °C for additional 24 h. Subsequently, biofilms were rinsed once with PS and the cells still present were collected by previously described. The number of CFU/ml was determined by conventional plating. A minimum of three samples both for the control and treatment with SeNPs was analyzed and this was repeated on at least two separate days.

#### *Determination of the minimum inhibitory concentration (MIC) of biogenic NPs*

The susceptibility of each strain to used to infect the dermis to Sm-SeNPs was determined in triplicate according to the Clinical and Laboratory Standard Institute (CLSI, 2016) protocol using the broth microdilution method in flat-bottom 96 well microtiter plates, as previously described. TSB was used as growing medium and fresh plasma was dissolved in it. MICs obtained with this method were then compared to the ones obtained using TSB medium alone.

#### **4.5 FLOW CELLS GROWTH MODEL**

Biofilms were grown in continuous flow culture chambers (flow cells), constructed as described by Pamp et al. (Pamp, 2008). A conventional microscope glass slide and a coverslip as the bottom and upper part of the chamber respectively, were fixed by a silicon sheet to a polycarbonate aluminium flow cells and were used to form the two separate rectangular channels. TSB medium



diluted 8 times was used as growth medium and connected through silicon tubes to the flow cell. A bubble trap was mounted between the two to avoid bubble formation. The system was filled with medium using a peristaltic pump (*Watson Marlow*, Calmough, Cornwall, England) with a consistent flow rate of 0.2 ml/min. An effluent reservoir was then placed at the most downstream part of the system (Fig.4).

An overnight culture of *P. aeruginosa* PAO1 and INT strain, grown in TSB medium at 37°C, was used to prepare an inoculum of 0.05 OD at 590nm. The continuous flow was stopped and each channels, one for the control and one for the treatment, was independently inoculated with 5 ml of bacterial suspension. The flow cells were then incubated for 1 h to allow attachment of the bacterial cells to the substratum and then the flow was restarted. After 3 days of incubation at 37°C, the continuous flow of fresh medium was stopped, the tubes connected to the chamber corresponding to the treatment clamped, and the bottle of medium substituted with one containing fresh medium supplemented with selenium nanoparticles at a final concentration of 128 µg/ml. The flow was then restarted and the mature biofilm was exposed to the SeNPs treatment for 24 hours. Some drops of the effluent from the flow cells were aseptically collected during the treatment at the time zero (immediately after that the flow was restarted) then after 1, 4, 24 hours of treatment and the number of CFU/ml was determined by conventional plating in TSA medium (*Oxoid*) and compared to a non treated control collected at the same times.

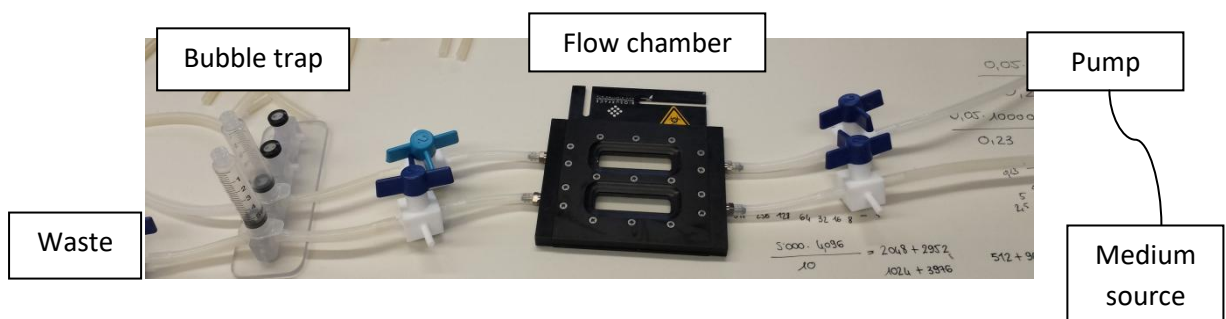


Figure 4. Schematic representation of the flow cells system.

#### Quantification of cells in biofilms

After 24 h of treatment with continuous flow at room temperature, coverslips were aseptically removed from the flow cells, and the cells in biofilms collected by adding 1 ml of PS on the surface of the glass and scratching with a sterile cell scraper. The bacterial suspension was then serially diluted in PS and the number of CFU/ml still present in the biofilm determined by conventional planting in TSA medium and compared to a non treated control.

#### **4.6 CAENORHABDITIS ELEGANS: A SIMPLE “IN VIVO” MODEL**

*Caenorhabditis elegans* strain N2  $\Delta$ glp-4  $\Delta$ sek-1 was used and worms were grown as previously described by Vandecandelaere et al (2017). This strain is incapable of producing progeny at 25 °C ( $\Delta$ glp-4) (Beanan, 1992) and exhibits an enhanced sensitivity to various pathogens ( $\Delta$ sek-1) (Kim, 2002).

#### Preparation of Nematode Growth Medium (NGM) plates

Nematodes were grown on Nematode Growth Medium (NGM) agar which has been prepared adding 3 g NaCl, 17g Agar, 2.5 g peptone to 975 ml H<sub>2</sub>O. The solution was then autoclaved and once cooled down, 1 ml CaCl<sub>2</sub> 1M, 1 ml cholesterol (5mg/ml in ethanol), 1 ml MgSO<sub>4</sub> 1M and 25 ml KPO<sub>4</sub> 1M were added. The medium has been then aseptically poured into *Petri* dishes. Before use the plates were leaved 2-3 days at room temperature to allow detection of contaminants and to allow excess moisture to evaporate.

#### Preparation of bacterial food source (*E. coli* OP50)

Briefly, a single colony of *E. coli* OP50 was aseptically inoculate in TSB broth and incubated overnight at 37°C. Using an inoculating loop approximately 100  $\mu$ l of the O/N suspension were spread on NGM agar plates and incubated at 37°C for 6 h to allow the formation of a thin bacterial layer. The worms tend to spend most of the time in bacteria and these plates can be used to keep the *C. elegans* nematodes in culture.

#### Transferring the worms (“chunking” technique)

This technique was used to transfer *C. elegans* from one petri plate to another. A stainless steel spatula was sterilized by holding it on the flame and cooled down in sterile MilliQ water. An NGM plate containing nematodes was cut approximately in 1 cm<sup>2</sup> pieces and 1-3 pieces were transferred to another NGM plate with an *E. coli* OP50 lawn. The worms will crawl out of the chunk and spread out onto the bacterial lawn on the plate. The plates were stored at 15°C for 2 weeks for culturing.

#### Obtaining a synchronised *C. elegans* population (“bleaching”)

The plates containing *C. elegans* were washed with sterile PS and collected in a falcon tube. The nematodes were let sink down and washed another times. Worms were then bleached by adding 1 mL 5% sodium hypochlorite (*Sigma*) and 0.5 mL 4 M NaOH (*Sigma*) and by vortexing for 10 sec every 2 minutes for a total of 10 minutes. The resulting eggs were incubated for 3–4 days at 25 °C on NGM medium plates previously precultured with *E. coli* OP50 strain, to obtain L4 stage worms (Brenner, 1974).

#### *C. elegans* infection assay

In a 24-well flat-bottomed microtiter plate, approximately 30 L4 stage worms were added per well in growth medium containing 95% M9 buffer (3 g KH<sub>2</sub>PO<sub>4</sub>, 6 g Na<sub>2</sub>HPO<sub>4</sub>, 1 ml 1 M MgSO<sub>4</sub> per litre), 5% Brain Heart Infusion broth (*Difco Laboratories*, Detroit, MI, USA) and 0.1 v/v % of a 5 mg/ml cholesterol solution (*Sigma*). Worms were infected by adding 25 µl of a bacterial cell suspension (10<sup>7</sup>-10<sup>8</sup> CFU/mL). The effect of different dilutions of SeNPs on infected *C. elegans* was evaluated and compared to the same number of wells treated with PS as a negative control. The total volume per well was 1 mL. The plates were incubated at 25 °C and scored for live and dead worms every 24 h (up to 48 h). Worms were considered dead if they were straightened and if no movement was observed.

#### **4.7 FLUORESCENCE MICROSCOPY**

Live/Dead staining (*Life Technologies*) was prepared adding to 994  $\mu$ l of PS, 6  $\mu$ l of Syto9 and propidium iodide (PI). Some drops of the staining were then added on the biofilm formed on the glass slide. After an incubation period of 15 minutes, the staining was removed and some drops of PS were added to avoid biofilm drying, a coverslip was then mounted on the slides and the glasses were observed at fluorescence microscope (Evos FL Auto, *Life Technologies*).

The commercial kit used for the assay is composed by two different nucleic acid stains that can allow to rapidly distinguish live bacteria with intact plasma membranes from dead bacteria with compromised membranes. Indeed cellular and membrane integrity is considered to be one criterion distinguishing between dead and viable bacterial cells. These last ones are assumed to have intact and tight cell membranes that cannot be penetrated by some staining compounds, whereas dead cells are considered to have disrupted and/or broken membranes. The red-fluorescent nucleic acid stain Propidium Iodide (PI) intercalates to DNA with no sequence preference with one dye molecule per four to five base pairs, identifying dead cells in the bacterial population stained. PI is not permeable through bacterial membranes and is usually excluded by living cells. On the contrary, the green-fluorescent nucleic acid stain SYTO9 is a membrane-impermeable-dye that can enter both live and dead bacterial cells. When both dyes are present, PI exhibits a stronger affinity for nucleic acids than SYTO9, and hence, SYTO9 is displaced by PI (Pamp, 2008).

#### **4.8 SeNPs TOXICITY IN AN “IN VIVO” MOUSE MODEL**

Animals were maintained under conventional housing conditions and acclimatized for at least 5 days before the experiment to the local animal facility conditions (room temperature: 20–24°C; relative humidity: 40–70%), having free access to standard rat chow and tap water. The experiments were conducted according to the Principles of Animal Care (publication no. 85–23, revised 1985)

of the National Institutes of Health and with the current law of the European Union and Italy (D. L.vo 116/92).

Female congenic C57BL/6J WT and gut-corrected CFTR<sup>tm1UNC</sup> (8-10 weeks old) mice were purchased from Cystic Fibrosis animal Core facility (San Raffaele Hospital, Milan, Italy). Prior to use, animals were acclimatized for at least 5-7 days to the local vivarium conditions, having free access to standard rodent chow and tap water.

#### Intratracheal challenge of Sm-SeNPs(-)

Mice were anesthetized with 2.5% isoflurane and placed on an intubation platform hanging by their incisor teeth. After visualization of the opening of the trachea using a laryngoscope, SeNPs solution at different concentrations were instilled by an intubation tube connected to a pressure control system. The animals were observed for viability and clinical signs of toxicity on the day of dosing (after 3 h) and then daily up to 5 days. In a similar trial, the negative control group received 0.9% apyrogenic sterile NaCl.

## **4.9 EVALUATION OF SeNPs CYTOTOXIC EFFECT IN HUMAN CELL CULTURES**

#### Preparation and culture of dendritic cells and fibroblasts

After written informed consent was received from donors, and approval by the Ethical Committee (Prot. no. 5626, February 2nd 2012, and Prot. no. 43318, September 4<sup>th</sup> 2013), buffy coats from the venous blood of normal healthy volunteers were obtained from the Blood Transfusion Centre at the University Hospital of Verona. Peripheral blood mononuclear cells were isolated by Ficoll-Hypaque and Percoll density gradient centrifugation (*GE Healthcare Life Sciences*, Little Chalfont, UK) and used for the immunomagnetic isolation (*Miltenyi Biotec*) of CD14<sup>+</sup> cells as previously described (Zenaro, 2009). DCs were isolated by incubating  $1 \times 10^6$  monocytes per ml at 37°C in 5% CO<sub>2</sub> for 5–6

days in six-well tissue culture plates (*Greiner Bio-One, Nurtingen, Germany*) in RPMI 1640 medium supplemented with heat-inactivated 10% low-endotoxin FBS, 2 mM L-glutamine, 50 ng/ml GM-CSF and 20 ng/ml IL-4. The final DC population was 98% CD1a+, as measured by FACS analysis.

Human primary fibroblast CCD112Sk cells (ATCC®CRL-2429) were purchased from ATCC (Manassas, VA, USA) and cultured in DMEM supplemented with 10% heat-inactivated FBS plus 2 mM L-glutamine at 37°C in 5% CO<sub>2</sub>.

#### Quantification of cytokine production

Cytokine production in cell culture supernatants was determined by ELISA using Ready-Set-Go ELISA kits (*eBioscience, San Diego, CA, USA*) according to the manufacturer's instructions. We measured the levels of IL-12 (range 4–500 pg/ml), TNF- $\alpha$  (range 4–500 pg/ml) and IL-6 (range 2–200 pg/ml). The ELISA development kit (*Mabtech, Nacka Strand, Sweden*) was used to determine the level of IL-8 (CXCL8 range 4–400 pg/ml). Briefly, DCs were treated with different concentrations of SeNPs for 24 h, and then the supernatants were collected. DCs were also activated with 100 ng/ml LPS as a positive control. The plates were read at 450 nm with Victor3 1420 Multilabel Counter (*Perkin Elmer, Waltham, MA, USA*).

#### Cell viability evaluation

Cell viability was assessed using the *AlamarBlue* assay (*Invitrogen, Thermo Fischer Scientific, Waltham, MA, USA*) according to the manufacturer's instructions. After incubation for 24 h with SeNPs, the reagent was added to the culture medium a final concentration of 10% before measuring the absorbance at 570 and 600 nm.

### **4.10 STATISTICAL ANALYSIS**

All the data are expressed as means plus Standard Error Mean (SEM) or Standard Deviation (SD). Statistical analyses, including t-Test and One-Way and Two-Way analysis of variance (ANOVA), was performed using GraphPad Prism 6.0

(GraphPad Software Inc., La Jolla, CA, USA). The level of significance was set at P value < 0.05.

## 5. RESULTS

---

### 5.1 BIOGENIC SELENIUM NANOPARTICLES: CHARACTERIZATION, ANTIMICROBIAL AND ANTIBIOFILM ACTIVITY

Biogenic SeNPs were produced by exploiting the selenite reduction capability of *Bacillus mycoides* SeITE01 and *Stenotrophomonas maltophilia* SeITE02, two different environmental bacterial isolates. The biogenic SeNPs were compared with synthetic Ch-SeNPs in terms of their physicochemical characteristics: as indicated by scanning electron microscopy (SEM) analysis, all the three types of nanoparticles were spherical. EDAX microanalysis of the purified SeNPs revealed the characteristic selenium absorption peaks at 1.37 (SeL $\alpha$ ), 11.22 (SeK $\alpha$ ) and 12.49 keV (SeK $\beta$ ) (Fig. 5). However, SeNPs differently synthesized showed different elemental composition (Tab.2): the ones synthesized by Sm-SeNPs(-) showed a selenium percentage in weight of 11.01% and Bm-SeNPs(+) a selenium percentage of 9.26. On the other hand, Ch-SeNPs exhibited a higher percentage in selenium, 31.61%. Furthermore, the composition of biogenic SeNPs, showed that they were rich in C, O, P and S, this suggesting the presence of biological macromolecules surrounding the nanomaterials. It is possible to hypothesize that this biogenic SeNPs cap include proteins, membrane phospholipids (P peaks) and also some cellular residues.

A possible composition and characterization of the biomolecular capping surrounding SeNPs biosynthesized by *S. maltophilia* SeITE02 has been already reported. Actually, the analysis of Sm-SeNPs(-) through Fourier transform infrared spectroscopy (FTIR) evidenced the presence of proteins, lipids and carbohydrates associated with the nanomaterial (Lampis, 2016) while in Ch-SeNPs, the same elements are present in different percentage (60.91% in weight of C, 4.97% in weight of O, 1.88% in weight of P and 0.63% in weight of S). This difference is probably due to the procedure used for the synthesis, where through the bacterial secretion of NPs some organic molecules may bind to the surface of nanoparticles. The average sizes has been also investigated using dynamic light scattering measurements: Sm-SeNPs(-) showed a size of  $170.6 \pm 35.12$  nm, Bm-SeNPs(+)  $160.6 \pm 52.24$  nm and Ch-SeNPs  $102.5 \pm 29.44$  nm (Fig. 6). All three



types of SeNPs are able to generate large negative zeta potentials (between -70 and -80 mV) in solution (Fig. 6) suggesting they are unlikely to form aggregates as a neutral and negatively charged NPs. From the literature we know that NPs tend to have long half-lives in human serum and are not taken up by cells in a nonspecific manner (Alexis, 2008). This is an important information looking at nanoparticles as potential in vivo applications as antimicrobial reagents.

Table 2. Elemental composition of Ch-SeNPs, Sm-SeNPs(-) and Bm-SeNPs(+) calculated through EDAX analysis.

Element	Ch-SeNPs	Sm-SeNPs(-)	Bm-SeNPs(+)
C	60.91	73.13	75.75
O	4.97	10.44	10.82
Se	31.61	11.01	9.26
P	1.88	4.42	3.14
S	0.63	1.00	1.04

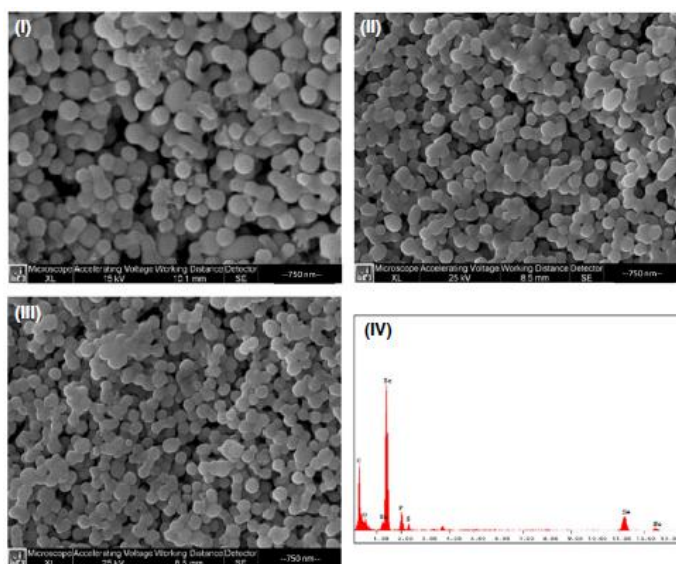


Figure 5. SEM analysis of SeNPs produced by *Stenotrophomonas maltophilia* SeITE02 (I), SeNPs produced by *Bacillus mycoides* SeITE01 (II) and chemically synthesized SeNPs (III). EDAX analysis of biogenic SeNPs (IV).

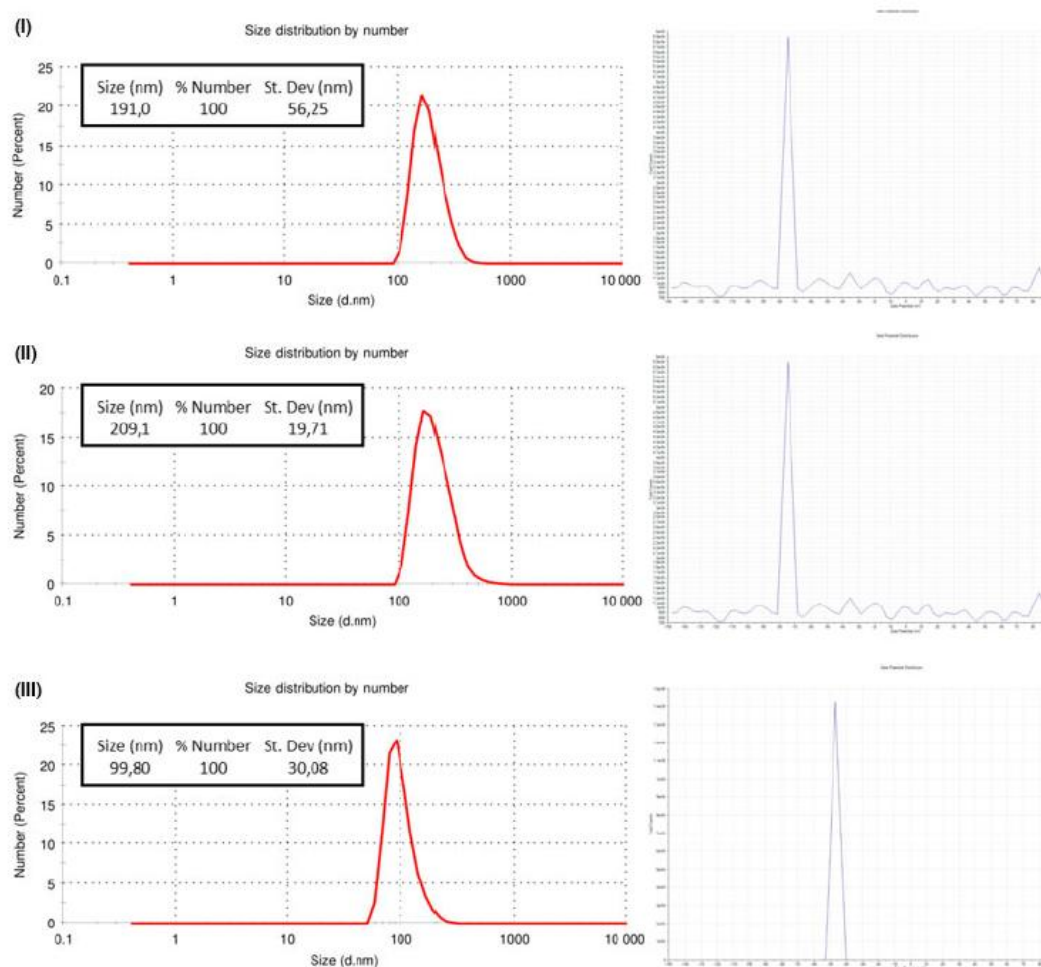


Figure 6. DLS analysis and zeta potential of SeNPs produced by *Stenotrophomonas maltophilia* SeITE02 (I), SeNPs produced by *Bacillus mycoides* SeITE01 (II) and chemically synthesized SeNPs (III).

Determination of Minimum Inhibitory Concentration (MIC) for SeNPs against *P. aeruginosa* PAO1

In a very first part of the study, in order to evaluate the antimicrobial effect of biogenic and synthetic SeNPs as well as to understand the putative role of the biomolecular cap of the biogenic nanoparticles, we determined the minimum inhibitory concentration (MIC) values against the reference strain *Pseudomonas aeruginosa* PAO1 (Tab.3). MIC determination was carried out for the biogenic SeNPs (Sm-SeNPs(-) and Bm-SeNPs(+)), the chemically synthesized Ch-SeNPs,

the Ch-SeNPs exposed to cell free extract (CFX) of *S. maltophilia* SeITE02 (CFX(Sm)-Ch-SeNPs) and *B. mycooides* SeITE01 (CFX(Bm)-Ch-SeNPs)) and CFX of *S. maltophilia* SeITE02 (CFX(Sm)) and *B. mycooides* SeITE01 (CFX(Bm)) alone. With the term CFX is usually indicated the fluid obtained by breaking bacterial cells, which contains most of the soluble molecules and components present in that microorganisms. We decided to perform this kind of experiment to clearly understand if the antimicrobial activity of the biogenic NPs was due to the toxicity of the elemental selenium contained in them, to the presence of biological molecules derived from the exploitation mechanism or both.

Table 3. Minimum inhibitory concentration (MIC) values of Sm-SeNPs(-), Bm-SeNPs(+), Ch-SeNPs, CFX(Sm)-SeNPs, CFX(Bm)-SeNPs, CFX(Sm), CFX(Bm) against *P. aeruginosa* PAO1.

Types of NPs	MIC $\mu\text{g/ml}$
Sm-SeNPs(-)	8
Bm-SeNPs(+)	64
Ch-SeNPs	>128
CFX(Sm)-Ch-SeNPs	256
CFX(Bm)-Ch-SeNPs	256
CFX(Sm)	>512
CFX(Bm)	>512

As we can see from Table 3, Ch-SeNPs, Sm-SeNPs(-) and Bm-SeNPs(+) evidenced a different MIC value: the Sm-SeNPs(-) seem to have the highest activity against *P. aeruginosa* PAO1 with a MIC value of 8  $\mu\text{g/ml}$ . On the contrary, the NPs synthesized by *B. mycooides* are less active with an higher MIC value (64  $\mu\text{g/ml}$ ). Ch-SeNPs showed a very low activity, with an MIC value >128

µg/ml towards the strain tested, similar to the one of CFX(Sm)-Ch-SeNPs and CFX(Bm)-Ch-SeNPs (256 µg/ml). Finally, CFX alone from both *S. maltophilia* SeITE02 and *B. mycooides* SeITE01 did not exhibit antimicrobial activity at any of the concentration tested. The values obtained are very high (> 512 µg/ml) thus indicating that the isolated cap alone is not responsible for the antimicrobial effect of the SeNPs.

These very preliminary results clearly indicate that the antimicrobial activity observed is exactly due to the nanoparticles and the biomolecular cap to them associated through the biosynthetic mechanism and not only to the selenium core of the NPs or their biomolecular cap.

Based on these findings, from here on with the term “biogenic selenium nanoparticles” we refer to nanoparticles produced by the *B. mycooides* SeITE01 and the *S. maltophilia* SeITE02 strains, composed by a selenium core surrounded by a complex capping structure (coating) formed by organic elements as proteins and carbohydrates, to date not completely characterized both in its composition and structure.

#### Antimicrobial activity of SeNPs against clinical isolates of *P. aeruginosa*

The antibacterial activity of the SeNPs, was tested against a series of clinical strains of *P. aeruginosa*, which, because of their surrounded polysaccharide biofilm matrix, are resistant to eradication by antibiotics and to clearance by the immune system. Such kind of strains are recurrent in chronic lung diseases as for instance Cystic Fibrosis, chronic obstructive pulmonary disease (COPD) and asthma. The ability of SeNPs to inhibit bacterial growth was tested by challenging the bacterial isolates and reference strains with different concentrations of SeNPs according to the Clinical and Laboratory Standards Institute (CLSI, 2016) broth microdilution method. *P. aeruginosa* PAO1 and ATCC 27853 were included as reference strains. Three strains BR1, BR2 and BR3 were clinically isolated from patients through bronchoalveolar lavages. The strains CFC20, CFC21, CFCA and CFCB were included being clinical isolates from patient affected by Cystic Fibrosis. The TN1 strain was isolated from a nasal swab and the UST1 strain from

a burn wound. The *P. aeruginosa* INT strain, isolated from a urinary tract infection, was chosen to provide a particularly challenging target being a multidrug-resistant strain that carries a class 1 integron containing multiple antibiotic-resistant gene cassettes.

As shown in Table 4, the MIC of Sm-SeNPs(-) varied widely among the different *P. aeruginosa* strains. Against some clinical isolates from low respiratory tract infections (CFC20, CFC21, CFCA,CFCB, BR1 and BR2) and the reference strain PAO1 SeNPs showed low MIC values ranging from 8 to 32 µg/ml, while other strains as the *P. aeruginosa* INT and BR3 presented MIC values ranging from 64 to 256 µg/ml. Finally, among the strains considered, two clinical isolates (TN1 and FUS1) as well as the reference strain ATCC27853 seemed to have high MIC values ranging from 256 to 512 µg/ml.

The MIC of Bm-SeNPs(+) also varied among the strains but was generally 2–4 times higher than Sm-SeNPs (Table 4). The MIC of Ch-SeNPs indicated that these SeNPs are no effective against the bacterial growth of *P. aeruginosa* (Tab.4).

We investigated also the antibiotic susceptibility of the same strains by calculating the MIC values, according to the CLSI standard method. The analysis demonstrated that the *P. aeruginosa* clinical strains were resistant to beta-lactams (MIC values varying between 16 and  $\geq 64$  µg/ml) and other antibiotics such as gentamicin (MIC values 8-16 µg/ml), ciprofloxacin (MICs between 2 and  $\geq 4$  µg/ml) and sulphonamides (MIC values 20-320 µg/ml).

However, a possible correlation between the SeNPs susceptibility (Tab.4) and the antibiotic resistance reported above is not conceivable.

Table 4. Minimum inhibitory concentration (MIC) values of Sm-SeNPs(-), Bm-SeNPs(+) and Ch-SeNPs against different *P. aeruginosa* reference and clinical strains.

Strain Name	MIC $\mu\text{g/ml}$		
	Sm-SeNPs (-)	Bm-SeNPs(+)	Ch-SeNPs
PAO1	8	64	>128
ATCC27853	512	512	>512
INT	64	512	>512
BR1	32	128	>512
BR2	8	128	>512
BR3	256	512	>1024
CFC20	16	64	128
CFC21	8	32	128
CFCA	16	64	>128
CFCB	16	32	>128
FUS1	512	>1024	>1024
TN1	512	>1024	>1024

To tentatively evaluate the susceptibility of bacterial strains to SeNPs, the MIC values obtained were compared to those obtained using antibiotics. Lacking reference MIC values (breakpoints) which could help us in determining the sensitivity or the resistance to the SeNPs, we can only refer to the obtained values in term of low or high and try to compare these results to the ranges of antibiotics clinical exposure.

Because the MIC values of SeNPs for some of the clinical isolates and the reference strain PAO1 fall within the range of clinical exposures adopted during typical antibiotic treatments (Tab.4), we can hypothesize that biogenic SeNPs could be used to treat antibiotic resistant clinical strains, eventually overcoming the potential risks of antibiotic resistance manifestation. Moreover, in some cases the MIC values of biogenic SeNPs is lower than those of antibacterial drugs

supporting the idea of these new nanomaterial as a possible alternative strategies in the fighting of drug-resistant bugs.

#### *Inhibition of P. aeruginosa strains biofilm formation by SeNPs*

The effect of SeNPs on *P. aeruginosa* biofilm synthesis was analyzed treating the clinical isolates showing low or intermediate MIC values to SeNPs and the two reference strains PAO1 and ATCC27853 with different concentrations of Sm-SeNPs(-), Bm-SeNPs(+) and Ch-SeNPs for 24 h at 37°C. Biofilm formation was quantified by methylene blue staining as previously described. The percentage of biofilm inhibition was calculated by comparing the microbial cultures exposed to the SeNPs with a culture control growing in the absence of SeNPs. As seen in Tables 5 and 6, the quantity of biofilm produced by *P. aeruginosa* varied among the different strains as reported in brackets but all the strains were considered efficient biofilm producers. The lowest concentrations of biogenic SeNPs used (50 and 100 µg/ml) inhibited biofilm synthesis by *P. aeruginosa* strains CFC20, CFC21 and CFCA by 70-90%, and confirmed that NPs are particularly active against these strains as previously indicated by MIC values (Tab.5). In contrast, in the clinical strains CFCB and INT, as well as in the reference strains, SeNP showed a significant inhibition of biofilm synthesis (at least 70%) only in the presence of concentrations  $\geq 250$  µg/ml. Surprisingly, the BR3 strain, showed a very resistant biofilm against the action of SeNPs with an inhibition of 50% only up to 500 µg/ml. Table 5 also shows that Sm-SeNPs(-) were usually more efficient than Bm-SeNPs(+) and that the synthetic Ch-SeNPs were only active at concentrations of 250–500 µg/ml against most of the strains, the exception being *P. aeruginosa* CFC20, which was the most susceptible isolate tested.

#### *Degradation of P. aeruginosa biofilms by SeNPs*

We next investigated whether the SeNPs were able to cause the degradation of biofilms by measuring the amount of biofilm remaining after exposing for 24 h the mature synthesized exopolysaccharide matrix to different concentrations of

biogenic and synthetic SeNPs (Tab.6). Also in this case, the *P. aeruginosa* CFC20 biofilm was highly susceptible to SeNP-induced disaggregation, resulting in 90% degradation in the presence of 50 µg/ml SeNPs, confirming that this strain is more susceptible to SeNPs than the other strains. In all the strains, the biofilm degradation did not increase at higher SeNPs concentrations. Sm-SeNPs(-) were slightly more efficient than Bm-SeNPs(+) in the eradication of *P. aeruginosa* biofilms. As regard the reference strains, the biofilm formed by PAO1 can be considered highly susceptible to SeNPs activity, showing a disaggregation of more than 70% also at the lowest concentration. Conversely, against the reference strain ATCC27853 and the clinical isolates INT, CFCB and CFCA as well, SeNPs demonstrated a lower disaggregating activity ranging from 40 to 60% for all the concentration tested. Only one of the clinical isolates, the *P. aeruginosa* CFC21, was not sensitive to the SeNPs disaggregating activity, showing only a 20% reduction of the exopolysaccharide matrix. Similarly to the inhibiting activity, the Ch-SeNPs had not a good antibiofilm activity. The difference between the MIC values and the inhibiting and disaggregating activity among the same strain was probably due to the type, the quantity and the thickness of biofilm formed by the different strains.



Table 5. Percentages of inhibiting activity in different *Pseudomonas aeruginosa* strains caused by Sm-SeNPs, Bm-SeNPs and Ch-SeNPs (mean±SD).

Strain name	Se NPs-Sm (-) µg/ml				Se NPs-Bm (+) µg/ml				Ch Se NPs µg/ml			
	50	100	250	500	50	100	250	500	50	100	250	500
PAO1	40±2.5	45±3	70±2.5	96±1	33±3	47±6	63±4.5	95±1.2	9±0.7	21±2.1	94±0.7	96±1.4
ATCC27853	15±0.7	30±0.7	41±0.7	66±2.1	15±4.2	17±2	44±2.8	64±1	4±1.4	10±0.7	35±2.1	44±2
INT	23±1	34±1	59±3.5	95±1	25±4.5	29±3.5	49±2.5	94±1.5	2±3.5	2±1.4	20±0.7	30±0.7
BR1	71 ± 0.7	75 ± 2.1	73 ± 6	76 ± 4.9	20 ± 1.4	30 ± 4.2	28 ± 0.1	50 ± 3.5	7 ± 0.1	10 ± 4.9	13 ± 5.6	16 ± 1.4
BR2	75 ± 4.9	69 ± 7	74 ± 4.2	69 ± 3.7	22 ± 1.4	33 ± 1.2	45 ± 0.7	60 ± 3.5	0	0	26 ± 2.8	59 ± 2.8
CFC21	66±5	86±0.5	95±2	96±1.5	37±5.5	66±3.5	93±1.7	95±2	10±3.5	33±3.5	71±1.4	65±1.4
CFC20	75±0.5	82±1	86±1	93±1.5	72±2	76±0.5	85±1	91±2	53±0.7	90±0.7	95±1	95±1
CFCA	39±1	94±1	94±3.5	96±1	25±5	25±1.5	94±0.5	96±1	5±0.7	6±0.7	96±1	97±1.5
CFCB	31±1	39±3	39±2	88±4	28±1.5	34±5	81±4.5	85±5	1±0.5	1±0.5	97±0.7	98±1

Table 6. Percentages of disaggregating activity in different *Pseudomonas aeruginosa* strains caused by Sm-SeNPs, Bm-SeNPs and Ch-SeNPs (mean±SD).

Strain name	Se NPs-Sm (-) µg/ml				Se NPs-Bm (+) µg/ml				Ch Se NPs µg/ml			
	50	100	250	500	50	100	250	500	50	100	250	500
PAO1	73±5	72 ±2	76 ±2	73±5	52±1	62±4.5	57±1	73±6	16±0.7	18±4.2	37±0.7	53±1
ATCC27853	49±1.4	53±1.4	53±1.4	43±0.7	31±4.9	43±1.4	51±7	45±7	23±1.4	35±1	40±2.5	46±0.7
INT	63±5.5	53±0.5	61±1.5	41±4.5	65±4.5	44±0.5	58.2±3	32±1.5	15±6.3	15±6.3	8±2.8	8±4.5
BR1	23±3.5	28±3.7	44±3	40±0.7	2±4.9	2±4.9	14±2.8	10±1.4	10±1.2	14±2	21±0.7	19±1
BR2	14±4.9	10±0.1	36±4.1	43±6.3	10±1.4	7±3.5	17±0.1	19±4.1	0	6±1.2	9±0.7	8±0.1
CFC21	21±1	45±3.5	53±5.5	63±2	44±4.5	16±3	33±1.5	61±0.5	8±1.4	5±0.7	16±1.4	1±0.7
CFC20	87±3	84±0.5	85±1	85±0.5	80±1	86±1	86±1.7	82±2	17±3.5	13±2.8	29±4.2	50±2.8
CFCA	53±4	58±3	56±3	64±2	25±1	27±5	51±2.5	47±3	0	4±1.4	57±1.4	72±0.7
CFCB	44±2.5	44±2.5	39±1	53±2	28±4	20±2.5	40±2.5	53±1	0	2±0.7	66±0.7	73±0.7

Antimicrobial activity of SeNPs against clinical isolates of Candida

Table 7. Minimum inhibitory concentration (MIC) values of Sm-SeNPs(-), Bm-SeNPs(+) and Ch-SeNPs against different yeasts strains.

Yeast strain	MIC µg/ml		
	Sm-SeNPs(-)	Bm-SeNPs(+)	Ch-SeNPs
<i>C. albicans</i> CVr-21	64	256	>512
<i>C. parapsilosis</i> CPVr-5	64	128	>512

We also evaluated the anti-fungal activity of SeNPs by testing *in vitro* their ability to inhibit the growth of *C. albicans* and *C. parapsilosis* clinical strains. The SeNPs from *Stenotrophomonas malthophilia* SeIT02 resulted to have mild MIC values (64 µg/ml) against the three strains tested. The NPs from *Bacillus mycooides* SeIT01 and chemically synthesized resulted poorly effective against *Candida* strains with MICs values ranging from 128 to more than 512 µg/ml.

Inhibition of the formation and degradation of Candida strains biofilm by SeNPs

Then the inhibiting and disaggregating activity of SeNPs was evaluated on *Candida* biofilms (Tab.8). Interestingly, the lowest SeNP dose tested (50 µg/ml) was sufficient to inhibit biofilm formation for 60–70% in the two yeast isolates, and no significant improvement was achieved at the higher doses of 100 and 250 µg/ml tested (Tab.9). Sm-SeNPs(-) and Bm-SeNPs(+) had similar effects on biofilm formation in the yeast strains, whereas the Ch-SeNPs had no significant effect.

Table 8. Percentage of biofilm synthesis inhibition in different fungal strains caused by Sm-SeNPs(-), Bm-SeNPs(+), Ch-SeNPs (mean±SD).

Strain name	Sm-SeNPs(-)				Bm-SeNPs(+)				Ch-SeNPs			
	50	100	250	500	50	100	250	500	50	100	250	500
CVr-21	61±0.5	60±3	60±1	94±1	60±6.5	69±2	74±2.5	93±0.5	0	0	0	9±0.7
CPVr-5	72±1.5	79±0.5	73±1	95±1	75±1.5	73±0.5	72±3	94±0.5	0	0	0	5±0.7

Table 9. Percentage of biofilm disaggregation in different fungal strains caused by Sm-SeNPs(-), Bm-SeNPs(+), Ch-SeNPs (mean±SD).

Strain name	Sm-SeNPs(-)				Bm-SeNPs(+)				Ch-SeNPs			
	50	100	250	500	50	100	250	500	50	100	250	500
CVr-21	26±2.5	43±2.5	47±3.5	60±2	11±2.5	32±2	48±1.5	60±3.5	0	0	2	0
CPVr-5	52±2	48±1.5	48±2.5	64±2	48±3	38±2	47±2	42±2.5	0	1	0	0

## 5.2 INVESTIGATION OF THE BIOGENIC COATING AS A POSSIBLE MODULATOR FOR THE SeNPs ANTIMICROBIAL AND ANTIBIOFILM ACTIVITY

In a first part of the study we demonstrated that biogenic selenium nanoparticles produced by two different environmental isolates were able to inhibit biofilm synthesis by *P. aeruginosa* and can efficiently disaggregate the mature exopolysaccharide matrix produced by these microorganisms. The antimicrobial potential of these biogenic SeNPs is greater than that of synthetic SeNPs, probably due to the presence of a bacterial protein layer coating the surface of the NPs. Furthermore, SeNPs produced by the Gram-negative species *S. maltophilia* are more efficient antibacterial and antibiofilm agents than those produced by the Gram-positive species *B. mycoides*. This could suggest that SeNPs with similar dimensions but originating from taxonomically distinct bacterial isolates may show different activities, probably due to the different composition of their organic surface layer.

In a second part of the study, in order to evaluate the influence of this organic matter on the physical characteristics of biogenic nanoparticles, different and progressively more aggressive denaturant treatments were applied to the Sm-SeNPs(-). Taken in consideration that the NPs produced by the Gram-negative strain *S. maltophilia* were more active against the strains tested, we decided to focus our attention on this type of biogenically produced nanoparticles.

The macromolecular contents and the physical and electrical properties were determined in each type of SeNPs including those obtained after treatments. The SeNPs obtained after the three different denaturing treatment were then tested for their antibacterial and antibiofilm activity and compared to the SeNPs biogenically produced by *S. maltophilia* SeITE02 (Untreated) in order to correlate the composition and the presence of the whole coating on the surface of the NPs and their antimicrobial activity.

Characterization of Sm-SeNPs(-) as biogenic products and after different denaturing treatments

As shown in Figure 7, the protein content associated with the organic coating of SeNPs decreases after the different denaturant treatments. Biogenic SeNPs present protein concentration of  $0.46 \pm 0.05$  mg/mgNPs that progressively decreases with the increase in treatment intensity reaching a value of  $0.05 \pm 0.01$  mg/mgNPs after exposure to 10% sodium dodecyl sulfate (SDS) and 30 min boiling. A similar pattern was observed for carbohydrate concentration (Fig.5B): untreated biogenic SeNPs present a concentration of  $0.33 \pm 0.04$  mg/mgNPs which decreases after the different treatments reaching a value of  $0.02 \pm 0.01$  mg/mgNPs.

Dynamic light scattering measurements (Tab.10) showed that the exposure to different treatments induced a progressive increasing of the nanoparticles size, up to  $270 \pm 24$  nm, after the treatment with 10% SDS and 30 min boiling. More precisely, as shown in Figure 8, the loss of cap is associated to an increase in the number of SeNPs with high trend to aggregation and not to the formation of SeNPs with higher dimensions. On the other hand, nanoparticles showed a reduction of Z-potential with values ranging between -17.40 and -3.97 mV after the different treatments (Tab.10). Figure 8 describes in detail the changes associated with the denaturing conditions indicating that there is an increase both in size and in the agglomeration state in a high number of the NPs due to the removal of the organic coat.

With the aim to demonstrate that the decreasing antibacterial activity of the completely denaturated SeNPs (treatment with 10%SDS+30' boiling) was not only due to the biggest dimension but also to the complete loss of the coating surrounding the surface of the NPs, another type of SeNPs (Sm-SeNPs(48)) was also taken into consideration. These Sm-SeNPs(48) were obtained from bacterial cultures after 48 hours of incubation with sodium selenite and showed a diameter of  $276 \pm 26$  nm, with a Z-potential value of -29.27 mV (Tab.10). In fact, Lampis et al (Lampis, 2014) demonstrated that the size of SeNPs is dependent on the incubation times: by increasing the incubation time is possible to produce biogenic particles with a greater size.

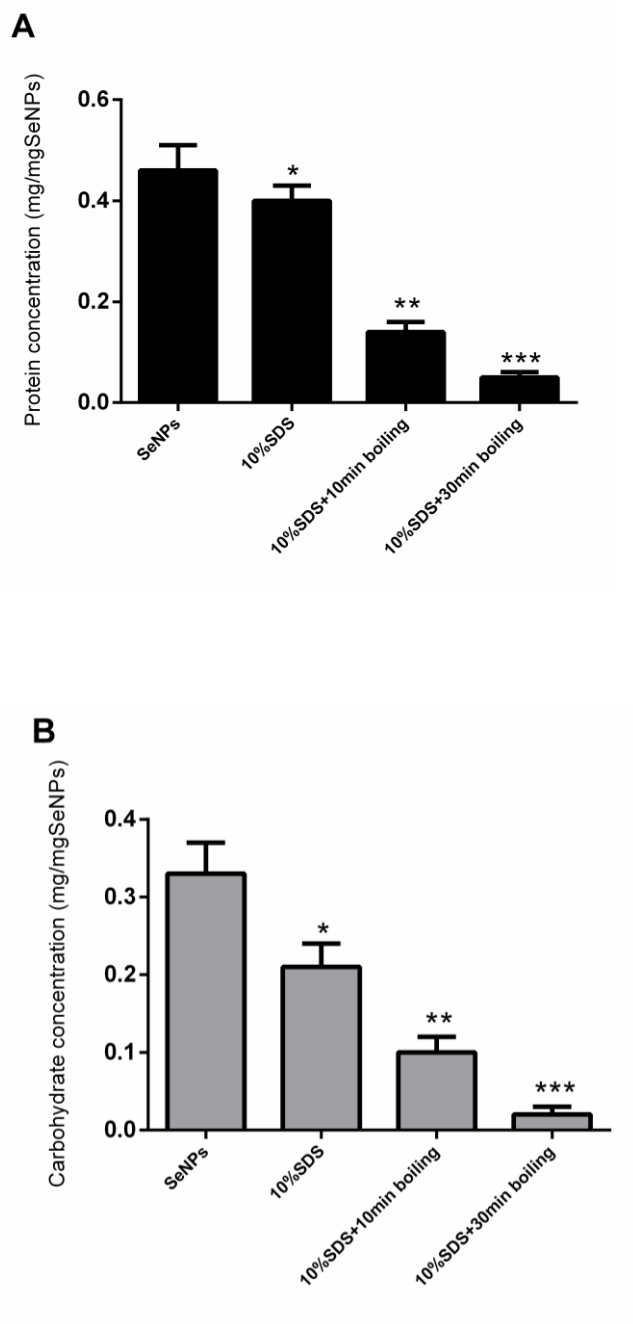


Figure 7. Protein (A) and carbohydrate (B) content on the coating of Sm-SeNPs(-) after different denaturant treatments compared to the native SeNPs (first column) (mean±SD; n=3; p<0.05).

Table 10. DLS analysis and zeta potential of Sm-SeNPs(-) as biogenic product, after different treatments and after 48 h of incubation.

	Diameter (nm)	Z-potential (mV)
SeNPs	181±20	-32.01±2.67
10% SDS	209±25	-17.40±3.45
10% SDS+10min boiling	233±19	-10.02±2.36
10% SDS+30min boiling	270±24	-4.06±1.34
Sm-SeNPs(48)	276±26	-29.27±2.5

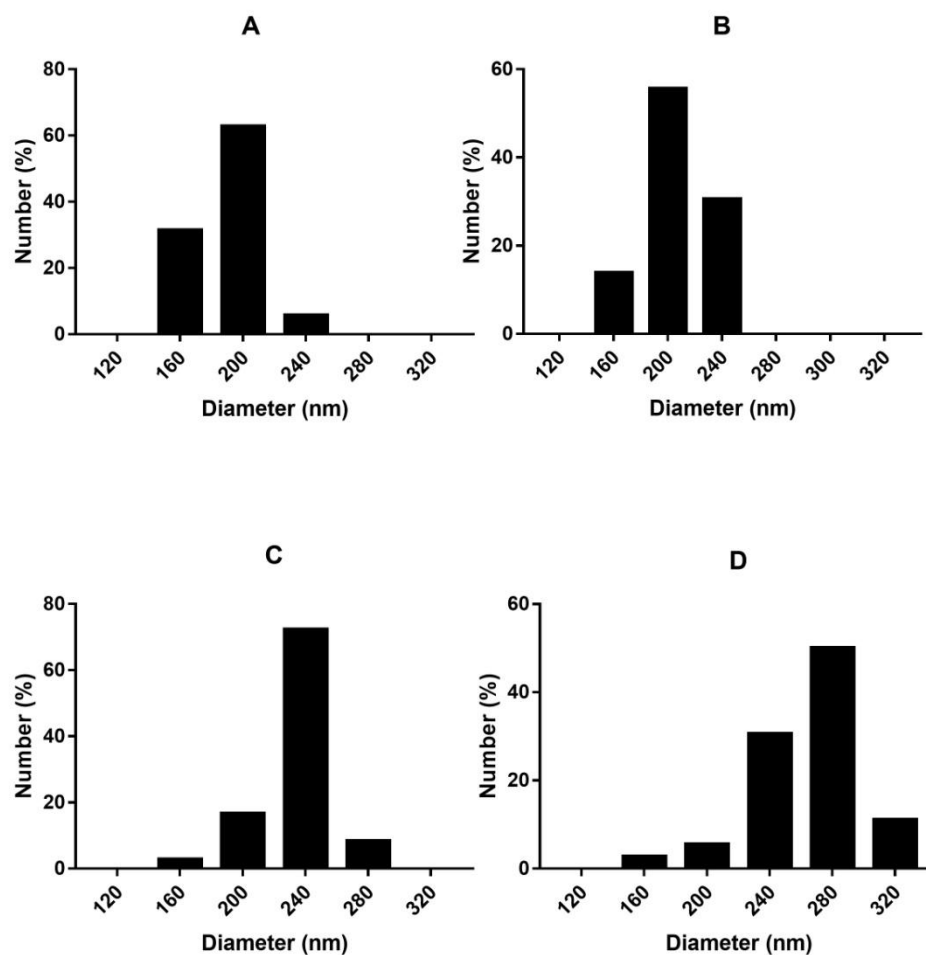


Figure 8. Diameter distribution of SeNPs extracted from *Stenotrophomonas maltophilia* SeITE02. Biogenic SeNPs (A), SeNPs after treatment with 10% SDS

(B), SeNPs after treatment with 10% SDS +10 min boiling (C), SeNPs after treatment with 10% SDS + 30 min boiling (D).

#### Characterization and antimicrobial activity for Sm-SeNPs(48)

SeNPs extracted after 48h of incubation with *Stenotrophomonas maltophilia* SeITE02 were first of all characterized for chemical and physio-chemical characteristics. Sm-SeNPs(48) showed a diameter of  $276\pm 26$  nm, with a Z-potential value of  $-61.16$  mV (Tab.10), which is an indicator of the surface charge on SeNPs and consequently of their stability. As shown in Fig.9 the proteins concentration associated with these biogenic nanomaterials was  $0.48\pm 0.07$  mg/mgSeNPs, while the carbohydrates concentration was  $0.35\pm 0.03$  mg/mgSeNPs. Comparing the size distribution of the different types of NPs to the one of the Sm-SeNPs(48) (Fig.8 and Fig.9) we can clearly notice that they had similar dimensions while the percentage of biomolecules supposed to form the organic coating is completely different, especially comparing the Sm-SeNPs(48) with the ones treated with the harsher conditions (10%SDS+30'boiling). The MIC values of the Sm-SeNPs(48) were measured against four selected strains, two *P. aeruginosa* (PAO1 and BR2), *S. maltophilia* VR20 and *S. aureus* UR1 (Tab.11) and compared to the other types of nanoparticles. Depending on the strain tested, the results obtained evidenced variable MIC values between 16 to 256  $\mu\text{g/ml}$ , generally 1-2 times higher than the values obtained with the untreated Sm-SeNPs.

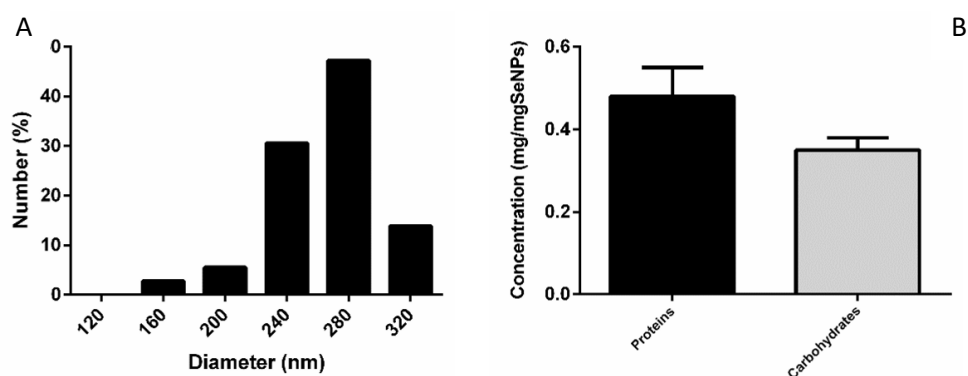


Figure 9. Distribution (A), protein and carbohydrate concentrations (B) of biogenic



SeNPs produced by *S. maltophilia* after 48 h of incubation (average $\pm$ SD; n=3).

#### Antimicrobial activity of the various kinds of selenium nanoparticles

Some of the *P. aeruginosa* strains used for the first part of the study and a number of other bacterial strains belonging to different species were screened for their susceptibility to native and treated SeNPs. This to underline and evaluate the susceptibility to SeNPs among different bacterial species and different bacterial strains among the same species. The selection was made on the basis of the frequent involvement of these strains in infections mediated by biofilm: this is the case of the well-known *P. aeruginosa* and *Burkholderia cenocepacia* and the emergent *Achromobacter xylosoxidans* and *Stenotrophomonas maltophilia* pathogens causing chronic lung infections in cystic fibrosis and other respiratory diseases (Bjarnsholt, 2013). Four strains of *P. aeruginosa* were tested: the clinical isolates from a bronchial lavage BR1 and BR2, the MDR strain *P. aeruginosa* INT and the reference strain PAO1. Two strains of *S. maltophilia* (VR10 and VR20), both isolated from patient affected by low respiratory infections and the *B. cenocepacia* LMG16656 isolated from a patient affected by cystic fibrosis were also included. Finally the *A. xylosoxidans* C strain, from a low respiratory infection, and the *Acinetobacter baumannii* LMG 10531, isolated from a wound infection, were used as representatives of that class of Gram-negative microorganisms which have become challenging to treat due to the increasing appearance of multi drug resistance among these bacterial species (Chan-Tompkins, 2011)

In this second part of the study also Gram-positive species were taken into account. Two *S. aureus* strains were considered: the MDR Mu50, as reference strain, and the clinical isolate from an urine sample UR1. The *S. epidermidis* ET024, clinically isolated from an endotracheal tube, and the *S. haemolyticus* UST1, isolated from a burn wound, were also tested. It is well known that staphylococci are important producers of biofilms associated with infections from medical devices and skin pathologies (Paharik, 2016). Moreover, also the *Propionibacterium acnes* LMG16711 isolated from a human facial acne sample,

was included in the study as another representative of another Gram-negative species.

As shown in Table 11, in accordance to the results obtained in the first part of the study, the MIC values of biogenic SeNPs varied widely among the different microbial species and even among various strains belonging to the same species, ranging from 4 to 64 µg/ml.

Looking at the results is evident that some of the Gram-negative strains tested showed low MIC values ranging from 4 to 16 µg/ml. Is the case of the *P. aeruginosa* PAO1 and BR2 strains, the *B. cenocepacia* LMG16656 and the *A. Baumannii* LMG10531. Five of the nine Gram-negative strains tested showed mild MIC values of 32-64 µg/ml. As regard the Gram-positive strains, the UR1, UST1 and ET024 staphylococci and the *P.acnes* LMG16711 strain showed a very low MIC values form 4 to 16 µg/ml. Only one of the strains tested, the *S. aureus* Mu50, demonstrated the highest MIC value of 128 µg/ml, probably due to the presence of the capsule.

Then, we decided to evaluate the possible effect of removing the SeNP cap, on their antibacterial activity. For this purpose, we tested the antimicrobial effect of the SeNPs as biogenic products and after different denaturing treatments. Data reported in Table 11 showed, for almost all the strains evaluated, a decrease in the SeNP activity with the progressive denaturation of the coat surrounding the nanoparticles, as indicated by progressively higher MIC values.

The antimicrobial activity of Sm-SeNPs(48) was also evaluated to test the bioactivity of SeNPs showing a size similar to that of the completely denatured nanoparticles (treatment 3) but surrounded by the organic cap. What we observe is that the increase in NP size and the induction of the aggregation state, associated to the loss of antibacterial effect, seems to be mediated by the loss of the organic coat surrounding the NPs. In fact, the removal of this coat causes an increase in aggregation and size of NPs, a change in their electric properties (Tab.10) and a loss of the antibacterial activity (Tab.11).

To prove that, we used those strains that have shown the gradually lowest SeNPs activity after various denaturing treatments, namely *P. aeruginosa* PAO1, *P. aeruginosa* BR2, *S. maltophilia* VR20 and *S. aureus* UR1. As reported in Tab.10,

the MIC values were lower than those obtained with completely denatured SeNPs. The experiments conducted with the different denaturant treatments together with the one performed with Sm-SeNP(48) highlighted that the organic coating is in some way involved in the antibacterial activity of NP. The completely denatured NPs are less efficient against the microorganisms tested not only for their bigger dimensions but also for the lack of organic surface elements.

Table 11. MIC of different types of SeNPs against various bacterial strains. Untreated: native biogenic SeNPs; Treatment 1: 10% SDS; Treatment 2: 10% SDS+10 min boiling; Treatment 3: 10% SDS+30 min boiling, Sm-SeNPs(48): SeNPs obtained after 48 h of incubation.

Bacterial species	Strain name	MIC $\mu\text{g/ml}$				
		Untreated SeNPs	Treatment 1	Treatment 2	Treatment3	Sm-SeNPs(48)
<i>P. aeruginosa</i>	PAO1	8	16	128	64	16
<i>P. aeruginosa</i>	INT	64	512	>512	>512	-
<i>P. aeruginosa</i>	BR1	32	64	32	64	-
<i>P. aeruginosa</i>	BR2	8	16	32	128	32
<i>S. maltophilia</i>	VR10	32	16	32	64	-
<i>S. maltophilia</i>	VR20	64	256	512	>512	256
<i>A. xylooxidans</i>	C	64	>512	>512	>512	-
<i>B. cenocepacia</i>	LMG16656	16	16	32	32	-
<i>A. baumannii</i>	LMG10531	8	16	32	128	-
<i>S. aureus</i>	Mu50	128	128	256	512	-
<i>S. aureus</i>	UR1	4	16	32	64	16
<i>S. haemolyticus</i>	UST1	16	8	32	64	-
<i>S. epidermidis</i>	ET024	4	8	16	64	-
<i>P. acnes</i>	LMG16711	8	8	16	32	-
<i>C. albicans</i>	SC5314	64	128	>512	>512	-

### Anti-biofilm effect of untreated and treated SeNPs

Subsequently, the anti-biofilm effect of the different types of SeNPs, either as native products or after various denaturant treatments, was evaluated. These experiments were conducted on a selection of strains, namely three strains of *P. aeruginosa* (PAO1, BR1 and BR2), the *B. cenocepacia* LMG16656 strain and the *S. haemolyticus* UST1 strain. These were chosen on the basis of their low MIC values and the fact they are efficient biofilm formers. On the other hand, the methicillin-resistant and vancomycin-intermediate (VISA) strain *S. aureus* Mu50 was also examined, being resistant to antibiotics and SeNPs. Based on the results obtained in the first part of this whole study, the anti-biofilm activity of the different NP types was tested using a selenium nanoparticles concentration representing the lowest concentration having a significant effect on biofilm formation (128 µg/ml).

First the total biofilm biomass was quantified using crystal violet (CV) staining. The CV stain measured the total biofilm biomass grown, in the case of the strains tested, on the bottom and on the walls of the microwells. Then, the number of culturable cells (colony forming units/ml, CFU/ml) still present within the biofilms was determined after their removal and plating on a growth medium. For all *P. aeruginosa* strains, exposure of biofilms to 128 µg/ml of various types of SeNPs resulted in a clear decrease in the CV signal: this was more pronounced with untreated SeNPs than with completely denatured SeNPs (Fig.10A). The number of culturable cells per ml of *P. aeruginosa* PAO1 decreased significantly after treatment with all kind of SeNPs tested except when completely denatured NPs were used (Fig.10B); the number of CFU/ml recovered from *P. aeruginosa* BR1 and BR2 biofilms decreased significantly only when exposed to the untreated SeNPs (Fig.10B) that showed the highest bactericidal activity with a reduction of 5-2 log<sub>10</sub> CFU/ml, depending on the strain considered. A particularly interesting case is that of *B. cenocepacia* LMG16656, which produces a very susceptible biofilm that is completely disaggregated by all the SeNP types, including completely denatured nanoparticles. Also the number of culturable cells recovered from these biofilms was, in any experimental condition, significantly lower than the control biofilms (Fig.11). Regarding the untreated SeNPs we

obtained a 7 log<sub>10</sub> reduction in the number of cells still present in the biofilm after challenging, while for the other types of NPs the number of CFU/ml is reduced by about 3 logarithms.

Despite its low susceptibility to the action of SeNPs in the planktonic state (MIC of 128 µg/ml), the Mu50 strain of *S. aureus* produced a biofilm matrix easily degradable by any type of SeNPs. The results showed a decrease in the number of culturable biofilm bacterial cells after treatment with the untreated nanoparticles with a significant difference of 5 log<sub>10</sub> if compared to the control. The reduction in the number of CFU/ml is progressively less evident when treated SeNPs were applied. Surprisingly, the *S. haemolyticus* UST1 represented a different case, as we can see from the figure is possible that this strain synthesizes a very SeNP-resistant biofilm and showed no decrease in the culturable cell number after any nanoparticle treatment (Fig.11).

Comparing the effects on biofilm biomass and cell viability between the different types of SeNPs tested (Fig.10 and 11) it is evidenced a significant difference not only referred to the control but also among the various denaturing treatment applied to the NPs. In all the strains tested, except for the *S. haemolyticus* UST1 strain, the progressive loss of the biomolecular cap on the surface on NPs is related to a progressive loss of their antimicrobial activity demonstrated by an increasing value of CV signal and increasing number of CFU/ml. The statistic analysis reported, indeed point out a significant difference especially between the antimicrobial activity of the untreated NPs and the ones exposed to the harsher denaturing treatment (Treatment 3) able to remove and denature the majority of the capping molecules present on the surface of the nanoparticles.

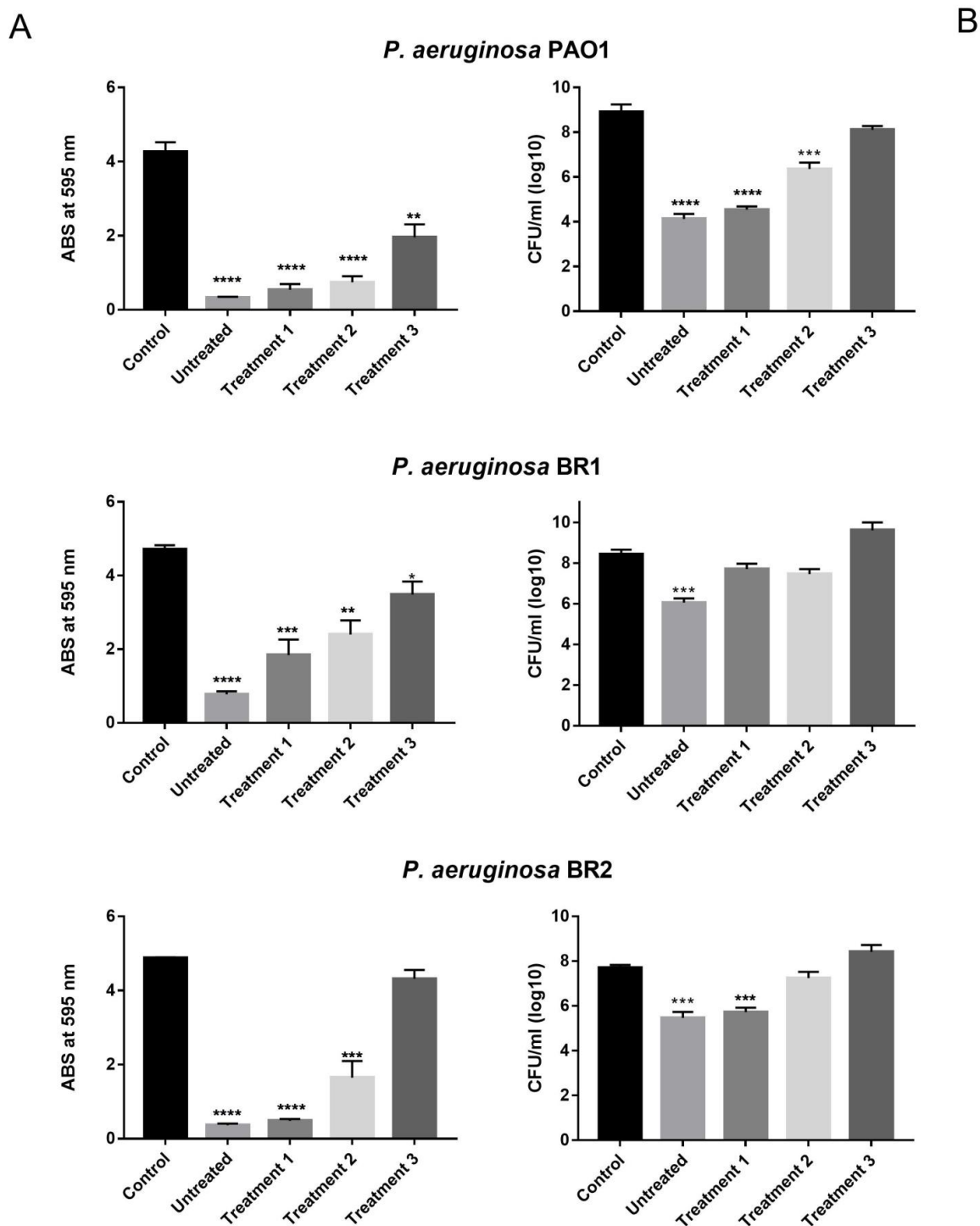


Figure 10. Anti-biofilm activity of different types of SeNPs measured by CV staining (effect on biofilm biomass) (A) and colony counting (effect on cell viability) (B), compared to a biofilm grown in the absence of SeNPs (Control) as regard *P.aeruginosa* strains PAO1, BR1 and BR2 (n=3, Average  $\pm$ SEM;  $p < 0.05$ ).

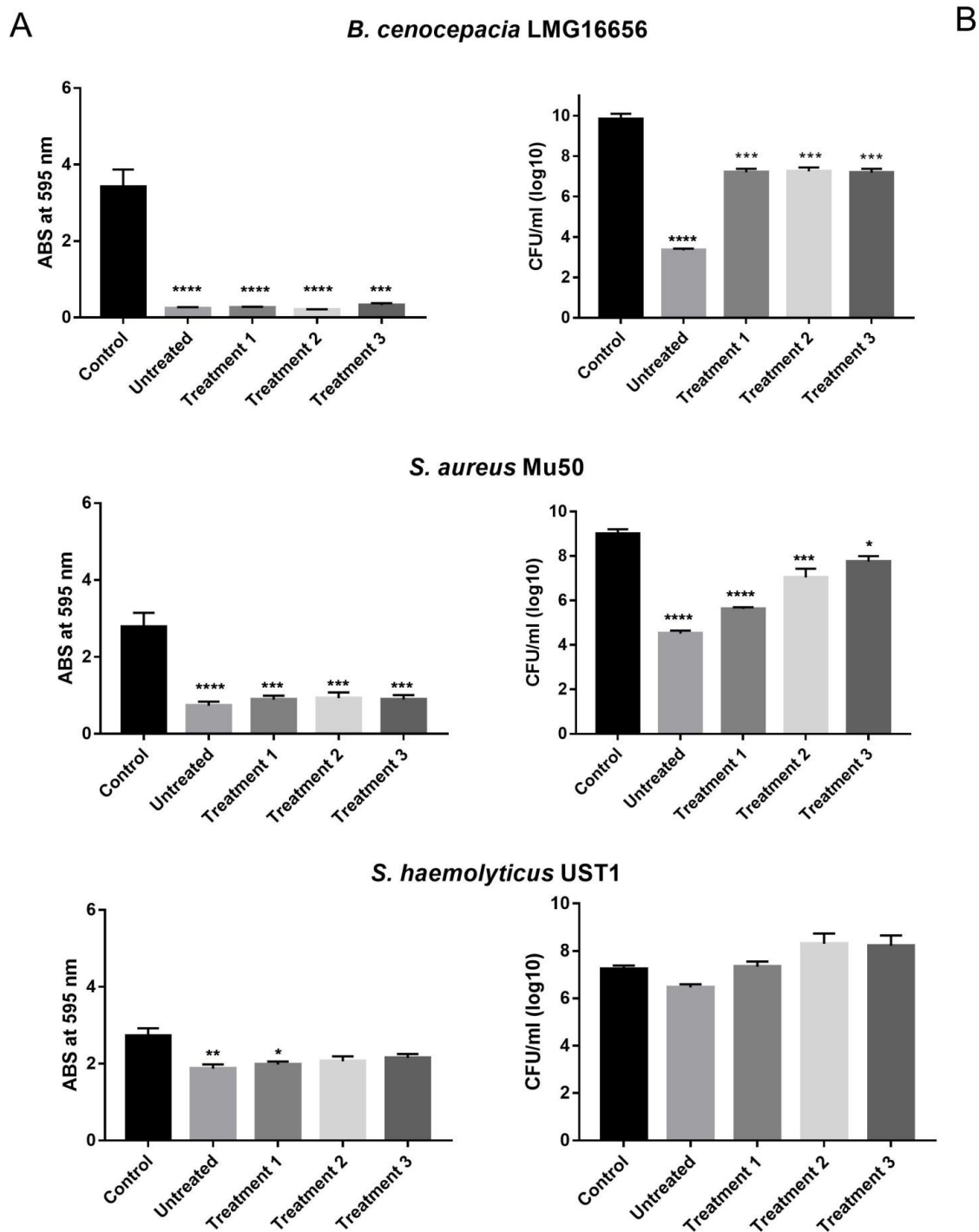


Figure 11. Anti-biofilm activity of different types of SeNPs measured by CV staining (effect on biofilm biomass) (A) and colony counting (effect on cell viability) (B), compared to a biofilm grown in the absence of SeNPs (Control) as regard *B. cenocepacia* LMG 16656, *S.aureus* Mu50 and *S. haemolyticus* UST1 (n=3, Average  $\pm$ SEM;  $p < 0.05$ ).

### Fluorescence microscopy

In Figure 13 are reported the images of different biofilms observed at fluorescence microscope after staining with *Live/Dead* dye. Comparing the control biofilms to the treated with 128  $\mu\text{g/ml}$  of Sm-SeNPs(-) we can clearly notice that the structure of the biofilm matrix is completely different in the treated ones. The major difference seems to be in the number and not in the viability of cells still remaining in biofilms: as reported by CV assay there was a clear decrease in the staining signal but not in cell viability. Even if there was a lower number of cells they are still able to replicate on the growth medium (CFU/ml).

### Ros production

The production of reactive oxygen species (ROS) in response to SeNPs treatment was analysed in the three selected strains *P. aeruginosa* PAO1, *S. aureus* Mu50 and *B. cenocepacia* LMG16656. As shown in Figure 12, for all bacterial strains tested there was an increase in the quantity of ROS produced after treatment with biogenic nanoparticles compared to the untreated controls. Reactive oxygen species are important elements in the bacterial response to lethal stress and have been associated with the killing action of multiple antimicrobial agents (Van Acker, 2017).

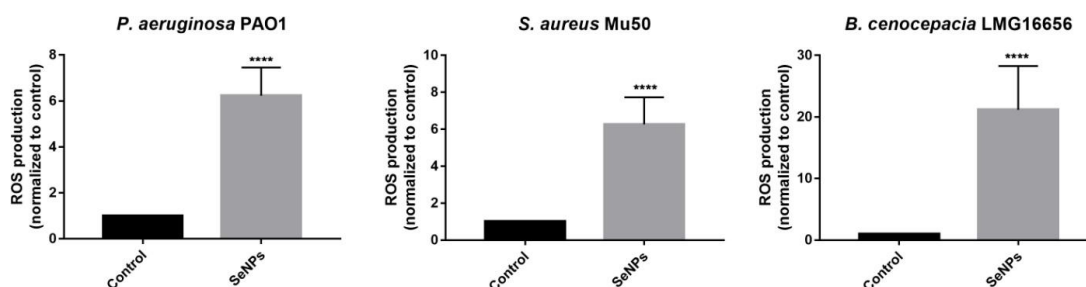


Figure 12. Formation of ROS in *P. aeruginosa* PAO1, *B. cenocepacia* LMG16656, *S. aureus* Mu50 planctonic cells exposed to 128  $\mu\text{g/ml}$  of SeNPs for 24 hours normalized to cells not exposed to NPs (Control) (n=3; Average  $\pm$  SEM; p<0.05).



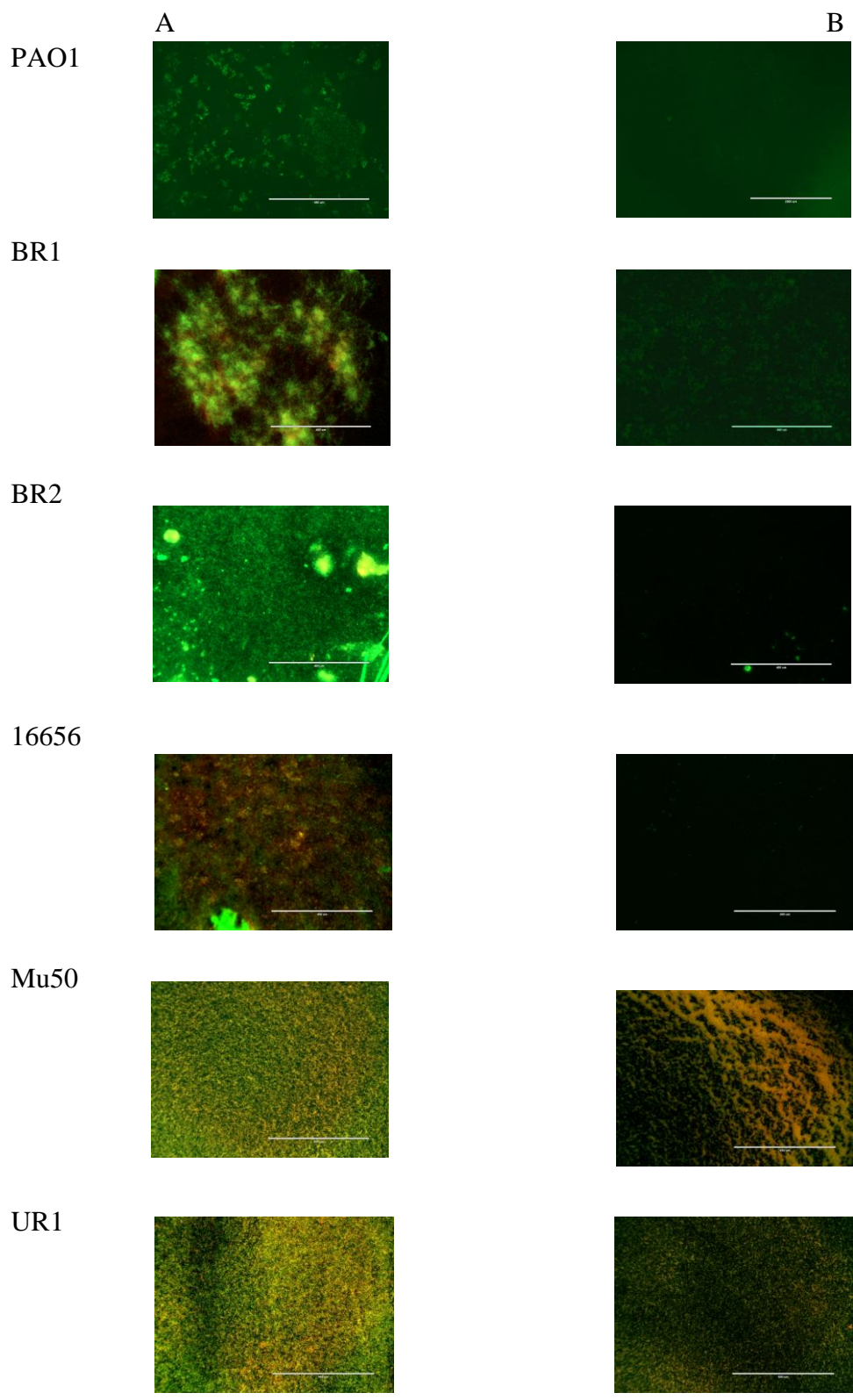


Figure 13. Fluorescence microscopy images of different bacterial biofilms treated with 128  $\mu\text{g/ml}$  Sm-SeNPs(-) (B) compared to a non treated control (A).

### 5.3 EVALUATION OF THE POSSIBLE SYNERGIC EFFECT OF BIOGENIC SELENIUM NANOPARTICLES AND ANTIBIOTICS

Then we investigated the possible in vitro synergistic antibacterial and antibiofilm activities of biogenic Sm-SeNPs(-) in combination with some conventional antibiotics. For this part of the study we focused our attention on those strains that showed the greater antibiotic resistance and we compared them to reference strains belonging to the same bacterial species. Specifically, we analyzed the *P. aeruginosa* INT strains, isolated from an human urine sample. This strain was considered particularly relevant showing the presence of a class 1 integron, that confer resistance to a large panel of antibiotics. A second interesting strain used was the *S. aureus* Mu50 strain, originally isolated from a burn wound and considered a reference strain, was selected being a Vancomycin Intermediate- and Methicillin-resistant. *P. aeruginosa* PAO1 and *S. aureus* UR1 (isolated from an urine sample and showing a great antibiotic susceptibility) were also included in the study.

The strains selected were first tested for their antibiotic susceptibility against various antimicrobial drugs, commonly used in the clinical practice. Among those compound we highlighted the one to whom the strains tested showed a resistance. For *Pseudomonas* strains Clarithromycin, a protein synthesis inhibitor, Tobramycin, a protein synthesis inhibitor frequently used in patient affected by Cystic Fibrosis, and Trimethoprim/Sulfamethoxazole, an inhibitor of folate synthesis, were used. For *S. aureus* strains we selected Levofloxacin, an inhibitor of DNA replication, Oxacillin and Vancomycin, two inhibitor of the synthesis of bacterial cell walls. Usually, the resistance to Oxacillin correlates with the resistance to the whole class of  $\beta$ -lactams.

The FIC index of Sm-SeNPs(-) and the various antibiotic combination were summarized in Tables 12 and 13. Nanoparticles were able to potentiate the effect of Clarithromycin against *P. aeruginosa* PAO1 strain ( $FIC \leq 0.5$ ) and partially potentiate the effect of Trimethoprim/Sulfamethoxazole and Tobramycin ( $FIC \leq 1$ ) (Tab.12). The antibiotic effect of the three different agents tested against *P. aeruginosa* INT strain is partially potentiated by the combination with NPs ( $0.5 \geq FIC \leq 1$ ). As regard the *S. aureus* strains, for both Levofloxacin and Vancomycin

there is a synergistic activity ( $FIC \leq 0.5$ ) with SeNPs (Tab.13). On the contrary, the combination of SmSeNPs and Oxacillin, results in a partial synergic or additive effect for *S. aureus* UR1 and Mu50 respectively.

Table 12. Fractional inhibitory Concentration (FIC) index of *P. aeruginosa* PAO1 and INT strains for the combination of Sm-SeNPs(-) and Clarithromycin, Tobramycin and Trimethoprim/Sulfamethoxazole (n=3).

Bacterial strain	Clarithromycin		Tobramycin		Trimethoprim/Sulfamethoxazole	
	FIC index	Outcome	FIC index	Outcome	FIC index	Outcome
<i>P. aeruginosa</i> PAO1	0.5	Synergy	1	Additive	1	Additive
<i>P. aeruginosa</i> INT	0.56	Partial synergy	0.75	Partial Synergy	1	Additive

Table 13. Fractional inhibitory Concentration (FIC) index of *S. aureus* Mu50 and UR1 strains for the combination of Sm-SeNPs(-) and Levofloxacin, Oxacillin and Vancomycin (n=3).

Bacterial strain	Levofloxacin		Oxacillin		Vancomycin	
	FIC index	Outcome	FIC index	Outcome	FIC index	Outcome
<i>S. aureus</i> Mu50	0.5	Synergy	0.6	Partial Synergy	0.5	Synergy
<i>S.aureus</i> UR1	0.5	Synergy	2	Additive	0.5	Synergy

#### Antibiofilm activity of different combination of SeNPs and antibiotics

The antibiofilm activity of different combinations of antibiotics and nanoparticles was tested using a concentration of 128  $\mu\text{g/ml}$  of SeNPs, considered the lowest concentration having a significant effect on biofilm formation, as previously

demonstrated, combined to a concentration 2×MIC of CLA (Clarithromycin) and TRIM (Trimethoprim/Sulfamethoxazole) for *P. aeruginosa* strains. Antimicrobial activity of 128 µg/ml SeNPs against *S.aureus* strains was tested in addition to 2×MIC of both LEV (Levofloxacin) and VAN (Vancomycin). The concentration of antibiotics used was decided basing on the idea that the tolerance of mature biofilms against most antimicrobial agents is often many times higher, if compared with their planktonic counterpart (Bjarnsholt, 2013). We decided to combine the SeNPs and antibiotics at the same time because in previous experiments (data not shown) we tested the activity of a 2 h NPs treatment followed by a 22 h treatment of antibiotic with no significant reduction neither in biofilm biomass nor in cell viability.

First, the biofilm biomass was quantified using Crystal Violet staining (CV assay). Then the number of culturable cells (CFU/ml) still present in the mature biofilms after treatment, was quantified by plating on TSA growth medium. The results obtained for *P. aeruginosa* biofilms (Fig.14) showed that this reference strain was more susceptible to SeNPs than to CLA and TRIM, resulting in a clear disaggregation of mature biofilm with a low value of CV signal and a significant decrease in the number of CFU/ml. It is interesting to notice that the antibiofilm activity of antibiotics combined with NPs is very similar to the one of the SeNPs alone and more pronounced than the one of the antibacterial agents alone. Particularly interesting is the case of the multi-drug resistant *P. aeruginosa* INT strain: despite the low susceptibility to antibiotics due to the carrying of a class 1 integron, the combination with SeNPs potentiate the antibacterial activity with a clear reduction in the biofilm biomass (CV signal) and in the number of CFU/ml (Fig.14) with a significant difference of 2-3 log<sub>10</sub> compared to the non treated control and compared to the SeNPs or CLA/TRIM alone. The combination with SeNPs do not exhibit a synergistic antibiofilm effect, the activity of the combination of NPs and antimicrobial drugs is very similar to the one of nanoparticles alone. Thus suggesting that the SeNPs can be considered a more potent antibiofilm agent than the common antimicrobial drugs. Very relevant are the results regarding the MRSA and VISA strain Mu50 (Fig. 15) where we can observe that the SeNPs had greater effect on the biofilm than the antibiotic alone.

Also the combination between the two, seemed to be more effective than the antibiotic treatments. Figure 15 shows the effect of Levofloxacin or Vancomycin and SeNPs as well as their combination, on 24 h old *S. aureus* biofilms. The NPs alone had substantial effect on *S. aureus* Mu50 and UR1 biofilms but no effect is reported when treated with LEV or VAN alone.

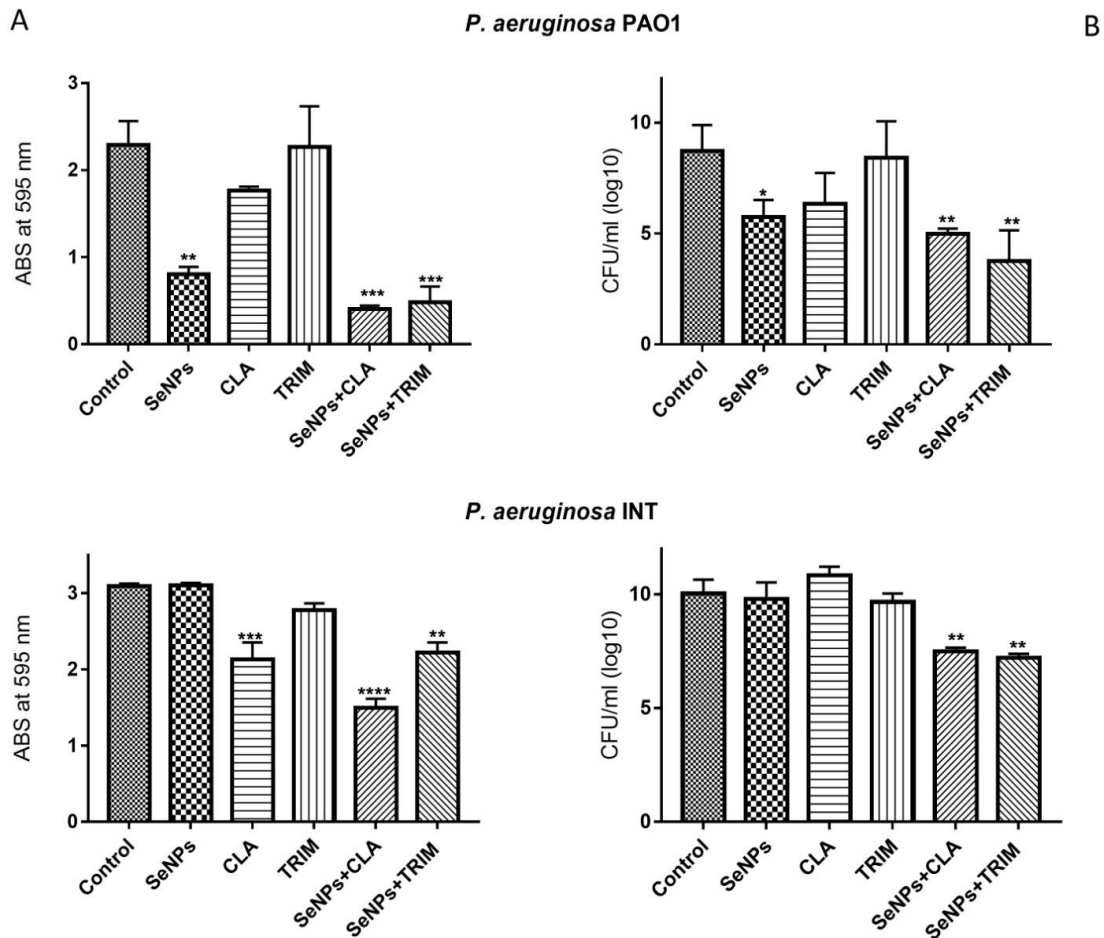


Figure 14. Antibiofilm activity of SeNPs (128 µg/ml) alone and in combination with *Clarithromycin* (1024 µg/ml) and *Trimethoprim/Sulfamethoxazole* (160 µg/ml for *P. aeruginosa* PAO1 and 640 µg/ml for INT strain respectively) measured by CV staining (effect on biofilm biomass) (A) and colony counting (effect on cell viability) (B), compared to a control biofilm (n=3, Average ±SEM; p<0.05).

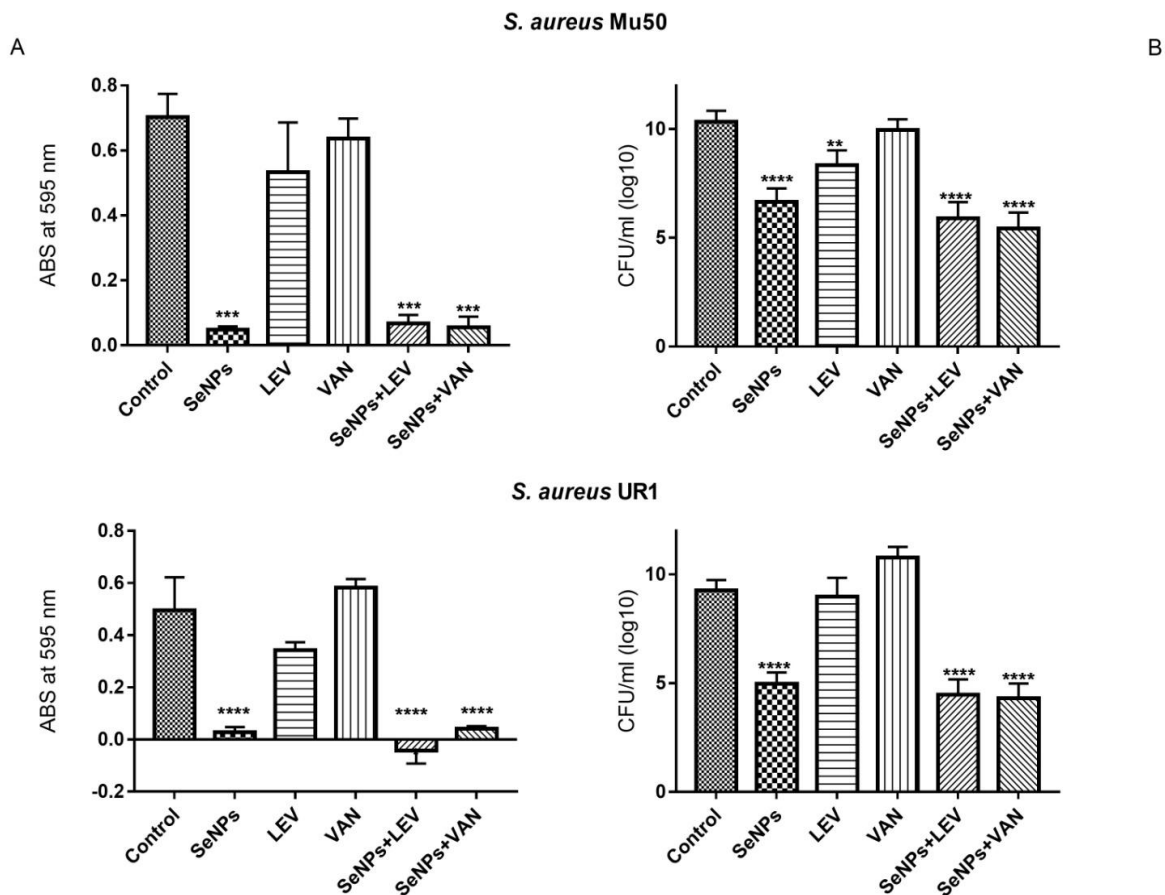


Figure 15. Antibiofilm activity of SeNPs (128  $\mu\text{g/ml}$ ) alone and in combination with *Levofloxacin* (16  $\mu\text{g/ml}$ ) and *Vancomycin* (2  $\mu\text{g/ml}$ ) measured by CV staining (effect on biofilm biomass) (A) and colony counting (effect on cell viability) (B), compared to a control biofilm, as regard *S.aureus* Mu50 and UR1 strains (n=3, Average  $\pm$ SEM; p<0.05).

#### 5.4 EVALUATION OF THE ANTIBIOFILM ACTIVITY OF BIOGENIC Sm-SeNPs(-) IN COMPLEX “IN VITRO” AND “IN VIVO” MODELS

##### Chronic wound model

The in vitro model used in this study displays specific aspects of wound biofilms, mimicking the real conditions in chronic wound and soft tissue infections having a surface consisting of hyaluronic acid and collagen (representing the nutritional

conditions present in an infection site). Biofilms were grown on artificial dermis (AD) as previously described (Fig.16). We decided to focus our attention on two *S. aureus* strains, the MRSA Mu50 strain (considered as a reference strain) and the clinical isolate UR1 as they belonged to a bacterial species recurrent in chronic wound and ulcers infections (Wang, 2017). Then we decided to include also *P. aeruginosa* PAO1 strain, as representative of Gram-negative bacteria.

The biofilm inhibiting and eradicating activity of Sm-SeNPs(-) was tested using the concentration of 128 µg/ml. Results were reported in Figure 17. For all the strains tested and in both inhibiting and eradicating activity the number of bacterial cells (CFU/dermis) still present in the biofilms after treatment with NPs were no significantly different from the untreated control. Indicating that in this model Sm-SeNPs(-) have no effectively antibiofilm activity. Then we decided to increase the concentration of NPs used to treat the different biofilms. Also using the highest dose of 256 µg/ml of SeNPs, no relevant antibiofilm activity was detected for all the strains tested (data not shown).

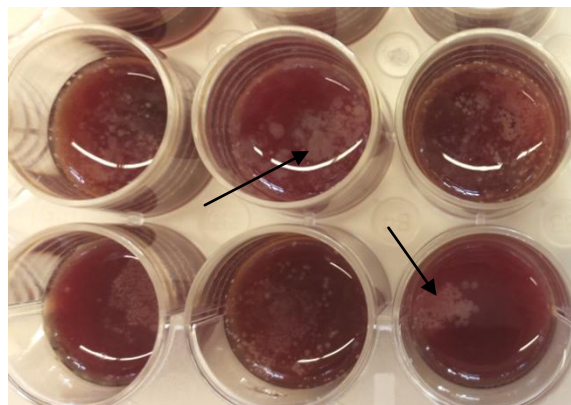


Figure 16. AD infected with *S. aureus* Mu50. Arrows indicate the bacterial biofilm formed on the surface of the dermis after 24h of incubation at 37 °C.

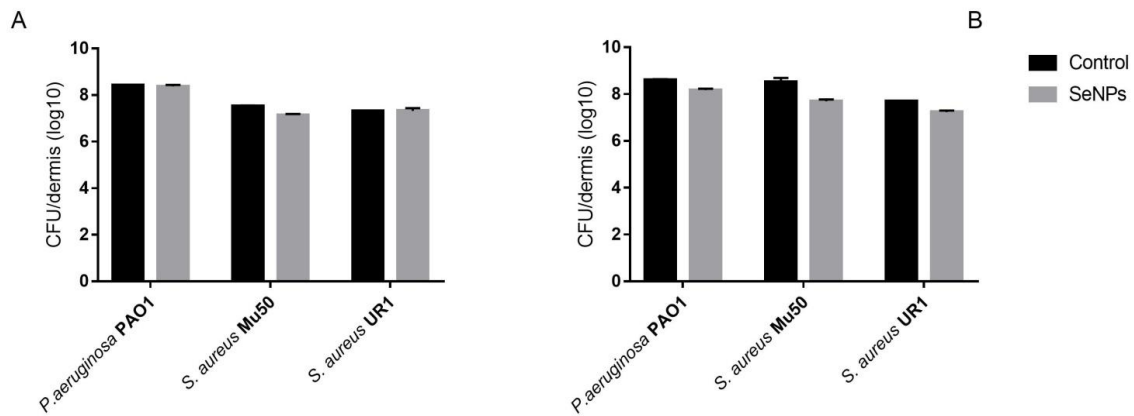


Figure 17. Biofilm inhibitory effect (A) and biofilm eradicating effect (B) of 128 µg/ml Sm-SeNPs(-) on *P. aeruginosa* PAO1, *S. aureus* Mu50 and *S. aureus* UR1 mature biofilms. Results were expressed as log CFU/dermis (mean ± SEM; n=3; p< 0.05) and compared to an untreated control.

Biofilms grown on AD were also stained with *Live/Dead* staining as described in “Material and Methods” and directly poured on their surface. After the incubation period the AD was overturned and the surface covered by the biofilm observed at the fluorescence microscope (Fig. 18). The observation was only possible for the *S. aureus* strains because in the case of *P. aeruginosa*, during the infection process the bacterial cells are able to produce an anticoagulant enzyme able to liquefy the dermis. Here, we reported two pictures about the Mu50 strain (Fig.18). The treated biofilm appeared different in shape but the cells green fluorescence emission suggest that they are still alive after treatment with SeNPs (Fig.18B). This data was confirmed by the colony counting (Fig.17).

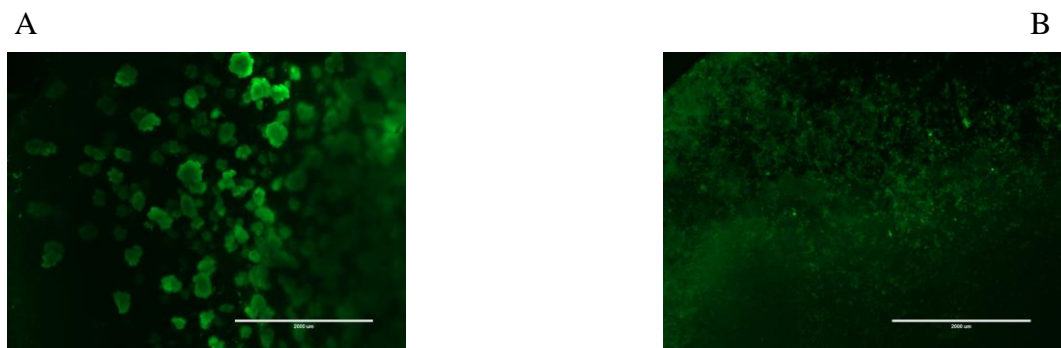


Figure 18. Observation at fluorescence microscope of AD infected by *S. aureus* Mu50 biofilm compared to an infected AD treated with Sm-SeNPs.



Trying to hypothesize a possible explanation for this lack of activity of SeNPs, we decided to test the antimicrobial activity of Sm-SeNPs(-) against the three strains considered using the TSB medium enriched with fresh plasma, one of the components of the used to prepare the medium necessary for the infection protocol. The MIC values obtained were then compared to the ones previously calculated using simple TSB medium. From the results (Tab.14) is evident that a medium added with plasma can interfere with the antimicrobial activity of SeNPs probably binding to some of the component of the organic layer surrounding the surface on NPs. Thus resulting in a 2-4 times increase of the MIC values. From the literature we have examples reporting the different activity of metal nanoparticles depending on the type and the composition of the medium used, that in some cases, could affect the toxicity of NPs (Loza, 2014).

Table 14. Minimum inhibitory concentration values of Sm-SeNPs(-) calculated using the tryptone soy broth (TSB) medium enriched with plasma compared to the simple medium.

	<b>Sm-SeNPs(-) MIC µg/ml</b>	
	<b>TSB</b>	<b>TSB+Plasma</b>
<i>P. aeruginosa</i> PAO1	8	32
<i>S. aureus</i> Mu50	64	>512
<i>S. aureus</i> UR1	4	256

### Flow cells

Due to their complexity, natural microbial communities and biofilms have been challenging objects of investigation also because they are often located at places that are difficult to access, which makes a direct and continuous examinations very difficult (Pamp 2009). To reduce complexity and facilitate investigations under controlled and reproducible laboratory conditions, a number of complex biofilm model systems have been established, including the flow-cell-grown

biofilms, whose setup allow the cultivation of biofilms under continuous hydrodynamic conditions.

*Pseudomonas aeruginosa* is an opportunistic human pathogen especially adept at forming surface-associated biofilms including catheter-associated urinary tract infection and ventilator-associated pneumonia (Cole, 2014). To test the antibiofilm activity of SeNPs in this complex *in vitro* model, we decided to focus our attention on two strains of *P. aeruginosa*: the reference strain PAO1 and the multi-drug resistant strain named INT, isolated from a human urine sample.

Bacterial suspensions were inoculated in the flow-cell-grown model as previously described and the biofilm was allowed to grow for 3 days under a continuous flow of medium. Then, the biofilm formed inside the flow chamber was treated with a continuous flow of 128 µg/ml of Sm-SeNPs(-). At the starting time (Time point 0) and during the treatment (at 1, 4 and 24 h) a sample of the effluent was collected and the number and the viability of the cells (CFU/ml) released by the mature biofilm during the treatment with NPs was evaluated. From our results (Fig.19) we can observe that during the 24 hours of treatment a constant number of cells was released by the control biofilm. Regarding the 4-old-days biofilms treated with SeNPs (Fig.19) there is a release of a lower number of culturable cells during the time of the treatment. This result can be probably explained considering that NPs are able to kill part of the bacterial cells that compose the biofilm.

After 24 h of treatment with SeNPs the number of cells (CFU/ml) still present in the biofilms were determined both by conventional plating on TSA medium and microscopy and compared to an untreated control. The chamber used in the flow model was formed by two glass slides, the upper one was scratched and used to collect the biofilm after treatment with SeNPs, considered the one formed by bacterial cells that can actively bind the glass surface. The other glass slide was used for microscopy analysis.

The results in Figure 20 confirmed the data previously reported indicated that the treatment of *P. aeruginosa* biofilms with a continuous flow of Sm-SeNPs(-) results in a killing of bacterial cells with a significant reduction in the number of colony forming unit. Is interesting to notice that, regarding the drug-resistant INT

strain, in this model the NPs seems to have an higher antibiofilm activity if compared to the results obtained in the *in vitro* microtiter plate assays. This is probably due to a different conformation of the biofilm structure formed inside the flow chamber compared to the one on the bottom of the microwells. The incessant supply of nutrients brought by the fresh medium could lead to the formation of a less resistant biofilm matrix, more sensitive to the NPs antimicrobial activity.

The observation of *P. aeruginosa* PAO1 and INT biofilms at fluorescence microscope, after *Live/Dead* staining, highlighted the presence of a large number of dead cells (red staining) in biofilms of both strains tested, if compared to the untreated control.

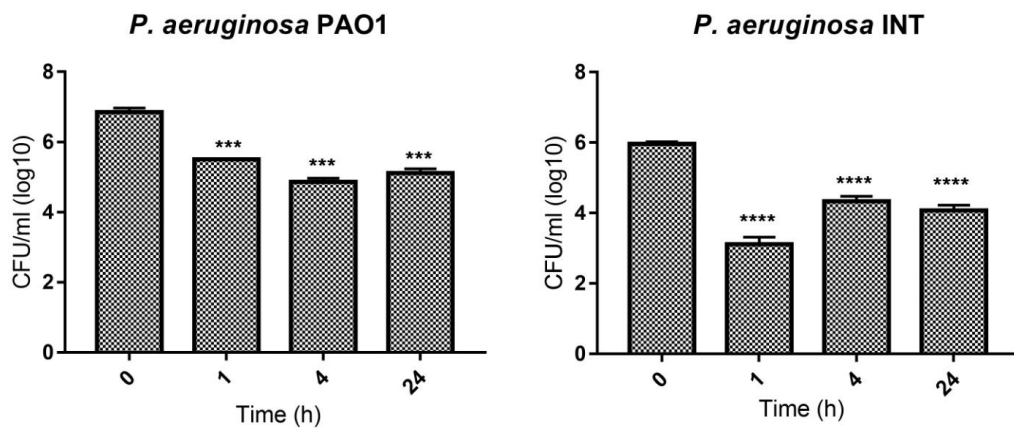


Figure 19. Antibacterial activity of Sm-SeNPs(-) evaluated by collecting the effluent from the flow chamber system during the 24 h of treatment. The number of CFU/ml is compared to the one of the time point zero that can be considered as a control (mean±SEM, n=3, p<0.05).

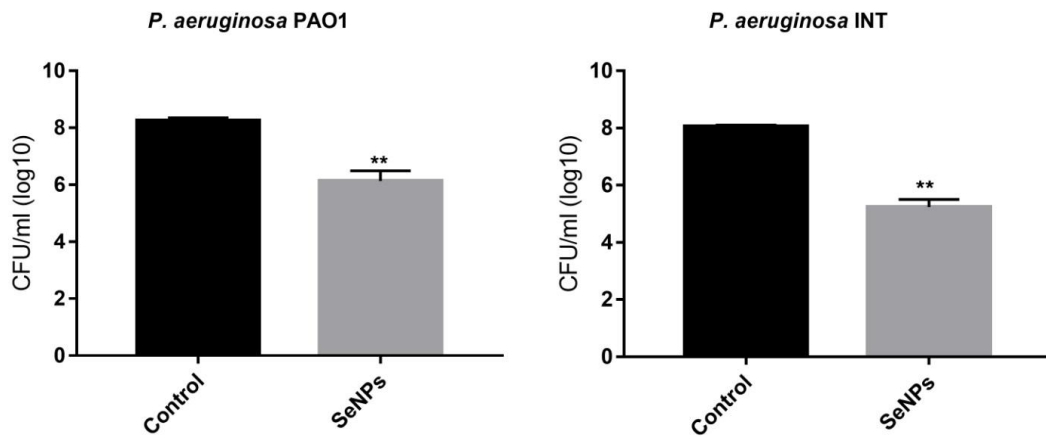


Figure 20. Antibiofilm activity of Sm-SeNPs(-) measured by CFU/ml counting (cell viability). Four days-old *P. aeruginosa* PAO1 and INT biofilms were treated for 24 h with a continuous flow of 128  $\mu\text{g/ml}$  per minute (mean  $\pm$ SEM, n=3,  $p < 0.05$ ).

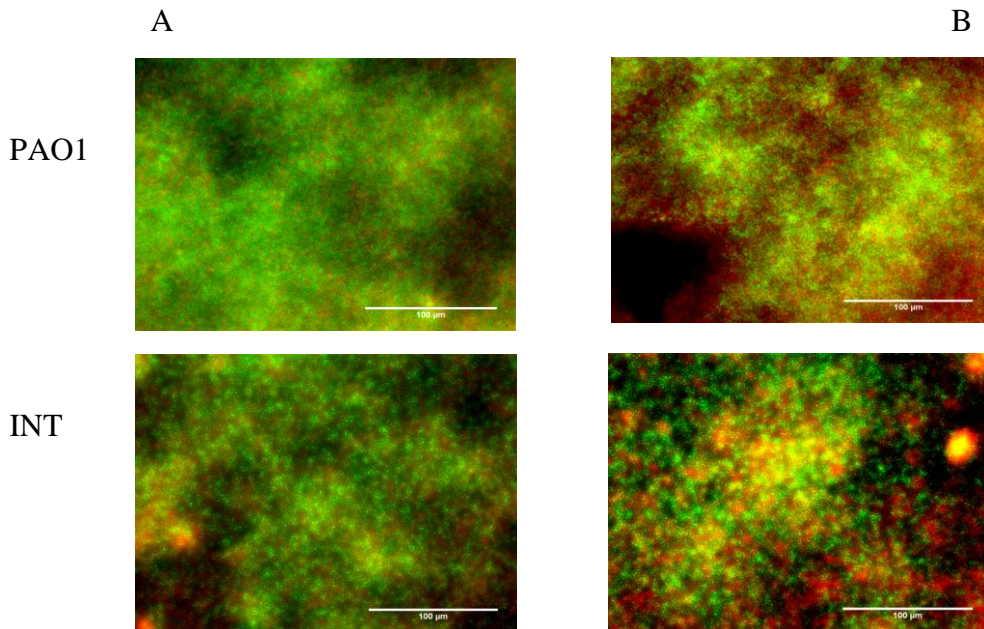


Figure 21. *P. aeruginosa* PAO1 and INT 4 days old biofilms stained with *Live/Dead* dye. The mature biofilms treated for 24 h with a continuous flow of 128  $\mu\text{g/ml}$  (B) were compared to a non treated control (A).

As we can see from Figure 21 the structure of the control biofilm and the treated one appeared very similar but with a number of live cells (green) apparently different. After the treatment with SeNPs most of the cells still present in *P. aeruginosa* PAO1 and INT biofilms seemed to be dead (red staining). This results confirmed the ones obtained by counting the CFU/ml (Fig.20) after removal of the biofilms in the flow chambers and plating on a growth medium.

### *Caenorhabditis elegans*

*C. elegans* strain N2  $\Delta$ glp-4  $\Delta$ sek-1 was used. Nematodes were cultured as previously described in the “Materials and Methods” section and infected with *P. aeruginosa* PAO1 (Fig.22), *S. aureus* Mu50 and *S. haemolyticus* UST1 strains. Table 15 shows the percentage of survivor of the nematodes after 24 h after treatment with 128  $\mu$ g/ml of Sm-SeNPs(-). As we can clearly see the percentage of survivor is very low (less than 20%) for all the strains considered if compared to the non treated control (survivor of 100%).

After that we decided to treat *C. elegans* with different concentrations of SeNPs to see if the NPs alone had a toxic effects on warms viability (Tab.16). After 24 h of treatment we had only 2% of viability in nematodes challenged with 128  $\mu$ g/ml, which is the lowest concentration having a relevant *in vitro* antibiofilm activity (Fig.22). After 48 h of treatment this percentage is reduced to zero. On the contrary, as we can see form Table 16, with lower concentration the viability of *C. elegans* at 24 and 48 h is higher, with a percentage ranging from 90 to 100% at the lowest concentration tested (1-8  $\mu$ g/ml).

From our results we can conclude that the concentration of 128  $\mu$ g/ml of Sm-SeNPs(-) used to treat *C. elegans* infected with *P. aeruginosa* PAO1, *S. aureus* Mu50 and *S. haemolyticus* UST1 was to high resulting in a completely killing of the warms due to a possible toxic effect of the SeNPs and not to the infection process. The concentration that appeared non toxic for the *C. elegans* model were considered too low to have an antimicrobial or antibiofilm activity.

Table 15. Percentage of survivor of *C. elegans* infected with *P. aeruginosa* PAO1, *S. aureus* Mu50 and *S. haemolyticus* UST1, after treatment with 128 µg/ml Sm-SeNPs (-) for 24 h (n=2; average±SEM).

<i>P. aeruginosa</i> PAO1	<i>S. aureus</i> Mu50	<i>S. haemolyticus</i> UST1
2.8±2.7 %	0.4±1.2 %	13.6±2.7 %

Table 16. Percentage of survivor of *C. elegans* after 24 and 48 h of treatment with different concentration of Sm-SeNPs(-) (n=3; average±SEM).

TIME	SeNPs µg/ml							
	1	2	4	8	16	32	64	128
24H	100	100±2	100±0.5	92.8±3	100±4.5	98.6±0.5	95.2±3	2.8±13.5
48H	100	94.1±2.12	92.8±0.3	94.1±2.12	84.6±3.8	84.4±0.3	12.8±2.1	0

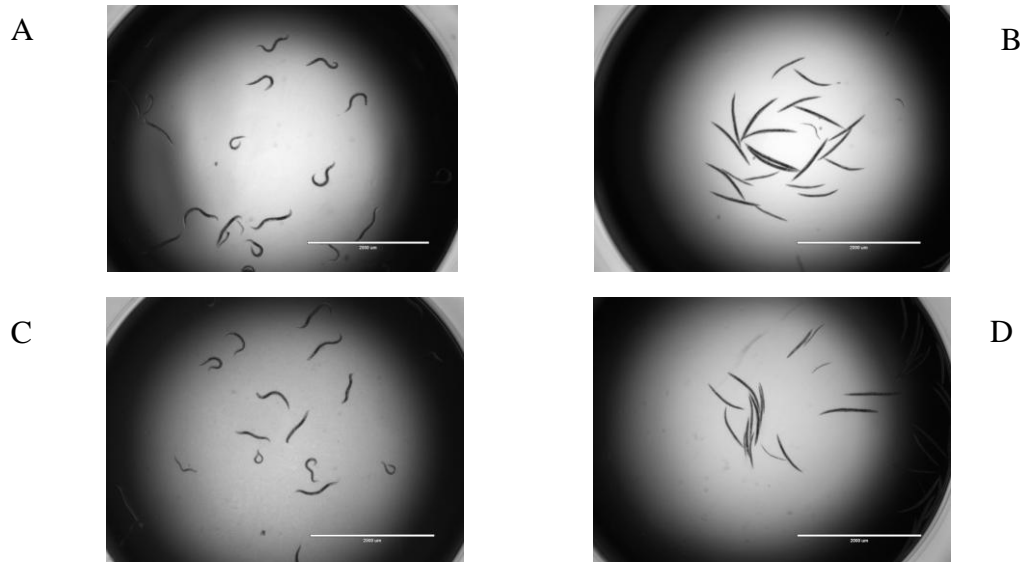


Figure 22. Microscope images of *C. elegans* nematodes uninfected and treated with 128 µg/ml of Sm-SeNPs(-) (B), infected with *P. aeruginosa* PAO1 (C), infected with PAO1 strain and treated for 24 h with 128 µg/ml of SeNPs,

compared to an uninfected and untreated control (A). At the end of the assay, worms were considered dead if they were straightened and if no movement was observed.

#### *Mouse model*

A number of 9 WT and 9 CF mice were intra-tracheally challenged with different concentrations (50µg/ml, 500 µg/ml and 5 mg/ml) of Sm-SeNPs and monitored for the 5 days after the treatment for the onset of toxic effect in term of viability, motility and adverse reaction to the administration of NPs. No toxic effect were detected in the treated mice compared to a control group intra-tracheally challenged with PS.

### **5.5 POSSIBLE TOXIC EFFECTS OF BIOGENIC SELENIUM NANOPARTICLES ON HUMAN DENDRITIC CELLS AND FIBROBLASTS**

#### *Evaluation of cell viability*

The biogenic SeNPs used in this study contain organic substances of bacterial origin, so it was necessary to determine whether they can damage human cells, or stimulate unanticipated effects in immune system cells. From the literature we have different examples of nanoparticles responsible for human cell stimulation and cytotoxicity (Di Gioacchino, 2011; Chang, 2010). We therefore investigated whether Sm-SeNPs(-) and Bm-SeNPs(+) affected the viability and activity of human dendritic cells (DCs), immune system components fundamentally involved in the inflammatory and immune response process (Schakel, 2009; Granucci, 2008). Ch-SeNPs, lacking biogenic molecules, were also tested and compared to the biogenic ones. Human blood monocytes were cultured for 5 days in the presence of Granulocyte-Colony Stimulating Factor (GM-CSF) and Interleukin 4 (IL-4) to obtain DCs, which were then challenged with different doses of SeNPs

or with the bacterial immunostimulator LPS, as a positive control. The effect of SeNPs on the viability and activity of cultured human fibroblasts was also analysed to determine whether SeNPs have adverse effects on non-immune cells. Cell viability was assessed using *Alamar blue*, a colorimetric redox assay of metabolic activity. Different concentrations of both biogenic and chemically synthesized SeNPs did not induce apoptosis in cultured DCs or fibroblasts, even at the highest dose of 500  $\mu\text{g/ml}$  (atypically high for standard in vitro cell stimulation protocols) (Fig.23).

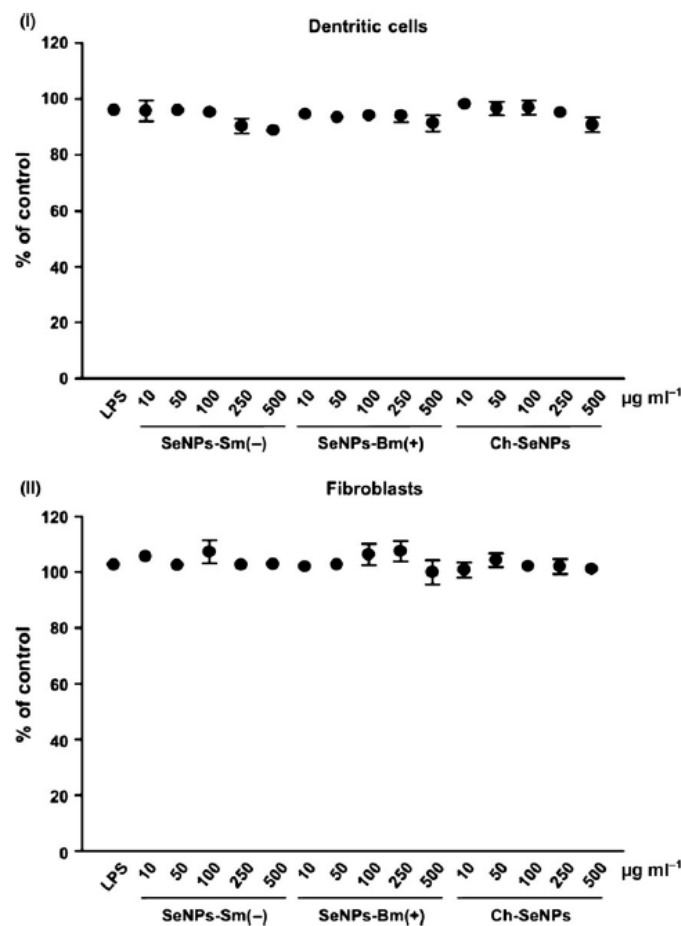


Figure 23. Evaluation of cell viability. DCs (I) and fibroblasts (II) were treated with the indicated concentrations of Sm-SeNPs(-), Bm-SeNPs(+) or Ch-SeNPs for 24 h, followed by 4 h incubation with Alamar blue. Cells were also incubated with 100 ng/ml LPS as a positive control. The values are expressed as the percentage



of Alamar blue reduction relative to untreated cells (designated as 100%). Data are means $\pm$ SD of four experiments.

#### Quantification of cytokine production

We then investigated whether SeNPs stimulate DCs to release of pro-inflammatory and immunostimulatory cytokines. Particularly we investigated the production of those involved in the activation of inflammatory and immune responses, such as IL-12, IL-8 IL-6 and tumor necrosis factor alpha (TNF- $\alpha$ ). The analysis of DC culture supernatants by enzymelinked immunosorbent assay (ELISA) revealed that SeNPs did not induce a significant increase in the release of IL-12, IL-6, IL-8 or TNF- $\alpha$  until the doses reached 250-500  $\mu$ g/ml, which are unlikely to be achieved *in vivo* (Fig.24). Cytokine release was stimulated more efficiently when DCs were challenged with Sm-SeNPs(-) rather than Bm-SeNPs(+), but bacterial LPS had a much more potent effect. Interestingly, the synthetic SeNPs did not induce the release of cytokines at any dose, suggesting that inorganic selenium is unable to stimulate human DCs alone and that the organic molecules coating the surface of biogenic SeNPs must be responsible for the observed effect. We also explored whether SeNPs influence the release of pro-inflammatory cytokines by human fibroblasts. We found that neither the biogenic SeNPs nor the Ch-SeNPs induced the secretion of IL-8, IL-6 or TNF-a by fibroblasts (data not shown), whereas 1  $\mu$ g/ml as a positive control induced human fibroblasts to secrete all three of these cytokines (data not shown). Collectively, our results demonstrate that although SeNPs inhibit bacterial growth, they are unable to cause significant damage to human DCs and fibroblasts or to stimulate the release of cytokines from the same cells.

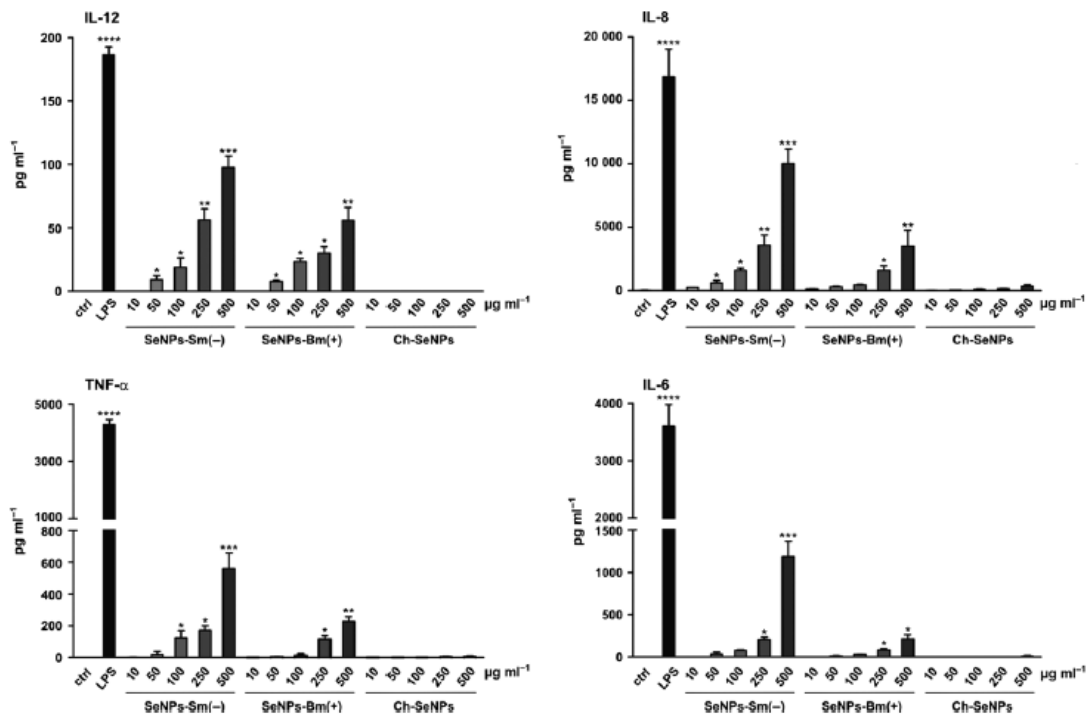


Figure 24. Quantification of cytokine production. DCs were challenged with the indicated amounts of Sm-SeNPs(-), Bm-SeNPs(+) or Ch-SeNPs for 24 h. DCs were also activated with 100 ng/ml LPS as a positive control. The release of the indicated cytokines into the culture supernatants was evaluated by ELISA test. The results are expressed as the mean value $\pm$ SD of three independent experiments. Statistical analysis: SeNP-treated DCs versus untreated cells ( $p < 0.05$ ).

## 6. DISCUSSION

---

Antibiotic-resistant infections in the last decades started to be more and more widespread, particularly in nosocomial contexts. Emergence of such pathogenic conditions can be responsible of longer hospital stays and an increased rate of mortality (Ferri, 2015). In such a scenario, major concerns are associated with multi-drug resistant (MDR) bacteria and bacterial communities able to grow forming biofilms. The widespread drug resistance is further exacerbated by the retreat of the pharmaceutical sector from new antibiotic development. These challenges highlight the demand for alternative and effective antimicrobial strategies.

Over the last few decades, the application of nanotechnology, particularly the use of nanoparticles for drug delivery, has generated significant impact in medicine. Several studies have already analysed the antimicrobial activity of different types of nanoparticles and specifically of chemically synthesized SeNPs towards different pathogenic bacterial strains. Chemically synthesized SeNPs were able to inhibit the growth of *Staphylococcus aureus* strains, including MRSA clinical isolates (Chudobova, 2014; Tran, 2011). Moreover, clinical isolates of *P. aeruginosa*, *S. aureus* and *P. mirabilis*, have been show to be particularly sensitive to SeNPs biogenically produced by a *Bacillus sp.* isolate (Shakibaie, 2014).

In the present study we analyzed, in a large number of bacterial isolates, the antimicrobial and antibiofilm activity of biogenic Selenium nanoparticles, produced by exploiting the selenite reduction capability of two environmental bacterial isolates. We consider the data obtained in this study would represent a contribution to investigate the possible use of these nanomaterials as an alternative strategy in the treatment of challenging drug resistant diseases.

In the first part of the study, the characteristics of different types of NPs were analyzed in order to identify and optimize the parameters associated with the highest NP efficiency as antimicrobial agents.

**The physiochemical characterisation of the three types of SeNPs tested in the study, revealed that the elemental composition of the biogenic SeNPs was very similar. On the contrary, the chemically synthesized NPs showed a**

different percentage in weight of Carbon, Oxygen, Selenium, Phosphorus and Sulphur. The higher content of these organic elements in the SeNPs produced by *B. mycooides* (Bm-SeNPs(+)) and *S. maltophilia* (Sm-SeNPs(-)), suggested the presence of biological macromolecules surrounding the nanomaterials. Both the fact that biogenic NPs showed a bigger size, if compared to the chemically synthesized, and the releasing mechanism from the intracellular environment hypothesized for NPs production by bacterial cells, give effort to this supposition. Indeed, Lampis and collaborators (Lampis, 2016) gave a partial description of the organic molecules bind to the Se<sup>0</sup> core of the NPs produced by *S. maltophilia* SeITE02, suggesting the presence of carbohydrates, lipids and proteins, totally absent or present in a smaller quantity in the synthetic counterpart. Other authors, investigated and confirmed the presence of functional groups typical of proteins and carbohydrates on biogenic SeNPs (BioSeNPs) suggesting the existence of extracellular polymeric substances (EPS) on the surface of these nanomaterials (Jain, 2014). There is also evidence that the EPS are able to govern the surface charge of BioSeNPs as well as contribute to their colloidal properties (Jain, 2014) of primary importance in mediating the antimicrobial activity of metallic NPs in general.

The cell free extract (CFX) obtained from SeNPs produced by *B. mycooides* and *S. maltophilia*, containing most of the soluble molecules and organic components deriving from the bacterial cells, by itself has not shown a relevant antimicrobial activity, as shown by calculating its minimum inhibitory concentration (MIC) against the bacterial growth, and comparing it to the MIC values of the native biogenic SeNPs and the chemical ones. The evidence that the CFX alone, as well as CFX simply added to synthetic SeNPs, showed no activity against the tested strain *P. aeruginosa* PAO1, may suggest that **the antimicrobial activity of biogenic SeNPs is primary due to the Selenium nanoparticle core surrounded by a complex biomolecular cap that is in some way associated to them as a result of the biosynthetic mechanism.** For that reason, is necessary to emphasize again that with the term biogenic Selenium nanoparticle (Bm-SeNPs(+)) and Sm-SeNPs(-) in the text), we refer to a nanomaterial composed by an elemental Selenium (Se<sup>0</sup>) core covered by a complex organic cap to date not completely

characterized.

The antibacterial activity of biogenic Bm-SeNPs(+) and Sm-SeNPs(-) was tested against a series of clinical and reference *P. aeruginosa* and *Candida* isolates and compared to the one of chemically produced SeNPs (Ch-SeNPs). Interestingly, the synthetic NPs, even though they showed a smaller size compared to the biogenic ones, seems to be not effective against the bacterial growth, as revealed by the very high MIC values recorded. Moreover, the two types of biogenic SeNPs showed a slightly different antimicrobial activity, with MIC values generally higher for the NPs produced by *B. mycooides*, suggesting a less efficient antimicrobial activity. As a matter of fact, from the literature is evident that the size of metallic nanoparticles is a key element in their antibacterial activity (Wang, 2017), the smallest they are, the highest antimicrobial activity could be detected. Sm-SeNPs(-) produced by *S. maltophilia*, turned out to be the most active, in term of antimicrobial activity, against the strains tested, revealing for some isolates (the reference strain PAO1 and the clinical BR2, CFC20, CFC21, CFCA, CFCB) low MIC values (ranging from 8 to 16 µg/ml) suggesting the possibility of using the biogenic Sm-SeNPs as a tool to avoid bacterial growth. Conversely, for other strains tested, the use of Sm-SeNPs(-) seemed not to be an efficient antimicrobial treatment, given the very high MIC values (512 µg/ml). In this contest, we can only describe the obtained values referring to them in term of high or low: is not possible to consider the strains tested as susceptible or resistant to NPs, lacking reference values as the standard breakpoints of the commonly used antibiotics.

Generally, it was detected a variable susceptibility among the strains tested that seemed to be dependent on the single isolate and not on the bacterial species. This observation was subsequently confirmed in a second part of the study for a wide range of bacterial isolates belonging to different species, both from Gram-positive and Gram-negative bacteria. As an example, within the species *P. aeruginosa*, a wide range of MIC values, from 8 to 512 µg/ml, was detected among the 12 strains tested, not being possible to associate the different susceptibility of the tested strains to any parameter such as the origin of the strain (ATTC collection or

clinical), the site of isolation or the type of patient involved in the study. Other parameters such as the physiological state or the cell surface charge have to be analyzed to understand the mechanisms underlying the bacteria susceptibility to NPs.

The investigations on the inhibitory and disaggregating activity of the three types of SeNPs on various bacterial biofilms confirmed the deep differences detected on the activity of chemical SeNPs compared to the biogenic ones, while a slight difference was evidenced between the two types of the NPs of bacterial origin. The SeNPs produced by *S. maltophilia* proved capable of inhibiting the biofilm formation also at the lowest concentration tested (50µg/ml) with a different antibiofilm activity depending on the strain considered. Indeed, some clinical isolates, collected from the sputum of CF patient and low respiratory infection, showed to be very susceptible to the NPs activity with percentage of inhibition up to 50% at the lowest concentration tested. Moreover, the Sm-SeNPs(-) inhibiting activity seemed to be dependent on the concentration.

Regarding the disaggregating activity on the mature biofilm polysaccharide matrix, the Ch-SeNPs confirmed their low activity, while Sm-SeNPs(-) showed a good antibiofilm activity being able to disaggregate the EPS matrix, for more than 40% already at 100µg/ml, in seven of the nine strains tested (except for BR1 and BR2 strains). Interestingly, the antibiofilm activity did not increase significantly at higher SeNP concentrations. Similarly, Sm-SeNPs(-) were able to disaggregate *Candida* biofilms of 40-60% already at the lowest concentration tested and no improvement at higher doses was detected. Bm-SeNPs(+) resulted slightly less efficient in eradicating the mature yeast biofilm than the one produced by *S. maltophilia* and the synthetic NPs had no substantial antibiofilm effect as already reported.

**The results regarding the antimicrobial and antibiofilm activity of biogenic SeNPs point out a different efficiency potential of the two types of NPs tested. In any case they are more active than their chemical counterpart. This, lead us to suppose that the different antimicrobial efficiency of nanoparticles originating from distinct taxonomically bacterial strains could be due to the presence of a different organic coating on the surface of the NP, as a result of**

### **the excretion mechanism by the producing bacterial cell.**

There is a significant gap in the knowledge of the biogenic SeNPs formation mechanism. In particular, it is unclear the way through they achieve the final control of the secreted nanoparticle and the composition of the originating particle. Several studies underlined the importance of proteins as key factors in the growth and final nucleation of metal nanoparticles (Dobias, 2011). For our purpose, native (Untreated) Sm-SeNPs(-), obtained as a result of 24 h incubation of *S. maltophilia* SeITE02 in the presence of selenite, were compared to the same biogenic nanoparticles undergoing increasingly stronger denaturing procedures namely i) denatured through a treatment with 10% SDS; ii) treated with 10% SDS and 10 min boiling, and iii) completely denatured with 10% SDS and 30 min boiling. **By increasing the strength of denaturing treatments, a progressive loss of proteins and carbohydrates from the organic coat surrounding Sm-SeNPs(-) was evidenced along with the increase of nanoparticle size and a change in their Z potential. Accordingly to data reported in literature (Dobias, 2011), the growth in size of biogenic selenium nanoparticles is a consequent effect of the denaturation process. Truly, the increase in NPs size is due to a gathering of particles that, deprived from their stabilizing coat, tend to aggregate. The partial loss of the external complex organic coating followed by an increase in the NPs size underline and confirm its pivotal role in preventing particle aggregation.** Furthermore, as well known (Hunter, 1981), the stability of treated SeNPs is reduced by the shift of Z potential measurements toward less negative values: NPs with charges close to a neutral value tend to agglomerate.

The anti-microbial activity of the four different types of SeNPs tested against different bacterial pathogens was quantified by MIC value determination. In accordance to the previous results, a wide variability of bacterial response to these nanoparticles was detected, not only among different species but also within strains belonging to the same species. Among the various clinical isolates and reference strains tested, belonging to both Gram-positive and Gram-negative species, some of them showed low MIC values (4-16 µg/ml) while other

evidenced higher MIC values (32-64  $\mu\text{g/ml}$ ), suggesting a good antimicrobial activity despite the different effectiveness. Equally, are reported in literature examples of a different susceptibility to metal NPs depending on the strains tested (Piacenza, 2017; Shakibaie, 2014), without an apparent explanation.

**As a general rule, despite the different susceptibility of the various strains, the anti-microbial efficacy of native Sm-SeNPs(-) decreased with the progressive loss of the organic coating layer. These findings suggested that antimicrobial activity of SeNPs is size-dependent, with the highest inhibiting effects associated to the smallest particles, which confirms the data already reported in previous studies (Zonaro, 2015; Chudobova, 2014; Lu, 2013). Indeed, removal of the external organic cap which leads to a progressive increase of particle dimensions overlap with a gradual decrease in anti-bacterial efficacy.**

To verify a direct influence of the organic capping surrounding these nanoparticles on their biocidal potential, not only as a particle stabilizing element, SeNPs from strain SeITE02 cultures after a 48 h incubation (Sm-SeNPs(48)) were tested for their antimicrobial activity and compared to those obtained after 24 h. The SeNPs obtained in that process appeared larger in size than those recovered as the product of a 24 h growth, but similar in dimension to the ones obtained by means of the strongest denaturing procedure (10%SDS+30'boiling) considered in this study. Indeed, the NPs size is depending on the age of the cultures (Lampis, 2014).

These biogenic Sm-SeNPs(48) owning their native surrounding layer, although as large as the ones deprived of the organic coating, showed MIC values significantly lower than those detected with fully denatured SeNPs, suggesting a role of the organic cap surrounding biogenic SeNPs in the efficacious anti-microbial interaction with target bacterial planktonic cells and biofilms.

With reference to the induction of loss of biofilm biomass, native Sm-SeNPs(-) were able to significantly disaggregate the exopolymeric matrix produced by all the bacterial strains tested. Moreover, quantification of culturable cells still embedded in bacterial biofilms after treatment confirmed the biocidal potential of



native Sm-SeNPs(-), with a marked reduction in colony forming units counting in five of the six strains tested, except *S. haemolyticus* UST1 which instead showed a high cell viability after treatment. **Results from the tests, carried out with partially denatured SeNPs or nanoparticles completely missing the outer coating layer, confirmed the key role played by the organic cap even in terms of anti-biofilm activity.**

Although the mechanisms through which metal/metalloid nanoparticles exert their anti-microbial activity are not completely understood and characterized, a number of authors addressed the production of reactive oxygen species (ROS) as one of the possible mode of action (Manke, 2013; Yan, 2013). In particular, anti-microbial effects of different selenium compounds have been attributed to the formation of free radicals (Tran, 2009). **In this study, exposure of three bacterial strains *P. aeruginosa* PAO1, *S. aureus* Mu50 and *B. cenocepacia* LMG16656, to Sm-SeNPs(-) actually caused an increase in ROS production compared to the controls.**

Taken together, the results regarding the antimicrobial activity of biogenic SeNPs, suggested their possible use as an efficient alternative strategy in the treatment of infectious diseases, including those particularly challenging for their resistance to different antimicrobial drugs. However, further investigation is needed to understand why some strains of a certain bacterial species respond to NPs while other strains of the same species appeared resistant to the action of the selenium nanomaterial.

The experiments on the possible synergistic activity of biogenic SeNPs produced by *S. maltophilia* and some selected antibiotics evidenced that, for several of the strains tested namely *P. aeruginosa* PAO1, *S. aureus* Mu50 and *S. aureus* UR1, there is a concomitant action but the biggest part in the disaggregating activity of the mature biofilm is due to the Sm-SeNPs(-) potential. **The NPs alone performed a very strong antibiofilm activity which is slightly increased when the nanoparticles are together with the antibiotics. Only in the case of the multi-resistant *P. aeruginosa* INT strain, a relevant biofilm disgregation is**

**detected only using a combination of our nanomaterials and drugs and not using SeNPs or antibiotic alone.**

The significant antibiofilm activity of the Sm-SeNPs(-) was confirmed also in the complex flow cells model. Due to their complexity, biofilm microbial communities have been challenging objects of investigation, also for the fact that biofilms are often located at places that are difficult to access and directly examine. A number of model systems have been established, including flow-cell-grown biofilms, that could facilitate these investigations in laboratory conditions and in combination with confocal laser scanning microscopy (CLSM) is considered the gold standard in biofilm research approach (Pamp, 2009). Moreover, such a system could help us in reproducing the conditions of constant nutrient supply characteristic of medical devices as urinary and venous catheters or heart valves. **In both the *P. aeruginosa* strains tested, the reference strain PAO1 and the multi-resistant INT, the biogenic SeNPs produced by *S. maltophilia* were able to significantly reduce the number of viable cells still present in the biofilm matrix inside the flow cell chamber after 24 h of continuous treatment. In addition, during the whole treatment, the number of viable cells released by the biofilm mass is steadily reduced.**

The complete characterization and understanding of biogenic SeNPs production mechanism and composition could finally lead us to explain the failure of the NPs antimicrobial activity in the chronic wound model and in the *in vivo* *C. elegans* nematode used in this study. As demonstrated by the obtained results for the wound model, is probably that some of the medium components may be able to interfere and modulate the interaction of NPs with bacterial cells. A series of studies have reported that the environmental conditions can significantly interfere with the nanoparticle antimicrobial activity. Temperature, pH, osmotic pressure and medium composition have a relevant role in determining the solubility of the NPs and consequently their efficacy (Wang, 2017; Loza, 2014).

On the contrary, inside the nematodes digestive system the SeNPs may result toxic by mechanical obstruction of the gut. Using the same model, Richter and

collaborators, (Richter, 2017) reported that quasi-spherical AgNPs of approximately 40 nm in diameter were able to successfully increase the survival rate of infected nematodes after treatment. X-ray tomography evidenced an accumulation of these AgNPs in the worm intestinal tract suggesting that the NPs were taken up by the nematodes during feeding. Probably, for the bigger size of our Selenium NPs (around 160 nm) and the presence of unknown biomolecular compounds on the surface of the particles, a high concentration of them resulted toxic. On the contrary, at lower concentrations the Sm-SeNPs(-) did not kill the treated worms.

Nowadays, the NPs antibacterial activity is limited to specific infections scenarios and we could only hypothesize their potentiality in clinical settings.

**Finally, the evaluation of the SeNPs toxic effect both in the mouse model and in human dendritic cells (DCs) and fibroblasts evidenced that the biogenic SeNPs used in this study, as well as those chemically synthesized, are not causing cell damage and toxic effects.** Different authors reported that nanomaterials and metallic NPs in general could be responsible for the induction of cytotoxicity and activation of human cell immuno-stimulatory molecules (Di Gioacchino, 2011; Chang, 2010). After challenging human DCs and fibroblasts with different concentration of SeNPs, neither adverse effect in cell viability nor relevant activation of immune-stimulatory cytokines as IL-6, IL-8, IL-12 or TNF $\alpha$  was reported, except at the highest concentration of 500  $\mu$ g/ml tested (which is very unlikely to be reached in an *in vivo* situation). Moreover, the mice treated with different concentration of Sm-SeNPs(-), by challenging the NPs intra-tracheally, did not reveal any adverse respiratory or systemic effect.

## 7. CONCLUSION AND PERSONAL CONSIDERATIONS

---

In conclusion, with the present investigation, we gave evidences that biogenic selenium nanoparticles, synthesized by an eco-friendly process, can reasonably be considered as reliable antimicrobial and antibiofilm agents able to efficaciously inhibit the growth of a number of challenging biofilm-producing bacteria of medical interest. Factors that basically are likely to affect the antimicrobial potential of the biogenic SeNPs used in this study are the constitutive elements, the size and the surface architecture and charge accordingly to the already published evidence (Wang, 2017; Zonaro, 2015). In addition to the formation of ROS and their relevant role for the biocidal potential, features of the organic coat surrounding the biogenic SeNPs show a marked influence on the antimicrobial properties of those nanoparticles. However, much is still to be clarified in order to elucidate the detailed nature of the external organic coating of biogenic metal nanoparticles and their mechanism of action against bacterial cells for an actual interpretation of the intimate biocidal mechanisms.

The information gained so far on biogenic SeNPs, together with the lack of toxicity against the mouse model and human cell lines, open a realistic perspective for a possible use of these nanostructured particles as a novel non-antibiotic antimicrobial tool to treat fastidious nosocomial infections, included biofilm-associated syndromes and those caused by multidrug-resistant bacteria.

Regarding the different susceptibility of the tested strains to the SeNPs, this remains a major concern. Further investigations are however required to elucidate in detail the actual mechanisms of action of these nanoparticles as well to evaluate their whole biological compatibility to the human body.

We must always keep in mind that as happened for antimicrobial drugs, there is the concrete possibility of the onset of resistance mechanisms also towards these nanomaterials. It is therefore necessary to avoid the indiscriminate use of such new alternative strategies and focus on prevention of infectious diseases and antibiotics stewardship.

The PhD thesis here presented is, in my opinion, the result of a very good

professional collaboration which led to new working contribution between different department of the Verona University and different European Universities. At the end of my project I can express my own satisfaction about the results obtained, moreover, I had the opportunity to travel and attend congresses, courses, meetings and collaborate with other students and researchers world renown.

## 8. ACKNOWLEDGMENTS

---

I will personally thank my academic tutors Prof. *Maria Lleo* and Dott. *Marzia Boaretti*, for the support and the aid during these three years of my PhD.

Prof. *Tom Coenye*, Dott. *Ilse Vandecandelaere*, *Jasper Wille* and all the people from the laboratory of Pharmaceutical Microbiology, for the warm welcome, the precious help and the suggestions provided during my stay at Ghent University.

Prof. *Giovanni Vallini*, Dott. *Silvia Lampis* and Dott. *Emanuele Zonaro* from the Laboratory of Environmental Microbiology, Dept. of Biotechnology, University of Verona and Prof. *Stefano Dusi* and Dott. *Marta Donini* from the Department of Pathology, University of Verona, for the kind collaboration.

Dott. *Paola Melotti* from the Regional Cystic Fibrosis Research Center in Verona for providing some of the strains used in the study.

## 9. BIBLIOGRAPY

---

Abedon ST. Phage therapy of pulmonary infections. *Bacteriophage*. 2015 Apr 18;5(1):e1020260. eCollection 2015 Jan-Mar. Review. PubMed PMID: 26442188.

Al-Haidari Ra, Shaaban Mi, Ibrahim Srm, Mohamed Ga. Anti-Quorum Sensing Activity Of Some Medicinal Plants. *Afr J Tradit Complement Altern Med*. 2016 Aug 12;13(5):67-71. Doi: 10.21010/Ajtcam.V13i5.10.

Ali L, Goraya MU, Arafat Y, Ajmal M, Chen JL, Yu D. Molecular Mechanism of Quorum-Sensing in *Enterococcus faecalis*: Its Role in Virulence and Therapeutic Approaches. *Int J Mol Sci*. 2017 May 3;18(5). pii: E960. doi: 10.3390/ijms18050960. Review.

Allison KR, Brynildsen MP, Collins JJ. Metabolite-enabled eradication of bacterial persisters by aminoglycosides. *Nature*. 2011 May 12;473(7346):216-20. doi: 10.1038/nature10069.

Ahmad SI. Treatment of post-burns bacterial infections by bacteriophages, specifically ubiquitous *Pseudomonas* spp. notoriously resistant to antibiotics. *Med Hypotheses*. 2002 Apr;58(4):327-31. PubMed PMID: 12027527.

Alexis, F., Pridgen, E., Molnar, L.K., and Farokhzad, O.C. (2008) Factors affecting the clearance and biodistribution of polymeric nanoparticles. *Mol Pharm* 5: 505–515.

Al-Wrafy F, Brzozowska E, Górska S, Gamian A. Pathogenic factors of *Pseudomonas aeruginosa* - the role of biofilm in pathogenicity and as a target for phage therapy. *Postepy Hig Med Dosw (Online)*. 2017 Feb 14;71(0):78-91. Review. PubMed PMID: 28258668.

Anutrakunchai C, Sermswan RW, Wongratanacheewin S, Puknun A, Taweechaisupapong S. Drug susceptibility and biofilm formation of *Burkholderia pseudomallei* in nutrient-limited condition. *Trop Biomed*. 2015 Jun;32(2):300-9. PubMed PMID: 26691259.

Arakha M, Pal S, Samantarrai D, et al. Antimicrobial activity of iron oxide nanoparticle upon modulation of nanoparticle-bacteria interface. *Sci Rep*. 2015;5:14813. Azeredo J, Sutherland IW. The use of phages for the removal of infectious biofilms. *Curr Pharm Biotechnol*. 2008 Aug;9(4):261-6. PubMed PMID: 18691087.

Azeredo J, Sutherland IW. The use of phages for the removal of infectious biofilms. *Curr Pharm Biotechnol*. 2008 Aug;9(4):261-6. PubMed PMID: 18691087.

Bagga P, Siddiqui HH, Akhtar J, Mahmood T, Zahera M, Khan MS. Gold Nanoparticles Conjugated Levofloxacin: For Improved Antibacterial Activity Over Levofloxacin Alone. *Curr Drug Deliv*. 2017;14(8):1114-1119. doi: 10.2174/1567201814666170316113432.

Bárdy P, Pantůček R, Benešík M, Doškař J. Genetically modified bacteriophages in applied microbiology. *J Appl Microbiol*. 2016 Sep;121(3):618-33. doi: 10.1111/jam.13207. Epub 2016 Jul 26. Review. PubMed PMID: 27321680.

Beyth N, Houry-Haddad Y, Domb A, Khan W, Hazan R. Alternative antimicrobial approach: nano-antimicrobial materials. *Evid Based Complement Alternat Med*. 2015;2015:246012. doi: 10.1155/2015/246012.

Bertolini, R. van Aerle, S. Lampis, K.A. Moore, K. Paszkiewicz, C.S. Butler, G. Vallini, M. van der Giezen, Draft genome sequence of *Stenotrophomonas maltophilia* SeITE02, a gammaproteobacterium isolated from selenite-contaminated mining soil, *Genome Announc*. 2 (3) (2014).

Biswas NN, Yu TT, Kimyon Ö, Nizalapur S, Gardner CR, Manefield M, Griffith R, Black DS, Kumar N. Synthesis of antimicrobial glucosamides as bacterial quorum sensing mechanism inhibitors. *Bioorg Med Chem*. 2017 Feb 1;25(3):1183-1194. doi: 10.1016/j.bmc.2016.12.024. Epub 2016 Dec 21. PubMed PMID: 28049617.

Bjarnsholt T, Ciofu O, Molin S, Givskov M, Høiby N. Applying insights from biofilm biology to drug development - can a new approach be developed? *Nat Rev Drug Discov*. 2013 Oct;12(10):791-808. doi: 10.1038/nrd4000. Review. PubMed PMID: 24080700.

Bjarnsholt T. The role of bacterial biofilms in chronic infections. *APMIS Suppl*. 2013 May;(136):1-51. doi: 10.1111/apm.12099. PubMed PMID: 23635385.

Boles, B. R., and A. R. Horswill. 2008. Agr-mediated dispersal of *Staphylococcus aureus* biofilms. *PLoS Pathog*. 4:e1000052.

Beanan MJ, Strome S. Characterization of a germ-line proliferation mutation in *C. elegans*. *Development*. 1992 Nov;116(3):755-66. PubMed PMID: 1289064.

Beheshti N, Soflaei S, Shakibaie M, Yazdi MH, Ghaffarifar F, Dalimi A, Shahverdi AR. Efficacy of biogenic selenium nanoparticles against *Leishmania major*: in vitro and in vivo studies. *J Trace Elem Med Biol*. 2013 Jul;27(3):203-7. doi: 10.1016/j.jtemb.2012.11.002.

Brackman G, Breyne K, De Rycke R, Vermote A, Van Nieuwerburgh F, Meyer E, Van Calenbergh S, Coenye T. The Quorum Sensing Inhibitor Hamamelitannin Increases Antibiotic Susceptibility of *Staphylococcus aureus* Biofilms by Affecting Peptidoglycan Biosynthesis and eDNA Release. *Sci Rep*. 2016 Feb 1;6:20321. doi: 10.1038/srep20321. PubMed PMID: 26828772; PubMed Central PMCID: PMC4734334

Brackman G, Cos P, Maes L, Nelis HJ, Coenye T. Quorum sensing inhibitors increase the susceptibility of bacterial biofilms to antibiotics in vitro and in vivo. *Antimicrob Agents Chemother*. 2011 Jun;55(6):2655-61. doi: 10.1128/AAC.00045-11.

Brackman, G., U. Hillaert, S. Van Calenbergh, H. J. Nelis, and T. Coenye. 2009. Use of quorum sensing inhibitors to interfere with biofilm formation and development in *Burkholderia multivorans* and *Burkholderia cenocepacia*. *Res. Microbiol*. 160:144–151

Bradshaw DJ, Homer KA, Marsh PD, Beighton D. Metabolic cooperation in oral microbial communities during growth on mucin. *Microbiology* 1994; 140: 3407–3412.)

Cao B, Christophersen L, Thomsen K, Sønderholm M, Bjarnsholt T, Jensen PØ, Høiby N, Moser C. Antibiotic penetration and bacterial killing in a *Pseudomonas aeruginosa* biofilm model. *J Antimicrob Chemother*. 2015 Jul;70(7):2057-63. doi: 10.1093/jac/dkv058. Epub 2015 Mar 18. PubMed PMID: 25786481.

Cha SH, Hong J, McGuffie M, Yeom B, VanEpps JS, Kotov NA. Shape-dependent biomimetic inhibition of enzyme by nanoparticles and their antibacterial activity. *ACS Nano*. 2015;9(9):9097–9105.

Chadha P, Katare OP, Chhibber S. In vivo efficacy of single phage versus phage cocktail in resolving burn wound infection in BALB/c mice. *Microb Pathog*. 2016 Oct;99:68-77. doi: 10.1016/j.micpath.2016.08.001. Epub 2016 Aug 4. PubMed PMID:27498362.

Chan-Tompkins NH. multidrug-resistant gram-negative infections. Bringing back the old. *Crit Care Nurs Q*. 2011 Apr-Jun;34(2):87-100. doi:10.1097/CNQ.0b013e31820f6e88.



Characklis, W. G., and K. C. Marshall. 1990. Biofilms: a basis for an interdisciplinary approach, p. 3–15. In W. G. Characklis and K. C. Marshall (ed.), *Biofilms*. John Wiley & Sons, New York, N.Y.

Chang, C., and Gershwin, M.E. (2010) Drugs and autoimmunity– a contemporary review and mechanistic approach. *J Autoimmun* 34: 266–275.

Chen T, Wong YS, Zheng W, Bai Y, Huang L. Selenium nanoparticles fabricated in *Undaria pinnatifida* polysaccharide solutions induce mitochondria-mediated apoptosis in A375 human melanoma cells. *Colloids Surf B Biointerfaces*. 2008 Nov 15;67(1):26-31. doi: 10.1016/j.colsurfb.2008.07.010. Epub 2008 Aug 3. PubMed PMID: 18805679.

Chhibber S, Shukla A, Kaur S. Transfersomal Phage Cocktail Is an Effective Treatment against Methicillin-Resistant *Staphylococcus aureus*-Mediated Skin and Soft Tissue Infections. *Antimicrob Agents Chemother*. 2017 Sep 22;61(10). pii: e02146-16. doi: 10.1128/AAC.02146-16. Print 2017 Oct. PubMed PMID: 28739792; PubMed Central PMCID: PMC5610514.

Cihalova K, Chudobova D, Michalek P, Moulick A, Guran R, Kopel P, Adam V, Kizek R. *Staphylococcus aureus* and MRSA Growth and Biofilm Formation after Treatment with Antibiotics and SeNPs. *Int J Mol Sci*. 2015 Oct 16;16(10):24656-72. doi: 10.3390/ijms161024656.

Ciofu, O., Giwercman, B., Pedersen, S. S. & Høiby, N. Development of antibiotic resistance in *Pseudomonas aeruginosa* during two decades of antipseudomonal treatment at the Danish CF Center. *APMIS* 102, 674–680 (1994)

Cole SJ, Records AR, Orr MW, Linden SB, Lee VT. Catheter-associated urinary tract infection by *Pseudomonas aeruginosa* is mediated by exopolysaccharide-independent biofilms. *Infect Immun*. 2014 May;82(5):2048-58. doi: 10.1128/IAI.01652-14.

Costerton, J. W., G. G. Geesey, and G. K. Cheng. 1978. How bacteria stick. *Sci. Am.* 238:86–95.)

Costerton JW, Cheng KJ, Geesey GG, Ladd TI, Nickel JC, Dasgupta M, Marrie TJ. Bacterial biofilms in nature and disease. *Annu Rev Microbiol*. 1987;41:435-64. Review.

Costerton, J. W., Z. Lewandowski, D. E. Caldwell, D. R. Korber, and H. M. Lappin-Scott. 1995. Microbial biofilms. *Annu. Rev. Microbiol.* 49:711–745.

Costerton JW, Stewart PS, Greenberg EP. Bacterial biofilms: a common cause of persistent infections. *Science*. 1999 May 21;284(5418):1318-22. Review.

Cremonini E, Zonaro E, Donini M, Lampis S, Boaretti M, Dusi S, Melotti P, Lleo MM, Vallini G. Biogenic selenium nanoparticles: characterization, antimicrobial activity and effects on human dendritic cells and fibroblasts. *Microb Biotechnol*. 2016 Nov;9(6):758-771. doi: 10.1111/1751-7915.12374.

Cuellar-Cruz, M., Lopez-Romero, E., Villagomez- Castro, J. C. & Ruiz-Baca, E. *Candida* species: new insights into biofilm formation. *Future. Microbiol.* 7, 755–771 (2012)

P, Mariani-Costantini R, Bernardini G. Immunotoxicity of nanoparticles. *Int J Immunopathol Pharmacol*. 2011 Jan-Mar;24(1 Suppl):65S-71S. Review. PubMed PMID:21329568.

Di Gioacchino, M., Tetrarca, C., Lazzarin, F., Di Giampaolo, L., Sabbioni, E., Boscolo, P., et al. (2011) Immunotoxicity of nanoparticles. *Int J Immunopath Pharmacol* 24: 65S–71S.

Di Gregorio S, Lampis S, Vallini G. Selenite precipitation by a rhizospheric strain of *Stenotrophomonas* sp. isolated from the root system of *Astragalus bisulcatus*: a biotechnological perspective. *Environ Int*. 2005 Feb;31(2):233-41. PubMed PMID: 15661289.

- Dobias, J., Suvurova, E.I., and Bernier-Latmani, R. (2011) Role of proteins in controlling selenium nanoparticle size. *Nanotechnology* 22: 195605.
- Donini M, Zenaro E, Tamassia N, Dusi S. NADPH oxidase of human dendritic cells: role in *Candida albicans* killing and regulation by interferons, dectin-1 and CD206. *Eur J Immunol.* 2007 May;37(5):1194-203. PubMed PMID: 17407098.
- Donlan RM. Biofilms: microbial life on surfaces. *Emerg Infect Dis.* 2002 Sep;8(9):881-90. Review. PubMed PMID: 12194761; PubMed Central PMCID: PMC2732559.
- Dunne WM Jr. 2002. Bacterial adhesion: Seen any good biofilms lately? *Clin Microbiol Rev* 15: 155–166.)
- Esfandiari N, Simchi A, Bagheri R. Size tuning of Ag-decorated TiO<sub>2</sub> nanotube arrays for improved bactericidal capacity of orthopedic implants. *J Biomed Mater Res A.* 2014;102(8):2625–2635.
- Ferri, M., Ranucci, E., Romagnoli, P., and Giaccone, V. (2015) Antimicrobial resistance: 405 a global 406 emerging threat to public health systems. *Crit Rev Food Sci Nutr* 407 doi:10.1080/10408398.2015.1077192.
- Flemming HC, Neu TR, Wozniak DJ. The EPS matrix: the "house of biofilm cells". *J Bacteriol.* 2007 Nov;189(22):7945-7. Epub 2007 Aug 3. PubMed PMID: 17675377; PubMed Central PMCID: PMC2168682.
- Fux CA, Costerton JW, Stewart PS, Stoodley P. Survival strategies of infectious biofilms. *Trends Microbiol.* 2005 Jan;13(1):34-40. Review. PubMed PMID:15639630.
- Fuqua, C., and E. P. Greenberg. 2002. Listening in on bacteria: acyl-homoserine lactone signaling. *Nat. Rev. Mol. Cell. Biol.* 3:685–695.
- Gupta D, Singh A, Khan AU. Nanoparticles as Efflux Pump and Biofilm Inhibitor to Rejuvenate Bactericidal Effect of Conventional Antibiotics. *Nanoscale Res Lett.* 2017 Dec;12(1):454. doi: 10.1186/s11671-017-2222-6. Epub 2017 Jul 13. Review. PubMed PMID: 28709374; PubMed Central PMCID: PMC5509568.
- Granucci, F., Zanoni, I., and Ricciardi-Castagnoli, P. (2008) Central role of dendritic cells in the regulation and deregulation of immune responses. *Cell Mol Life Sci* 65: 1683– 1697.
- Gu J, Liu X, Li Y, Han W, Lei L, Yang Y, Zhao H, Gao Y, Song J, Lu R, Sun C, Feng X. A method for generation phage cocktail with great therapeutic potential. *PLoS One.* 2012;7(3):e31698. doi: 10.1371/journal.pone.0031698. Epub 2012 Mar 1. PubMed PMID: 22396736; PubMed Central PMCID: PMC3291564.
- Gupta D, Singh A, Khan AU. Nanoparticles as Efflux Pump and Biofilm Inhibitor to Rejuvenate Bactericidal Effect of Conventional Antibiotics. *Nanoscale Res Lett.* 2017 Dec;12(1):454. doi: 10.1186/s11671-017-2222-6.
- He Y, Chen S, Liu Z, Cheng C, Li H, Wang M. Toxicity of selenium nanoparticles in male Sprague-Dawley rats at supranutritional and nonlethal levels. *Life Sci.* 2014 Oct 12;115(1-2):44-51. doi: 10.1016/j.lfs.2014.08.023. Epub 2014 Sep 16. PubMed PMID: 25219884.
- Huang Y, He L, Liu W, Fan C, Zheng W, Wong YS, Chen T. Selective cellular uptake and induction of apoptosis of cancer-targeted selenium nanoparticles. *Biomaterials.* 2013 Sep;34(29):7106-16. doi: 10.1016/j.biomaterials.2013.04.067. Epub 2013 Jun 22. PubMed PMID: 23800743.

Ishii S, Fukui K, Yokoshima S, Kumagai K, Beniyama Y, Kodama T, Fukuyama T, Okabe T, Nagano T, Kojima H, Yano T. High-throughput Screening of Small Molecule Inhibitors of the Streptococcus Quorum-sensing Signal Pathway. *Sci Rep.* 2017 Jun 22;7(1):4029. doi: 10.1038/s41598-017-03567-2. PubMed PMID: 28642545; PubMed Central PMCID: PMC5481443.

Jamal M, et al., Bacterial biofilm and associated infections, *Journal of the Chinese Medical Association* (2017), <https://doi.org/10.1016/j.jcma.2017.07.012>

Kim DH, Feinbaum R, Alloing G, Emerson FE, Garsin DA, Inoue H, Tanaka-Hino M, Hisamoto N, Matsumoto K, Tan MW, Ausubel FM. A conserved p38 MAP kinase pathway in *Caenorhabditis elegans* innate immunity. *Science.* 2002 Jul 26;297(5581):623-6. PubMed PMID: 12142542.

Khoei NS, Lampis S, Zonaro E, Yrjälä K, Bernardi P, Vallini G. Insights into selenite reduction and biogenesis of elemental selenium nanoparticles by two environmental isolates of *Burkholderia fungorum*. *N Biotechnol.* 2017 Jan 25;34:1-11. doi: 10.1016/j.nbt.2016.10.002. Epub 2016 Oct 4. PubMed PMID: 27717878

Kostakioti M, Hadjifrangiskou M, Hultgren SJ. Bacterial biofilms: development, dispersal, and therapeutic strategies in the dawn of the postantibiotic era. *Cold Spring Harb Perspect Med.* 2013 Apr 1;3(4):a010306. doi: 10.1101/cshperspect.a010306. Review.

Kundukad B, Seviour T, Liang Y, Rice SA, Kjelleberg S, Doyle PS. Mechanical properties of the superficial biofilm layer determine the architecture of biofilms. *Soft Matter.* 2016 Jun 29;12(26):5718-26. doi: 10.1039/c6sm00687f.

Kuramitsu HK, Wang BY. The whole is greater than the sum of its parts: dental plaque bacterial interactions can affect the virulence properties of cariogenic *Streptococcus mutans*. *Am J Dent.* 2011 Jun;24(3):153-4. Review. PubMed PMID: 21874934.

Lampis, S., Zonaro, E., Bertolini, C., Bernardi, P., Butler, C.S., and Vallini, G. (2014) Delayed formation of zerovalent selenium nanoparticles by *Bacillus mycoides* SeITE01 as a consequence of selenite reduction under aerobic conditions. *Microb Cell Fact* 13: 1–14.

Lampis, S., Zonaro, E., Bertolini, C., Cecconi, D., Monti, F., Micaroni, M., et al. (2016) Selenite biotransformation and detoxification by *Stenotrophomonas maltophilia* SeITE02: novel clues on the route to bacterial biogenesis of selenium nanoparticles. *J Hazard Mater* in press. doi:10.1016/j.jhazmat.2016.02.035

Lebeaux D, Ghigo JM, Beloin C. Biofilm-related infections: bridging the gap between clinical management and fundamental aspects of recalcitrance toward antibiotics. *Microbiol Mol Biol Rev.* 2014 Sep;78(3):510-43. doi: 10.1128/MMBR.00013-14. Review. PubMed PMID: 25184564; PubMed Central PMCID: PMC4187679.

Lewis K. Persister cells: molecular mechanisms related to antibiotic tolerance. *Handb Exp Pharmacol.* 2012;(211):121-33. doi: 10.1007/978-3-642-28951-4\_8. PubMed PMID: 23090599

Lewis K. Persister cells. *Annu Rev Microbiol.* 2010;64:357-72. doi: 10.1146/annurev.micro.112408.134306. Review. PubMed PMID: 20528688.

Li Z, Li H, Hu H. Selenite removal and reduction by growing *Aspergillus* sp. J2. *Biometals.* 2017 Nov 6. doi: 10.1007/s10534-017-0063-5. [Epub ahead of print] PubMed PMID: 29110163.

Lin, Z.H., and Wang, C.R.C. (2005) Evidence on the sizedependent absorption spectral evolution of selenium nanoparticles. *Mat Chem Phys* 92: 591–594.

Loza, K., Diendorf, C., Sengstock, C., Ruiz-Gonzalez, L., Gonzalez-Calbet, J.M., Vallet-Regi, M., et al. (2014) The dissolution and biological effects of silver nanoparticles in biological media. *J Mater Chem B* 2: 1634–1643.)

Lu, Z., Rong, K.L.J., Yang, H., and Chen, R. (2013) Size-dependent antibacterial activities of silver 423 nanoparticles against oral anaerobic pathogenic bacteria. *J. Mater Sci Mater Med* **24**: 1465–1471.

Magalhães AP, Lopes SP, Pereira MO. Insights into Cystic Fibrosis Polymicrobial Consortia: The Role of Species Interactions in Biofilm Development, Phenotype, and Response to In-Use Antibiotics. *Front Microbiol.* 2017 Jan 13;7:2146. doi: 10.3389/fmicb.2016.02146.

Mahmoudvand H, Shakibaie M, Tavakoli R, Jahanbakhsh S, Sharifi I. In Vitro Study of Leishmanicidal Activity of Biogenic Selenium Nanoparticles against Iranian Isolate of Sensitive and Glucantime-Resistant *Leishmania tropica*. *Iran J. Parasitol.* 2014 Oct-Dec;9(4):452-60. PubMed PMID: 25759725; PubMed Central PMCID:PMC4345083

Marques CN, Morozov A, Planzos P, Zelaya HM. The fatty acid signaling molecule cis-2-decenoic acid increases metabolic activity and reverts persister cells to an antimicrobial-susceptible state. *Appl Environ Microbiol.* 2014 Nov;80(22):6976-91. doi: 10.1128/AEM.01576-14.

Marsh PD, Moter A, Devine DA. Dental plaque biofilms: communities, conflict and control. *Periodontol* 2000. 2011 Feb;55(1):16-35. doi: 10.1111/j.1600-0757.2009.00339.x. Review. PubMed PMID: 21134226) Published online 2016 Feb 2. doi: 10.1016/j.freeradbiomed.2016.02.003

Mina EG, Marques CN. Interaction of *Staphylococcus aureus* persister cells with the host when in a persister state and following awakening. *Sci Rep.* 2016 Aug 10;6:31342. doi: 10.1038/srep31342. PubMed PMID: 27506163; PubMed Central PMCID: PMC4979210.

Mlynarcik P, Kolar M. Starvation- and antibiotics-induced formation of persister cells in *Pseudomonas aeruginosa*. *Biomed Pap Med Fac Univ Palacky Olomouc Czech Repub.* 2017 Mar;161(1):58-67. doi: 10.5507/bp.2016.057. Epub 2016 Nov 23. PubMed PMID: 27886280.

Moran Losada P, Chouvarine P, Dorda M, Hedtfeld S, Mielke S, Schulz A, Wiehlmann L, Tümmler B. The cystic fibrosis lower airways microbial metagenome. *ERJ Open Res.* 2016 May 9;2(2). pii: 00096-2015.

Nel A, Xia T, Mädler L, Li N. Toxic potential of materials at the nanolevel. *Science.* 2006 Feb 3;311(5761):622-7. Review. PubMed PMID: 16456071.

Nevius BA, Chen YP, Ferry JL, Decho AW. Surface-functionalization effects on uptake of fluorescent polystyrene nanoparticles by model biofilms. *Ecotoxicology.* 2012 Nov;21(8):2205-13. doi: 10.1007/s10646-012-0975-3.

Nguyen D, Joshi-Datar A, Lepine F, Bauerle E, Olakanmi O, Beer K, McKay G, Siehnel R, Schafhauser J, Wang Y, Britigan BE, Singh PK. Active starvation responses mediate antibiotic tolerance in biofilms and nutrient-limited bacteria. *Science.* 2011 Nov 18;334(6058):982-6. doi: 10.1126/science.1211037. PubMed PMID: 22096200; PubMed Central PMCID: PMC4046891.

O'Brien S, Fothergill JL. The role of multispecies social interactions in shaping *Pseudomonas aeruginosa* pathogenicity in the cystic fibrosis lung. *FEMS Microbiol Lett.* 2017 Aug 15;364(15). doi: 10.1093/femsle/fnx128. PubMed PMID: 28859314.

Odds F.C. 2013 Synergy, antagonism, and what the checkerboard puts between them *Journal of Antimicrobial Chemotherapy* (2003) **52**, 1DOI: 10.1093/jac/dkg301

- Orman MA, Brynildsen MP. Persister formation in *Escherichia coli* can be inhibited by treatment with nitric oxide. *Free Radic Biol Med*. 2016 Apr;93:145-54. doi: 10.1016/j.freeradbiomed.2016.02.003.
- Paczkowski JE, Mukherjee S, McCready AR, Cong JP, Aquino CJ, Kim H, Henke BR, Smith CD, Bassler BL. Flavonoids Suppress *Pseudomonas aeruginosa* Virulence through Allosteric Inhibition of Quorum-sensing Receptors. *J Biol Chem*. 2017 Mar 10;292(10):4064-4076. doi: 10.1074/jbc.M116.770552.
- Paharik AE, Horswill AR. The Staphylococcal Biofilm: Adhesins, Regulation, and Host Response. *Microbiol Spectr*. 2016 Apr;4(2). doi:10.1128/microbiolspec.
- Paganin P, Fiscarelli EV, Tuccio V, Chianciani M, Bacci G, Morelli P, Dolce D, Dalmastrì C, De Alessandri A, Lucidi V, Taccetti G, Mengoni A, Bevivino A. Changes in cystic fibrosis airway microbial community associated with a severe decline in lung function. *PLoS One*. 2015 Apr 21;10(4):e0124348. doi:10.1371/journal.pone.0124348.
- Pamp SJ, Sternberg C, Tolker-Nielsen T. Insight into the microbial multicellular lifestyle via flow-cell technology and confocal microscopy. *Cytometry A*. 2008 Feb;75(2):90-103. doi: 10.1002/cyto.a.20685. Review.
- Peeters E, Nelis HJ, Coenye T. Comparison of multiple methods for quantification of microbial biofilms grown in microtiter plates. *J Microbiol Methods*. 2008 Feb;72(2):157-65.
- Piacenza E, Presentato A, Zonaro E, Lemire JA, Demeter M, Vallini G, Turner RJ, Lampis S. Antimicrobial activity of biogenically produced spherical Se-nanomaterials embedded in organic material against *Pseudomonas aeruginosa* and *Staphylococcus aureus* strains on hydroxyapatite-coated surfaces. *Microb Biotechnol*. 2017 Jul;10(4):804-818. doi: 10.1111/1751-7915.12700. Epub 2017 Feb 23. PubMed PMID: 28233476; PubMed Central PMCID: PMC5481514.
- Pires DP, Melo L, Vilas Boas D, Sillankorva S, Azeredo J. Phage therapy as an alternative or complementary strategy to prevent and control biofilm-related infections. *Curr Opin Microbiol*. 2017 Sep 28;39:48-56. doi: 10.1016/j.mib.2017.09.004. [Epub ahead of print] Review. PubMed PMID: 28964986.
- Ranghar S. Nanoparticle-based drug delivery systems: promising approaches against infections. *Braz Arch Biol Techn*. 2012;57:209-222.
- Richter K, Facal P, Thomas N, Vandecandelaere I, Ramezanzpour M, Cooksley C, Prestidge CA, Coenye T, Wormald PJ, Vreugde S. Taking the Silver Bullet Colloidal Silver Particles for the Topical Treatment of Biofilm-Related Infections. *ACS Appl Mater Interfaces*. 2017 Jul 5;9(26):21631-21638. doi: 10.1021/acsami.7b03672.
- Ren Y, Zhao T, Mao G, Zhang M, Li F, Zou Y, Yang L, Wu X. Antitumor activity of hyaluronic acid-selenium nanoparticles in Heps tumor mice models. *Int J Biol Macromol*. 2013 Jun;57:57-62. doi: 10.1016/j.ijbiomac.2013.03.014. Epub 2013 Mar 13. PubMed PMID: 23500433.
- Samuel U, Guggenbichler JP. Prevention of catheter-related infections: the potential of a new nano-silver impregnated catheter. *Int J Antimicrob Agents*. 2004;23(suppl 1):75-78.
- Santi C, Bogusz D, Franche C. Biological nitrogen fixation in non-legume plants. *Ann Bot*. 2013 May;111(5):743-67. doi: 10.1093/aob/mct048.
- Schäkel, K. (2009) Dendritic cells—why can they help and hurt us. *Exp Dermatol* 18: 264–273.
- Schaudinn C, Carr G, Gorur A, Jaramillo D, Costerton JW, Webster P. Imaging of endodontic biofilms by combined microscopy (FISH/cLSM - SEM). *J Microsc*. 2009 Aug;235(2):124-7. doi: 10.1111/j.1365-2818.2009.03201.x.

Schmidt J, Musken M, Becker T, Magnowska Z, Bertinetti D, Moller S, Zimmermann B, Herberg FW, Jansch L, Haussler S. 2011. The *Pseudomonas aeruginosa* chemotaxis methyltransferase CheR1 impacts on bacterial surface sampling. *PLoS ONE* 6: e18184

Shaikh S, Rizvi SMD, Shakil S, Hussain T, Alshammari TM, Ahmad W, Tabrez S, Al-Qahtani MH, Abuzenadah AM. Synthesis and Characterization of Cefotaxime Conjugated Gold Nanoparticles and Their Use to Target Drug-Resistant CTX-M-Producing Bacterial Pathogens. *J Cell Biochem*. 2017 Sep;118(9):2802-2808. doi: 10.1002/jcb.25929.

Shaker MA, Shaaban MI. Formulation of carbapenems loaded gold nanoparticles to combat multi-antibiotic bacterial resistance: In vitro antibacterial study. *Int J Pharm*. 2017 Jun 15;525(1):71-84. doi: 10.1016/j.ijpharm.2017.04.019.

Shakibaie M, Forootanfar H, Golkari Y, Mohammadi-Khorsand T, Shakibaie MR. Anti-biofilm activity of biogenic selenium nanoparticles and selenium dioxide against clinical isolates of *Staphylococcus aureus*, *Pseudomonas aeruginosa*, and *Proteus mirabilis*. *J Trace Elem Med Biol*. 2015 Jan;29:235-41. doi: 10.1016/j.jtemb.2014.07.020. Epub 2014 Aug 9. PubMed PMID: 25175509.

Shakibaie M, Salari Mohazab N, Ayatollahi Mousavi SA. Antifungal Activity of Selenium Nanoparticles Synthesized by *Bacillus* species Msh-1 Against *Aspergillus fumigatus* and *Candida albicans*. *Jundishapur J Microbiol*. 2015 Sep 8;8(9):e26381. doi: 10.5812/jjm.26381.

Singh P, Kim YJ, Singh H, Wang C, Hwang KH, Farh Mel-A, Yang DC. Biosynthesis, characterization, and antimicrobial applications of silver nanoparticles. *Int J Nanomedicine*. 2015 Mar 31;10:2567-77. doi: 10.2147/IJN.S72313.

Sonkusre P, Singh Cameotra S. Biogenic selenium nanoparticles inhibit *Staphylococcus aureus* adherence on different surfaces. *Colloids Surf B Biointerfaces*. 2015 Dec 1;136:1051-7. doi: 10.1016/j.colsurfb.2015.10.052.

Soo VW, Kwan BW, Quezada H, Castillo-Juárez I, Pérez-Eretza B, García-Contreras SJ, Martínez-Vázquez M, Wood TK, García-Contreras R. Repurposing of Anticancer Drugs for the Treatment of Bacterial Infections. *Curr Top Med Chem*. 2017;17(10):1157-1176. doi: 10.2174/1568026616666160930131737. Review.

Thomsen H, Benkovics G, Fenyvesi É, Farewell A, Malanga M, Ericson MB. Delivery of cyclodextrin polymers to bacterial biofilms - An exploratory study using rhodamine labelled cyclodextrins and multiphoton microscopy. *Int J Pharm*. 2017 Oct 15;531(2):650-657. doi: 10.1016/j.ijpharm.2017.06.011.

Tran PA, Webster TJ. Selenium nanoparticles inhibit *Staphylococcus aureus* growth. *Int J Nanomedicine*. 2011;6:1553-8. doi: 10.2147/IJN.S21729.

Van Acker H, Coenye T. The Role of Reactive Oxygen Species in Antibiotic-Mediated Killing of Bacteria. *Trends Microbiol*. 2017 Jun;25(6):456-466. doi: 10.1016/j.tim.2016.12.008.

Van Acker H, Sass A, Bazzini S, De Roy K, Udine C, Messiaen T, Riccardi G, Boon N, Nelis HJ, Mahenthiralingam E, Coenye T. Biofilm-grown *Burkholderia cepacia* complex cells survive antibiotic treatment by avoiding production of reactive oxygen species. *PLoS One*. 2013;8(3):e58943. doi: 10.1371/journal.pone.0058943.

Vandecandelaere I, Van Nieuwerburgh F, Deforce D, Coenye T. Metabolic activity, urease production, antibiotic resistance and virulence in dual species biofilms of *Staphylococcus epidermidis* and *Staphylococcus aureus*. *PLoS One*. 2017 Mar 6;12(3):e0172700. doi: 10.1371/journal.pone.0172700.

- Wadhvani SA, Shedbalkar UU, Singh R, Chopade BA. Biogenic selenium nanoparticles: current status and future prospects. *Appl Microbiol Biotechnol*. 2016 Mar;100(6):2555-66. doi: 10.1007/s00253-016-7300-7.
- Wan G, Ruan L, Yin Y, Yang T, Ge M, Cheng X. Effects of silver nanoparticles in combination with antibiotics on the resistant bacteria *Acinetobacter baumannii*. *Int J Nanomedicine*. 2016 Aug 12;11:3789-800. doi: 10.2147/IJN.S104166.
- Wang H, Joseph JA. Quantifying cellular oxidative stress by dichlorofluorescein assay using microplate reader. *Free Radic Biol Med*. 1999 Sep;27(5-6):612-6. PubMed PMID: 10490282.
- Wang Q, Larese-Casanova P, Webster TJ. Inhibition of various gram-positive and gram-negative bacteria growth on selenium nanoparticle coated paper towels. *Int J Nanomedicine*. 2015 Apr 13;10:2885-94. doi: 10.2147/IJN.S78466.
- Wang L, Hu C, Shao L 2017 The antimicrobial activity of nanoparticles: present situation and prospects for the future *Int J Nanomedicine*. 2017 Feb 14;12:1227-1249. doi: 10.2147/IJN.S121956.
- Wang Q, Webster TJ. Nanostructured selenium for preventing biofilm formation on polycarbonate medical devices. *J Biomed Mater Res A*. 2012 Dec;100(12):3205-10. doi: 10.1002/jbm.a.34262.
- Waters EM, Neill DR, Kaman B, Sahota JS, Clokie MRJ, Winstanley C, Kadioglu A. Phage therapy is highly effective against chronic lung infections with *Pseudomonas aeruginosa*. *Thorax*. 2017 Jul;72(7):666-667. doi:10.1136/thoraxjnl-2016-209265.
- Williams, P. 2007. Quorum sensing, communication and cross-kingdom signalling in the bacterial world. *Microbiology* 153:3923–3938.
- Wood TK. Strategies for combating persister cell and biofilm infections. *Microb Biotechnol*. 2017 Sep;10(5):1054-1056. doi: 10.1111/1751-7915.12774.
- Xavier, K. B., and B. L. Bassler. 2003. LuxS quorum sensing: more than just a numbers game. *Curr. Opin. Microbiol*. 6:191–197.
- Yu C, Hu ZQ, Peng RY. Effects and mechanisms of a microcurrent dressing on skin wound healing: a review. *Mil Med Res*. 2014;1:24.
- Yu J, Zhang W, Li Y, et al. Synthesis, characterization, antimicrobial activity and mechanism of a novel hydroxyapatite whisker/nano zinc oxide biomaterial. *Biomed Mater*. 2014;10(1):015001.
- Zarabadi MP, Paquet-Mercier F, Charette SJ, Greener J. Hydrodynamic Effects on Biofilms at the Biointerface Using a Microfluidic Electrochemical Cell: Case Study of *Pseudomonas* sp. *Langmuir*. 2017 Feb 28;33(8):2041-2049. doi: 10.1021/acs.langmuir.6b03889.
- Zhang J, Wang H, Bao Y, Zhang L. Nano red elemental selenium has no size effect in the induction of seleno-enzymes in both cultured cells and mice. *Life Sci*. 2004 May 28;75(2):237-44. PubMed PMID: 15120575.
- Zonaro E, Lampis S, Turner RJ, Qazi SJ, Vallini G. Biogenic selenium and tellurium nanoparticles synthesized by environmental microbial isolates efficaciously inhibit bacterial planktonic cultures and biofilms. *Front Microbiol*. 2015 Jun 16;6:584. doi: 10.3389/fmicb.2015.00584.

## 10. SCIENTIFIC CONTRIBUTION FROM THE PhD THESIS

# microbial biotechnology

Open Access

## Biogenic selenium nanoparticles: characterization, antimicrobial activity and effects on human dendritic cells and fibroblasts

Eleonora Cremonini,<sup>1</sup> Emanuele Zonaro,<sup>2</sup> Marta Donini,<sup>3</sup> Silvia Lampis,<sup>2</sup> Marzia Boaretti,<sup>1</sup> Stefano Dusi,<sup>3</sup> Paola Melotti,<sup>4</sup> Maria M. Lleo<sup>1,\*</sup> and Giovanni Vallin<sup>2,\*\*</sup>

<sup>1</sup>Department of Diagnostic and Public Health, University of Verona, Strada Le Grazie 8, 37134 Verona, Italy.

<sup>2</sup>Department of Biotechnology, University of Verona, Strada Le Grazie 15, 37134 Verona, Italy.

<sup>3</sup>Department of Medicine, University of Verona, Strada Le Grazie 8, 37134 Verona, Italy.

<sup>4</sup>Cystic Fibrosis Regional Center, AOUI Verona, Verona, Italy.

### Summary

Tailored nanoparticles offer a novel approach to fight antibiotic-resistant microorganisms. We analysed biogenic selenium nanoparticles (SeNPs) of bacterial origin to determine their antimicrobial activity against selected pathogens in their planktonic and biofilm states. SeNPs synthesized by Gram-negative *Stenotrophomonas maltophilia* [Sm-SeNPs(-)] and Gram-positive *Bacillus mycoides* [Bm-SeNPs(+)] were active at low minimum inhibitory concentrations against a number of clinical isolates of *Pseudomonas aeruginosa* but did not inhibit clinical isolates of the yeast species *Candida albicans* and *C. parapsilosis*. However, the SeNPs were able to inhibit biofilm formation and also to disaggregate the mature glycocalyx in both *P. aeruginosa* and *Candida* spp. The Sm-SeNPs(-) and Bm-SeNPs(+) both achieved much stronger antimicrobial effects than synthetic selenium nanoparticles (Ch-SeNPs). Dendritic cells and fibroblasts exposed to Sm-SeNPs(-), Bm-SeNPs(+) and Ch-SeNPs did not show any loss of cell viability, any increase in the release of reactive oxygen species or any significant increase in

the secretion of pro-inflammatory and immunostimulatory cytokines. Biogenic SeNPs therefore appear to be reliable candidates for safe medical applications, alone or in association with traditional antibiotics, to inhibit the growth of clinical isolates of *P. aeruginosa* or to facilitate the penetration of *P. aeruginosa* and *Candida* spp. biofilms by antimicrobial agents.

### Introduction

Resistance to antimicrobial drugs has become more widespread over the last decades resulting in a significant threat to public health. Infections caused by antibiotic-resistant bacteria need higher doses of drugs, additional toxic treatments and extended hospital stays, and ultimately result in increased mortality (Gadakh and Van Aerschoot, 2015). Despite the need for new antibiotics, only limited resources have been allocated by the pharmaceutical industry to support the discovery of new antibacterial agents, largely because the financial returns are likely to be small. To prevent or overcome antimicrobial resistance, non-antibiotic therapies will be necessary to treat bacterial infections and alternative strategies that show promise for the management of resistant infections are already under investigation (Beyth *et al.*, 2015; Gill *et al.*, 2015).

Most antibiotics that are active against free microbes are less effective against the same species when present as a biofilm. This is a particular concern because microbial biofilms play a pivotal role in many infections, and biofilm-related traits may confer high-level antibiotic resistance in microbial communities (Penesyan *et al.*, 2015). The biofilm matrix can act as a mechanical barrier, hindering the penetration of antibacterial agents and immune response effectors. However, bacteria can also become highly resistant to antibiotics as a result of nutrient limitation or the emergence of a persistent but non-growing phenotype that allows microbial cells to cope efficiently with environmental stresses, including antibiotic challenge (Grant and Hung, 2013).

Strategies that prevent biofilm formation or dispersal are not fully effective in the absence of a treatment that also counters the growth of individual cells. For this reason, a combination of anti-biofilm therapy along with traditional antibiotics that target bacterial growth offers a

Received 22 January, 2016; revised 16 May, 2016; accepted 3 June, 2016. For correspondence: \*E-mail mafa.lleo@univr.it; Tel. +390458027194; Fax +390458027101. \*\*E-mail giovanni.vallin@univr.it; Tel. +390458027098; Fax +390458027928. Eleonora Cremonini and Emanuele Zonaro contributed equally to the research.  
*Microbial Biotechnology* (2016) 0(0), 000–000  
doi:10.1111/1751-7915.12374

© 2016 The Authors. *Microbial Biotechnology* published by John Wiley & Sons Ltd and Society for Applied Microbiology. This is an open access article under the terms of the Creative Commons Attribution License, which permits use, distribution and reproduction in any medium, provided the original work is properly cited.



promising approach for the control of biofilm-related infectious diseases. In such combination approaches, the anti-biofilm agent would force microbes into their planktonic growth state, thus facilitating the targeting of pathogens at the cellular level with traditional antibiotics (Kostakioti *et al.*, 2013).

Recent developments in nanotechnology allow the production of tailored metal/metalloid nanoparticles with physicochemical properties that can inhibit microorganisms. These nanoparticles have been shown to overcome existing drug resistance mechanisms, including slow drug uptake and accelerated efflux, biofilm formation and intracellular bacterial parasitism (Pelgrift and Friedman, 2013). In this context, selenium nanoparticles (SeNPs) possess antibacterial, antiviral and antioxidant properties, suggesting they could be suitable as therapeutic candidates to combat infectious diseases. In particular, nanostructured particles can be synthesized using bacterial and fungal cells as biological catalysts, providing a non-toxic and environmentally beneficial approach for the production of nanoparticles, including SeNPs (Xiangqian *et al.*, 2011). Several microbial strains can reduce the toxic selenite oxyanion to the less toxic elemental selenium through the formation of either intracellular or extracellular SeNPs, with a typical spherical shape and a diameter of 50–400 nm (Lampis *et al.*, 2014). Furthermore, recent studies with biogenic SeNPs have demonstrated that the particles have anti-biofilm activity against clinical isolates of bacterial pathogens (Shakibaie *et al.*, 2015). However, their antibacterial effects are not fully understood and their potential toxicity towards human tissues requires further investigation.

Another potential limitation affecting the clinical application of metal/metalloid nanoparticles is the ability of some nanostructured materials to stimulate the release, by dendritic cells (DCs) and other cells in the immune system, of reactive oxygen species and/or chemical mediators that trigger unwanted side-effects such as hypersensitivity reactions, autoimmune diseases and inflammatory responses (Chang and Gershwin, 2010; Di Gioacchino *et al.*, 2011). In particular, activated DCs produce oxygen free radicals that can cause severe tissue damage (Vulcano *et al.*, 2004; Donini *et al.*, 2007), and may also release cytokines that play a key role in the induction of inflammatory and immune responses (Elmqvist *et al.*, 1997; Suffredini *et al.*, 1999; Granucci *et al.*, 2008; Schäkel, 2009; Vignali and Kuchroo, 2012). Therefore, nanoparticle candidates suitable for clinical applications must not induce DC activation or have toxic effects against cells of the immune system and other tissues.

Here, SeNPs generated by two environmental bacterial isolates, namely a strain of the Gram-positive species *Bacillus mycoides* (Bm-SeNPs(+)) and a strain of the Gram-negative species *Stenotrophomonas maltophilia*

(Sm-SeNPs(-)), were compared with chemically synthesized SeNPs (Ch-SeNPs) in terms of their physical and biological properties, including toxicity and immunostimulatory activity *in vitro* against cultures of human DCs and fibroblasts. The antibacterial and anti-biofilm characteristics of the SeNPs were tested against clinical strains of *Pseudomonas aeruginosa* and clinical isolates of two *Candida* species.

## Results and discussion

### Biosynthesis and characterization of SeNPs

Biogenic SeNPs were produced by exploiting the selenite reduction capability of two different environmental bacterial isolates, namely *B. mycoides* SeITE01 and *S. maltophilia* SeITE02. The biogenic SeNPs were compared with synthetic Ch-SeNPs in terms of their physicochemical characteristics. Scanning electron microscopy (SEM) analysis indicated that all three SeNPs were spherical and EDAX microanalysis of the purified SeNPs revealed the characteristic selenium absorption peaks at 1.37 (SeL $\alpha$ ), 11.22 (SeK $\alpha$ ) and 12.49 keV (SeK $\beta$ ) (Fig. 1). Moreover, SeNPs differently synthesized showed different elemental composition (Table 1). For instance, biogenic SeNPs showed a selenium percentage in weight of 11.01% and 9.26% for Sm-SeNPs(-) and Bm-SeNPs(+) respectively. On the other hand, Ch-SeNPs exhibited a higher percentage in selenium, 31.61%. Furthermore, the composition of biogenic SeNPs, which were rich in C, O, P and S, suggests the presence of biological macromolecules surrounding the nanomaterials. Based on the presence and percentage of C, O and S, it is possible to hypothesize that biogenic SeNPs cap include proteins or enzymes and also some cellular residues and membrane phospholipids (P peaks). In particular, a tentative composition of the biomolecular capping surrounding SeNPs biosynthesized by *S. maltophilia* SeITE02 has been already reported. Actually, Fourier transform infrared spectroscopy (FTIR) analysis of Sm-SeNPs(-) evidenced the presence of proteins, lipids and carbohydrates associated with the nanomaterial (Lampis *et al.*, 2016).

In Ch-SeNPs, the same elements are present in different percentage: 60.91% in weight of C, 4.97% in weight of O, 1.88% in weight of P and 0.63% in weight of S: this is probably due to the procedure used for the synthesis.

Dynamic light scattering measurements indicated average sizes of  $170.6 \pm 35.12$  nm for the Sm-SeNPs(-),  $160.6 \pm 52.24$  nm for the Bm-SeNPs(+) and  $102.5 \pm 29.44$  nm for the Ch-SeNPs (Fig. 2).

All three SeNPs generated large negative zeta potentials (between -70 and -80 mV) in solution (Fig. 2) suggesting they are unlikely to form aggregates as a

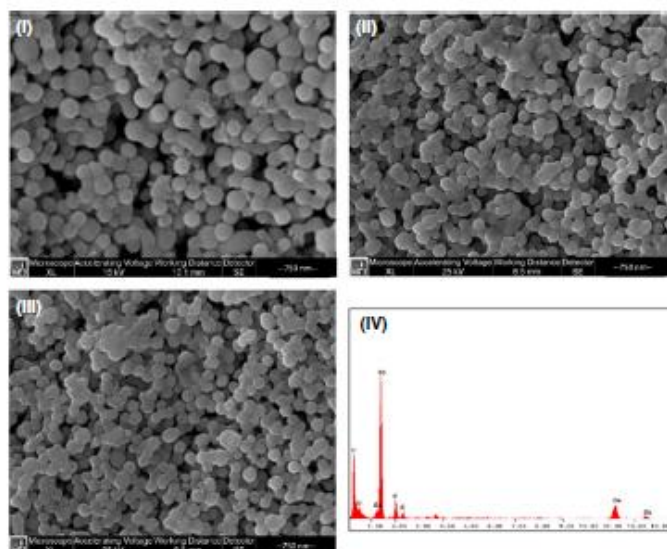


**Fig. 1.** Scanning electron microscopy analysis of SeNPs produced by *Stenotrophomonas maltophilia* SeITE02 (I), SeNPs produced by *Bacillus mycoides* SeITE01 (II) and chemically synthesized SeNPs (III). EDX analysis of biogenic SeNPs (IV).

**Table 1.** Elemental composition of Ch-SeNPs, Sm-SeNPs(–) and Bm-SeNPs(+) calculated through EDX analysis.

Element	Ch-SeNPs	Sm-SeNPs(–)	Bm-SeNPs(+)
C	60.91	73.13	75.75
O	4.97	10.44	10.82
Se	31.61	11.01	9.26
P	1.88	4.42	3.14
S	0.63	1.00	1.04

consequence of their electrostatic stability. Neutral and negatively charged NPs tend to have long half-lives in human serum and are not taken up by cells in a non-specific manner (Alexis *et al.*, 2008). This is important in the context of potential *in vivo* applications as antimicrobial reagents.

#### Determination of the minimum inhibitory concentration for SeNPs against *Pseudomonas aeruginosa* PAO1

In order to evaluate the effect of biogenic and synthetic SeNPs as antimicrobial agents, as well as to study the putative role of the biomolecular cap of the biogenic nanoparticles, the determination of minimum inhibitory concentration (MIC) values was first carried out against the reference strain *Pseudomonas aeruginosa* PAO1 (Table 2). MIC determination was carried out for the biogenic SeNPs, Sm-SeNPs(–) and Bm-SeNPs(+), the chemically synthesized Ch-SeNPs, the Ch-SeNPs

exposed to cell free extract (CFX) of *S. maltophilia* SeITE02 (CFX(Sm)-SeNPs) and *B. mycoides* SeITE01 (CFX(Bm)-SeNPs) and CFX of *S. maltophilia* SeITE02 (CFX(Sm)) and *B. mycoides* SeITE01 (CFX(Bm)) alone.

As we can see from Table 2, Ch-SeNPs, Sm-SeNPs(–) and Bm-SeNPs(+) evidenced a similar MIC value of  $128 \mu\text{g ml}^{-1}$ . On the other hand, CFX(Sm)-SeNPs and CFX(Bm)-SeNPs showed a lower activity towards the reference strain, with a MIC value of  $256 \mu\text{g ml}^{-1}$ . Finally, CFX from both *S. maltophilia* SeITE02 and *B. mycoides* SeITE01 did not exhibit antimicrobial activity at any of the concentration tested in the present analysis. These results clearly indicate that the antimicrobial activity observed is exactly due to the nanoparticles and the biomolecular cap to them associated through the biosynthetic mechanism. Several studies have already analysed the antimicrobial activity of SeNPs synthesized chemically towards different pathogenic bacterial strains. For instance, chemically synthesized SeNPs were able to inhibit the growth of *Staphylococcus aureus* (Tran and Webster, 2011), with higher efficiency than silver phosphate nanoparticles (Chudobova *et al.*, 2014).

#### Antimicrobial activity of SeNPs against clinical isolates of *P. aeruginosa* and *Candida* spp.

To test the antibacterial and anti-biofilm activity of the SeNPs, we selected a series of clinical strains of *P. aeruginosa*, whose surrounding polysaccharide biofilm

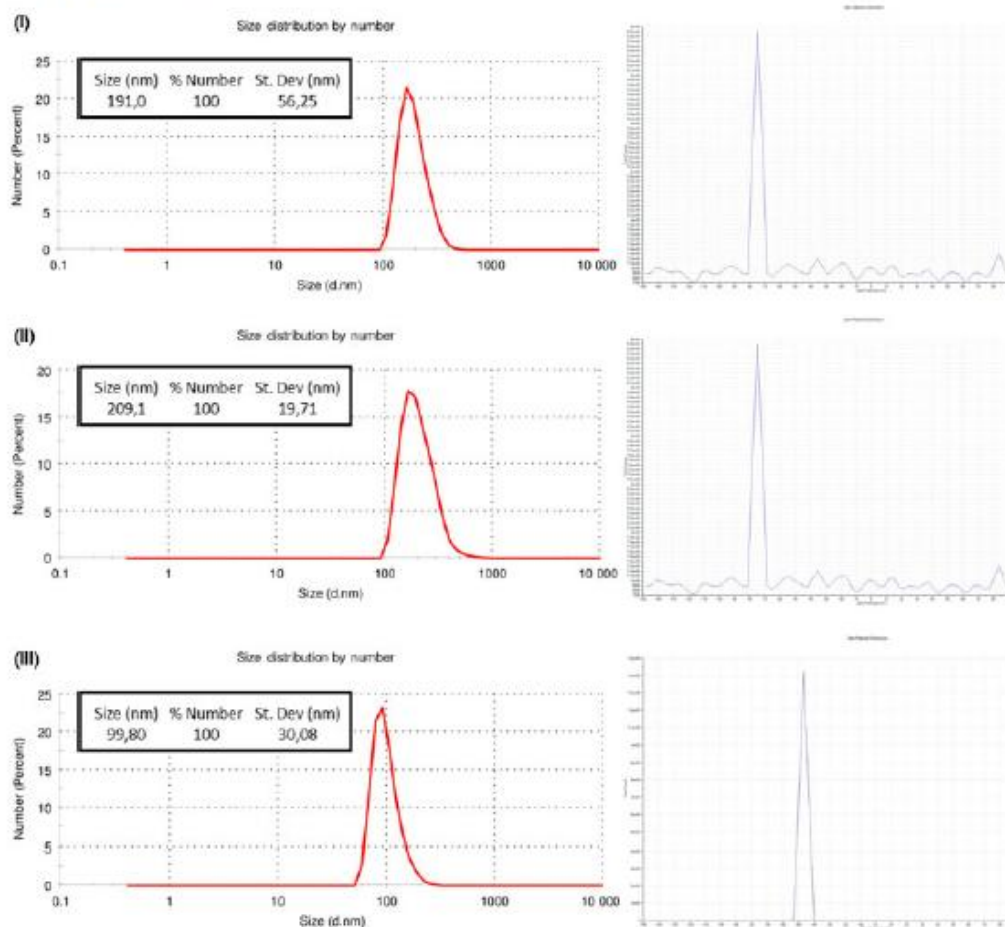


Fig. 2. Dynamic light scattering analysis and zeta potential of SeNPs produced by *Stenotrophomonas maltophilia* SeTE02 (I), SeNPs produced by *Bacillus mycoides* SeTED1 (II) and chemically synthesized SeNPs (III).

Table 2. Minimum inhibitory concentration (MIC) of Ch-SeNPs, Ch2-SeNPs, Sm-SeNPs(-), Bm-SeNPs(+), CFX(Sm)-SeNPs, CFX(Bm)-SeNPs, CFX(Sm) and CFX(Bm) against *Pseudomonas aeruginosa* PAO1.

Strain	Ch-SeNPs MIC ( $\mu\text{g ml}^{-1}$ )	Ch2-SeNPs MIC ( $\mu\text{g ml}^{-1}$ )	Sm-SeNPs(-) MIC ( $\mu\text{g ml}^{-1}$ )	Bm-SeNPs(+) MIC ( $\mu\text{g ml}^{-1}$ )	CFX(Sm)- SeNPs MIC ( $\mu\text{g ml}^{-1}$ )	CFX(Bm)- SeNPs MIC ( $\mu\text{g ml}^{-1}$ )	CFX(Sm) MIC ( $\mu\text{l ml}^{-1}$ )	CFX(Bm) MIC ( $\mu\text{l ml}^{-1}$ )
<i>Pseudomonas aeruginosa</i> PAO1	128	128	128	128	256	256	>512	>512

matrix confers resistance to eradication by antibiotics and clearance by the immune system. Such strains are recurrent in the chronic lung infections that characterize

cystic fibrosis, chronic obstructive pulmonary disease and asthma (Ciofu *et al.*, 2015). The multidrug-resistant isolate *P. aeruginosa* INT was chosen to provide a



particularly challenging target, whereas *P. aeruginosa* PAO1 and ATCC 27853 were included as reference strains. The ability of SeNPs to inhibit bacterial growth was tested by challenging the bacterial isolates and reference strains with different concentrations of SeNPs, then determining the MIC using the agar well diffusion assay and the broth dilution method.

As shown in Table 3, the MIC of Sm-SeNPs(-) varied widely among the different *P. aeruginosa* strains, ranging from 8 to 16  $\mu\text{g ml}^{-1}$  in strains isolated from low respiratory tract infections (CFC20, CFC21, CFCA and CFCB) to 128–512  $\mu\text{g ml}^{-1}$  against *P. aeruginosa* INT and both the reference strains. The MIC of Bm-SeNPs(+) also varied among the strains but was generally 2–4 times higher than Sm-SeNPs (Table 3). The MIC of Ch-SeNPs indicated that these SeNPs have no effect on the growth of *P. aeruginosa* (Table 3).

The susceptibility of the reference strains *P. aeruginosa* PAO1 and ATCC 27853 to Sm-SeNPs(-) was determined in a previous study and the reported MIC values were slightly different to those we observed (250  $\mu\text{g ml}^{-1}$ ) (Zonaro *et al.*, 2015). The difference probably reflects the distinct methods used to determine the MIC in each study and the use of different growth media, which is known to affect the toxicity of NPs (Loza *et al.*, 2014).

We found that *P. aeruginosa* clinical strains CFC20, CFC21, CFCA and CFCB were susceptible to Sm-SeNPs with MIC values in the range 2.5–20  $\mu\text{g ml}^{-1}$ , which is broadly in agreement with previous reports dealing with other nanoparticles (Habash *et al.*, 2014; Tomita *et al.*, 2014). Because these MIC values fall within the range of clinical exposures adopted during typical antibiotic treatments, biogenic SeNPs could be used to treat antibiotic-resistant clinical strains, eventually overcoming the potential risks of antibiotic resistance (Table 3). Our analysis of

antibiotic susceptibility carried out according to Clinical and Laboratory Standards Institute standard methods (Jorgensen and Ferraro, 2009) demonstrated that the four *P. aeruginosa* clinical strains were resistant to beta-lactams (MIC values varying between 16 and  $\geq 64 \mu\text{g ml}^{-1}$ ) and other antibiotics such as gentamicin (MIC values 8–16  $\mu\text{g ml}^{-1}$ ), ciprofloxacin (MICs between 2 and  $\geq 4 \mu\text{g ml}^{-1}$ ) and sulphonamides (MIC values 40–80  $\mu\text{g ml}^{-1}$ ).

Conversely, given the much higher MIC for *P. aeruginosa* INT ( $> 250 \mu\text{g ml}^{-1}$ ) compared with the clinical strains, it is unlikely that SeNPs could solve the problem of antibiotic resistance in this isolate.

We also evaluated the anti-fungal activity of SeNPs by testing *in vitro* their ability to inhibit the growth of *C. albicans* and *C. parapsilosis* clinical strains. The MIC values were very high ( $> 256 \mu\text{g ml}^{-1}$ ) indicating that SeNPs do not inhibit the growth of these yeast strains.

#### Inhibition of *P. aeruginosa* and *Candida* spp. biofilm formation by SeNPs

To analyse the effect of SeNPs on biofilm synthesis, the *P. aeruginosa* strains and the two *Candida* species were treated for 48 h at 37°C with different concentrations of Bm-SeNPs(+), Sm-SeNPs(-) and Ch-SeNPs, and biofilm formation was quantified by methylene blue staining. The percentage of biofilm inhibition was calculated by comparing the microbial cultures exposed to the SeNPs with the same strains growing in the absence of SeNPs.

The quantity of biofilm produced by *P. aeruginosa* strains CFCA and CFCB was greater than that produced by the other *P. aeruginosa* strains and by the yeast isolates, when values were averaged over six experiments (Table 4). The lowest concentrations of biogenic SeNPs (50 and 100  $\mu\text{g ml}^{-1}$ ) inhibited biofilm synthesis by *P. aeruginosa* strains CFC20, CFC21 and CFCA by 70–90%, indicating that they are particularly sensitive to the SeNPs. In contrast, clinical strains CFCB and INT, as well as the reference strains, were more resistant to the SeNPs, showing the significant inhibition of biofilm synthesis (at least 70%) only in the presence of SeNP concentrations  $\geq 250 \mu\text{g ml}^{-1}$ . Table 4 also shows that Sm-SeNPs(-) were usually more potent than Bm-SeNPs(+), and that the synthetic Ch-SeNPs were only active at concentrations of 250–500  $\mu\text{g ml}^{-1}$  against most strains, the exception being *P. aeruginosa* CFC20, which was the most susceptible isolate tested.

Interestingly, the lowest SeNP dose we tested (50  $\mu\text{g ml}^{-1}$ ) was sufficient for 60–70% biofilm inhibition in the two yeast isolates, and no significant improvement was achieved at the higher doses of 100 and 250  $\mu\text{g ml}^{-1}$  (Table 5). Sm-SeNPs(-) and Bm-SeNPs(+) had similar effects on biofilm formation in the yeast

**Table 3.** Minimal inhibitory concentrations (MICs) for *Stenotrophomonas maltophilia* (Sm)-SeNPs, *Bacillus mycoides* (Bm)-SeNPs and chemically synthesized (Ch)-SeNPs tested against different microbial strains isolated from clinical samples. MIC values in the clinical usage range are in bold.

Bacterial strain/ <i>Candida</i> species	MIC ( $\mu\text{g ml}^{-1}$ )		
	Sm-SeNPs	Bm-SeNPs	Ch-SeNPs
<i>Pseudomonas aeruginosa</i> PAO1	128	128	128
<i>P. aeruginosa</i> ATCC27853	512	512	>512
<i>P. aeruginosa</i> INT	256	512	>512
<i>P. aeruginosa</i> CFC20	<b>16</b>	<b>64</b>	128
<i>P. aeruginosa</i> CFC21	<b>8</b>	<b>32</b>	128
<i>P. aeruginosa</i> CFCB	<b>16</b>	<b>32</b>	>128
<i>P. aeruginosa</i> CFCA	<b>16</b>	<b>64</b>	>128
<i>Candida albicans</i>	256	512	>512
<i>C. parapsilosis</i>	512	512	>512

Table 4. Percentage of biofilm synthesis inhibition in different bacteria strains caused by Sm-SeNPs, Bm-SeNPs and Ch-SeNPs.

Bacterial strain <sup>a</sup>	Stenotrophomonas maltophilia-SeNPs ( $\mu\text{g ml}^{-1}$ )					Bacillus mycoides-SeNPs ( $\mu\text{g ml}^{-1}$ )					Chemically synthesized SeNPs ( $\mu\text{g ml}^{-1}$ )				
	50	100	250	500	500	50	100	250	500	500	50	100	250	500	500
<i>Pseudomonas aeruginosa</i> PAO1 (1,10)	40 ± 2.5	45 ± 3	70 ± 2.5	96 ± 1	96 ± 1.2	33 ± 3	47 ± 6	63 ± 4.5	96 ± 1.2	96 ± 1.4	9 ± 0.7	21 ± 2.1	74 ± 0.7	96 ± 1.4	96 ± 1.4
<i>P. aeruginosa</i> ATCC27853 (1,100)	15 ± 0.7	30 ± 0.7	41 ± 0.7	66 ± 2.1	64 ± 1	15 ± 4.2	17 ± 2	44 ± 2.8	64 ± 1	44 ± 2	4 ± 1.4	10 ± 0.7	35 ± 2.1	44 ± 2	44 ± 2
<i>P. aeruginosa</i> INT (1,00)	23 ± 1	34 ± 1	59 ± 3.5	95 ± 1	94 ± 1.5	25 ± 4.5	29 ± 3.5	49 ± 2.5	94 ± 1.5	20 ± 0.7	2 ± 3.5	2 ± 1.4	20 ± 0.7	30 ± 0.7	30 ± 0.7
<i>P. aeruginosa</i> CFC21 (1,20)	66 ± 5	86 ± 0.5	96 ± 2	96 ± 1.5	95 ± 2	37 ± 5.5	68 ± 3.5	93 ± 1.7	95 ± 2	71 ± 1.4	10 ± 3.5	33 ± 3.5	71 ± 1.4	65 ± 1.4	65 ± 1.4
<i>P. aeruginosa</i> CFC20 (1,10)	75 ± 0.5	82 ± 1	96 ± 1	93 ± 1.5	91 ± 2	72 ± 2	76 ± 0.5	85 ± 1	91 ± 2	95 ± 1	53 ± 0.7	81 ± 0.7	95 ± 1	95 ± 1	95 ± 1
<i>P. aeruginosa</i> CFCB (2,75)	31 ± 1	69 ± 3	79 ± 2	88 ± 4	86 ± 5	28 ± 1.5	34 ± 5	81 ± 4.5	86 ± 5	77 ± 0.7	1 ± 0.5	1 ± 0.5	77 ± 0.7	98 ± 1	98 ± 1
<i>P. aeruginosa</i> CFCB (3,00)	39 ± 1	94 ± 1	94 ± 3.5	96 ± 1	96 ± 1	25 ± 5	25 ± 1.5	94 ± 0.5	96 ± 1	96 ± 1	5 ± 0.7	6 ± 0.7	96 ± 1	97 ± 1.5	97 ± 1.5

a. Quantity of biofilm in arbitrary units.

The percentage of inhibition was calculated relative to the quantity of biofilm formed by each strain in the absence of nanoparticles. Data are the average of results obtained in three different experiments. Percentages of inhibition higher than 80% are shown in bold.

strains, whereas the Ch-SeNPs had no significant effect (Table 5). Previous investigation on the anti-fungal effect of biogenic SeNPs synthesized by *Klebsiella pneumoniae* on *C. albicans* strain TUMS R152 showed a MIC of  $2000 \mu\text{g ml}^{-1}$  (Kazempour *et al.*, 2013), a value higher than the concentrations tested in this analysis. Contrarily to recent results evidencing a clear anti-fungal activity of nanoparticles of different metals obtained by chemical synthesis (Lara *et al.*, 2015), chemically synthesized SeNPs, although capable of antimicrobial activity against a number of nosocomial bacterial pathogens, were not efficacious towards the pathogenic yeasts tested, namely *C. albicans* and *C. parapsilosis*. In the present study, proteins associated to SeNPs of biogenic nature (Wang *et al.*, 2010) apparently played a role in the anti-fungal activity against yeasts that seemed — on the other hand — not to be affected by chemically synthesized SeNPs. The anti-fungal activity of the biogenic SeNPs assayed was probably due to the disruptive interaction of their organic coat with the yeast outer wall layer, containing in *Candida* sp. mainly mannans and phosphorylated mannans. Permeabilization of the cell wall and subsequent disaggregation of the structural layers of the outer fungal cell wall are likely to be occurred. Nevertheless, the toxicity of metal nanoparticles towards yeasts and the associated toxic mechanisms remain controversial, and further investigation is needed in this area. Particularly, the cell wall constitutes the primary site for direct interaction with nanoparticles. Changes in yeast cell wall structure have been reported in response to many factors, e.g. growth conditions, mode of cultivation, compounds that block cell wall synthesis and anti-fungal substances. However, there is a lack of information concerning changes in the cell wall composition in response to nanoparticle exposure (Sun *et al.*, 2014).

#### Degradation of *P. aeruginosa* and *Candida* spp. biofilms by SeNPs

We next investigated whether the SeNPs were able to cause the degradation of biofilms by measuring the amount of biofilm remaining after exposing the synthesized exopolysaccharide to different concentrations of biogenic and synthetic SeNPs (Table 6 and Table 7). The *P. aeruginosa* CFC20 biofilm was highly susceptible to SeNP-induced disaggregation, resulting in 90% degradation in the presence of  $50 \mu\text{g ml}^{-1}$  SeNPs, confirming that this strain is more susceptible to SeNPs than the other strains. The exposure of the other *P. aeruginosa* strains to  $50$ – $100 \mu\text{g ml}^{-1}$  SeNPs resulted in  $50$ – $70\%$  biofilm degradation, and this did not increase at higher SeNP concentrations. Sm-SeNPs(–) were slightly more efficient than Bm-SeNPs(+) in the eradication of *P. aeruginosa* biofilms. Similarly, the biogenic SeNPs

**Table 5.** Percentage of biofilm synthesis inhibition in different fungal strains caused by Sm-SeNPs, Bm-SeNPs and Ch-SeNPs.

	15	30	50	60	100	120	250	325	400	500
Sm-SeNPs (-) $\mu\text{g ml}^{-1}$										
<i>Candida albicans</i>	40 ± 0.7	45 ± 0.5	61 ± 0.5	59 ± 0.7	60 ± 3	69 ± 1	60 ± 1	65 ± 2	77 ± 1	<b>94 ± 1</b>
<i>C. parapsilosis</i>	9 ± 3	42 ± 1	72 ± 1.5	60 ± 1.5	79 ± 0.5	70 ± 1	73 ± 1	72 ± 1	79 ± 3	<b>95 ± 1</b>
Bm-SeNPs(-) $\mu\text{g ml}^{-1}$										
<i>C. albicans</i>	51 ± 2	55 ± 2	60 ± 6.5	63 ± 3	69 ± 2	68 ± 2	74 ± 2.5	74 ± 1.5	<b>82 ± 0.5</b>	<b>93 ± 0.5</b>
<i>C. parapsilosis</i>	33 ± 2	49 ± 1	75 ± 1.5	70 ± 2.5	73 ± 0.5	70 ± 2	72 ± 3	71 ± 2	77 ± 1.5	<b>94 ± 0.5</b>
Ch-SeNPs(-) $\mu\text{g ml}^{-1}$										
<i>C. albicans</i>	0	0	0	0	0	0	0	0	5 ± 0.9	9 ± 0.7
<i>C. parapsilosis</i>	0	0	0	0	0	0	0	0	4 ± 1	5 ± 0.7

The percentage of inhibition was calculated relative to the quantity of biofilm formed by each strain in the absence of nanoparticles. Data are the average of results obtained in three different experiments. Percentages of inhibition higher than 80% are shown in bold.

eradicated 45–60% of the yeast biofilms at the lowest SeNP doses (50–100  $\mu\text{g ml}^{-1}$ ) and there was no improvement at higher doses. There was no significant difference in efficacy between the two types of biogenic SeNPs.

The comparison of SeNPs from different origins provides insights into the optimization of strategies to inhibit the synthesis of biofilms or destroy biofilms that already exist. Biogenic SeNPs at concentrations of 50–100  $\mu\text{g ml}^{-1}$  can suppress the synthesis of biofilms in three of the five clinical isolates of *P. aeruginosa* we tested, as well as two *Candida* species. SeNPs synthesized by the Gram-negative bacterium *S. maltophilia* SeITE02 were slightly more efficacious than those produced by the Gram-positive species *B. mycoides* SeITE01, although at concentrations  $\geq 250 \mu\text{g ml}^{-1}$  both SeNPs were remarkably potent. Nevertheless, different clinical isolates of *P. aeruginosa* varied in susceptibility at physiologically compatible concentrations of biogenic SeNPs. The most potent disaggregation effects (45–70%) against both *P. aeruginosa* and yeast were observed at a SeNP concentration of 100  $\mu\text{g ml}^{-1}$ , and higher doses did not achieve greater activity. The disaggregation of *P. aeruginosa* biofilms by SeNPs also showed strain-dependent efficacy, with strain CFC20 appearing particularly susceptible to biofilm disintegration probably due to the synthesis of a fragile exopolysaccharide matrix compared with the tougher and physically more resistant exopolysaccharide formations of the other isolates. Generally, the biogenic SeNPs at concentrations of 50–100  $\mu\text{g ml}^{-1}$  (and the Sm-SeNPs(-) in particular) were more effective in the destruction of existing biofilm structures than the inhibition of biofilm synthesis. This suggests that the anti-biofilm mechanism of these nanomaterials is possibly targeted to a component of the mature biofilm structure. The biogenic SeNPs were more effective than synthetic counterparts, indicating that organic molecules on the surface are likely to contribute to their antimicrobial activities and enhance the effect of the inorganic selenium component.

#### Effects of SeNPs on human cells

Some nanoparticles are known to be cytotoxic or to stimulate human cells, resulting in harmful off-target effects (Chang and Gershwin, 2010; Di Gioacchino *et al.*, 2011). The biogenic SeNPs in this study contain organic substances of bacterial origin, so it is necessary to determine whether they can damage human cells, or stimulate unanticipated effects, in the latter case particularly in immune system cells that recognize foreign structures and respond in order to neutralize and eliminate pathogens. We therefore investigated whether Sm-SeNPs(-) and Bm-SeNPs(+), as well as Ch-SeNPs lacking biogenic molecules, affected the viability and activity of DCs. These are immune system cells that are fundamentally involved in the orchestration of inflammatory and immune response (Granucci *et al.*, 2008; Schäkel, 2009). Human blood monocytes were cultured for 5 days in the presence of GM-CSF and interleukin 4 (IL-4) to obtain DCs, which were then challenged with different doses of SeNPs or with the bacterial immunostimulator LPS as a positive control. We also analysed the effect of SeNPs on the viability and activity of cultured human fibroblasts to determine whether SeNPs have adverse effects on non-immune cells. Cell viability was assessed using Alamar blue, a colorimetric redox assay of metabolic activity. Different concentrations of the biogenic SeNPs (and Ch-SeNPs) did not induce apoptosis in cultured DCs or fibroblasts, even at the highest dose of 500  $\mu\text{g ml}^{-1}$ , which is atypically high for standard *in vitro* cell stimulation protocols (Fig. 3).

We then investigated whether SeNPs stimulate DCs to release of pro-inflammatory and immunostimulatory cytokines (particularly those involved in the activation of inflammatory and immune responses), such as IL-12 which stimulates natural killer cells and T lymphocytes (Vignali and Kuchroo, 2012), IL-8 which causes leucocyte chemotaxis and activation (Admyre *et al.*, 2015), as well as IL-6 and TNF- $\alpha$  which elicit inflammation and the systemic acute phase reaction, characterized by fever,



Table 6. Percentages of biofilm degradation in different bacteria strains caused by Sm-SeNPs, Bm-SeNPs and Ch-SeNPs.

Bacterial strain <sup>a</sup>	Stenotrophomonas maltophilia-SeNPs ( $\mu\text{g ml}^{-1}$ )					Bacillus mycoides-SeNPs ( $\mu\text{g ml}^{-1}$ )					Chemically synthesized SeNPs ( $\mu\text{g ml}^{-1}$ )				
	50	100	250	500	500	50	100	250	500	500	50	100	250	500	500
<i>Pseudomonas aeruginosa</i> PAO1 (1,10)	73 ± 5	72 ± 2	76 ± 2	73 ± 5	73 ± 5	52 ± 1	62 ± 4.5	57 ± 1	73 ± 6	73 ± 6	16 ± 0.7	18 ± 4.2	37 ± 0.7	53 ± 1	53 ± 1
<i>P. aeruginosa</i> ATCC27853 (1,00)	49 ± 1.4	53 ± 1.4	53 ± 1.4	43 ± 0.7	43 ± 1.4	31 ± 4.9	43 ± 1.4	51 ± 7	55 ± 7	55 ± 7	23 ± 1.4	35 ± 1	40 ± 2.5	46 ± 0.7	46 ± 0.7
<i>P. aeruginosa</i> INT (1,00)	63 ± 5.5	53 ± 0.5	61 ± 1.5	41 ± 4.5	44 ± 0.5	65 ± 4.5	44 ± 0.5	58.2 ± 3	32 ± 1.5	32 ± 1.5	15 ± 6.3	15 ± 6.3	8 ± 2.8	8 ± 2.8	8 ± 2.8
<i>P. aeruginosa</i> CFC21 (1,20)	21 ± 1	45 ± 3.5	53 ± 5.5	63 ± 2	44 ± 4.5	16 ± 3	16 ± 3	33 ± 1.5	61 ± 0.5	61 ± 0.5	8 ± 1.4	5 ± 0.7	16 ± 1.4	1 ± 0.7	1 ± 0.7
<i>P. aeruginosa</i> CFC20 (1,10)	<b>97 ± 3</b>	<b>84 ± 0.5</b>	<b>85 ± 1</b>	<b>85 ± 0.5</b>	<b>80 ± 1</b>	<b>86 ± 1</b>	<b>86 ± 1</b>	<b>86 ± 1.7</b>	<b>82 ± 2</b>	<b>82 ± 2</b>	17 ± 3.5	13 ± 2.8	29 ± 4.2	50 ± 2.8	50 ± 2.8
<i>P. aeruginosa</i> CFCB (2,75)	53 ± 4	58 ± 3	56 ± 3	64 ± 2	25 ± 1	27 ± 5	27 ± 5	51 ± 2.5	47 ± 3	47 ± 3	0	4 ± 1.4	57 ± 1.4	72 ± 0.7	72 ± 0.7
<i>P. aeruginosa</i> CFC A (3,00)	44 ± 2.5	44 ± 2.5	39 ± 1	53 ± 2	28 ± 4	20 ± 2.5	20 ± 2.5	40 ± 2.5	53 ± 1	53 ± 1	0	2 ± 0.7	66 ± 0.7	73 ± 0.7	73 ± 0.7

a. Quantity of biofilm in arbitrary unit.

The percentage of degradation was calculated relative to the quantity of biofilm formed by each strain in the absence of nanoparticles. Data represent the means of three different experiments. Percentages of biofilm degradation higher than 80% are shown in bold.

headache, anorexia, nausea, emesis and changes in the sleep-wake cycle (Elmqvist *et al.*, 1997; Suffredini *et al.*, 1999).

The analysis of DC culture supernatants by enzyme-linked immunosorbent assay (ELISA) revealed that SeNPs did not induce a significant increase in the release of IL-12, IL-6, IL-8 or tumor necrosis factor alpha (TNF- $\alpha$ ) until the doses reached 250–500  $\mu\text{g ml}^{-1}$ , which are unlikely to be achieved *in vivo* (Fig. 4). Cytokine release was stimulated more efficiently when DCs were challenged with Sm-SeNPs(-) rather than Bm-SeNPs(+), but bacterial LPS had a much more potent effect. Interestingly, the synthetic SeNPs did not induce the release of cytokines at any dose, suggesting that inorganic selenium is unable to stimulate human DCs alone and that organic molecules on the surface of biogenic SeNPs must be responsible for the observed effect. The identity of these organic molecules will be the subject of future research. We also explored whether SeNPs influence the release of pro-inflammatory cytokines by human fibroblasts. We found that neither the biogenic SeNPs nor the Ch-SeNPs induced the secretion of IL-8, IL-6 or TNF- $\alpha$  by fibroblasts (data not shown), whereas 1  $\mu\text{g ml}^{-1}$  LPS as a positive control induced human fibroblasts to secrete all three of these cytokines (data not shown).

Activated human DCs can also release remarkable quantities of reactive oxygen species that cause oxidative damage to neighbouring cells (Vulcano *et al.*, 2004; Donini *et al.*, 2007). We therefore investigated whether SeNPs were able to induce human DCs to produce oxygen radicals using the cytochrome *c* reaction assay to measure the quantity of superoxide anion release by the cells (Vulcano *et al.*, 2004). We found that neither the biogenic SeNPs nor the Ch-SeNPs induced the release of superoxide anions by DCs, whereas microbial cell wall glucan, which is known to promote the release of superoxide anions by immune system cells (Gantner *et al.*, 2003; Donini *et al.*, 2007) was able to achieve this effect (data not shown). Collectively, our results demonstrate that although SeNPs inhibit bacterial growth, they are unable to cause significant damage to human DCs and fibroblasts or to stimulate the release of cytokines or reactive oxygen species from the same cells, making them suitable candidates for further development as *in vivo* antimicrobial reagents.

## Conclusions

We have demonstrated that SeNPs synthesized by both *B. mycoides* SeTE01 and *S. maltophilia* SeTE02 possess potent antibacterial activities with low MIC values against a number of clinical strains of *P. aeruginosa*, but no biocidal effects against two clinical isolates of

**Table 7.** Percentages of biofilm degradation in different fungal strains caused by Sm-SeNPs, Bm-SeNPs and Ch-SeNPs.

	15	30	50	60	100	120	250	325	400	500
Sm-SeNPs(-) $\mu\text{g ml}^{-1}$										
<i>Candida albicans</i>	0	5 $\pm$ 0.5	26 $\pm$ 2.5	30 $\pm$ 1	43 $\pm$ 2.5	30 $\pm$ 1.4	47 $\pm$ 3.5	49 $\pm$ 2	55 $\pm$ 3	60 $\pm$ 2
<i>C. parapsilosis</i>	0	0	52 $\pm$ 2	48 $\pm$ 1.4	48 $\pm$ 1.5	43 $\pm$ 1.5	48 $\pm$ 2.5	50 $\pm$ 0.5	59 $\pm$ 2.5	64 $\pm$ 2
Bm-SeNPs(-) $\mu\text{g ml}^{-1}$										
<i>C. albicans</i>	0	0	11 $\pm$ 2.5	12 $\pm$ 2	32 $\pm$ 2	41 $\pm$ 2	48 $\pm$ 1.5	51 $\pm$ 2	61 $\pm$ 1	60 $\pm$ 3.5
<i>C. parapsilosis</i>	0	0	48 $\pm$ 3	42 $\pm$ 1.5	38 $\pm$ 2	43 $\pm$ 1.5	47 $\pm$ 2	44 $\pm$ 1.5	47 $\pm$ 2	42 $\pm$ 2.5
Ch-SeNPs(-) $\mu\text{g ml}^{-1}$										
<i>C. albicans</i>	0	0	0	0	0	0	2	0	0	0
<i>C. parapsilosis</i>	0	0	0	0	1	0	0	0	0	0

The percentage of degradation was calculated relative to the quantity of biofilm formed by each strain in the absence of nanoparticles. Data represent the means of three different experiments.

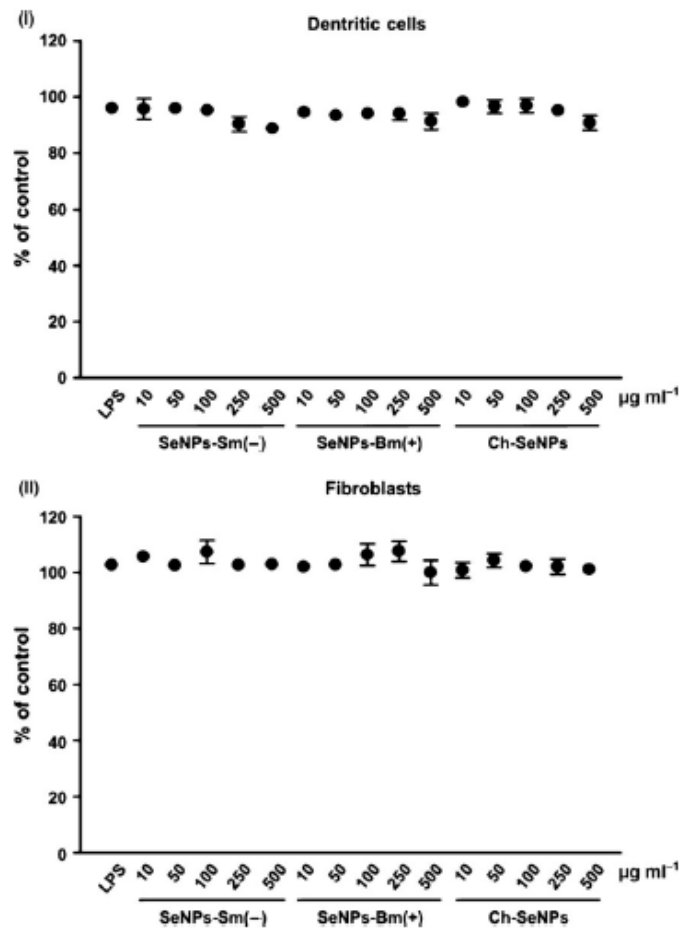


**Fig. 3.** Evaluation of cell viability. DCs (i) and fibroblasts (ii) were treated with the indicated concentrations of Sm-SeNPs(-), Bm-SeNPs(+), or Ch-SeNPs for 24 h, followed by 4-h incubation with Alamar blue. Cells were also incubated with 100  $\text{ng ml}^{-1}$  LPS as a positive control. The values are expressed as the percentage of Alamar blue reduction relative to untreated cells (designated as 100%). Data are means  $\pm$  SD of four experiments.



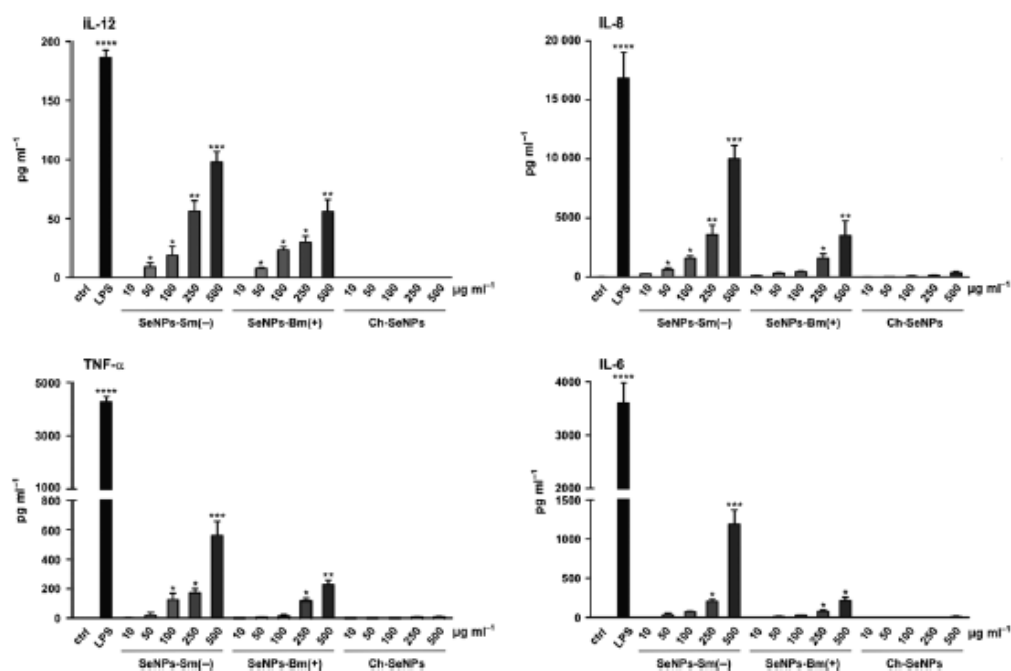


Fig. 4. Quantification of cytokine production. DCs were challenged with the indicated amounts of Sm-SeNPs(-), Bm-SeNPs(+) or Ch-SeNPs for 24 h. DCs were also activated with  $100 \text{ ng ml}^{-1}$  LPS as a positive control. The release of the indicated cytokines into the culture supernatants was evaluated by ELISA. The results are expressed as the mean value  $\pm$  SD of three independent experiments. Statistical analysis: SeNP-treated DCs versus untreated cells \* $P < 0.05$ , \*\* $P < 0.01$ , \*\*\* $P < 0.001$ , \*\*\*\* $P < 0.0001$ .

*C. albicans* and *C. parapsilosis*. To the best of our knowledge, this is the first report confirming that biogenic SeNPs are potentially suitable as antimicrobial agents against clinical strains isolated from patients with chronic lung diseases. We also show that the biogenic SeNPs can inhibit biofilm synthesis by *P. aeruginosa* and the two *Candida* species, and can efficiently disaggregate the mature exopolysaccharide matrix produced by these microorganisms. The antimicrobial potential of these biogenic SeNPs is greater than that of synthetic SeNPs, probably due to the presence of a bacterial protein layer coating the surface of the biogenic particles. Furthermore, SeNPs produced by the Gram-negative species *S. maltophilia* are more potent antibacterial agents than those produced by the Gram-positive species *B. mycoides*, suggesting that SeNPs with similar dimensions but originating from taxonomically distinct bacterial strains may show different activities, probably due to the different composition of their organic surface layer. Finally, neither the biogenic nor the synthetic SeNPs affected the viability of human DCs and fibroblasts, nor did they elicit the production of reactive oxygen species

or the substantial secretion of pro-inflammatory and immunostimulatory cytokines. Our data therefore suggest that the biogenic SeNPs are biocompatible structures that could be administered, either alone or in combination with antibiotics, in new therapeutic strategies to inhibit the growth of pathogens, including those resistant to antibiotics, or to facilitate the penetration of microbial biofilms.

#### Experimental procedures

##### Reagents

Analytical grade sodium selenite, selenous acid and reagents used for the chemical synthesis of SeNPs were purchased from Sigma-Aldrich (Milan, Italy). RPMI 1640, Dulbecco's modified Eagle's medium (DMEM) and L-glutamine were obtained from Lonza (Walkersville, MD, USA). Recombinant human GM-CSF and human IL-4 were purchased from Miltenyi Biotec GmbH (Bergisch Gladbach, Germany). Low-endotoxin FBS and *Saccharomyces cerevisiae* glucan were obtained from Sigma-Aldrich. All of the above reagents contained less than 0.125 endotoxin units per mL, as determined by the

Limulus amoebocyte lysate assay (Microbiological Associates, Walkersville, MD, USA). Ultrapure lipopolysaccharide (LPS 0111, B4 strain) from *Escherichia coli* was purchased from InvivoGen (San Diego, CA, USA). Mouse anti-human CD1a (HI149) antibody was obtained from Becton-Dickinson (San Jose, CA, USA).

#### Preparation of SeNPs

Two environmental isolates (Gram-positive *B. mycoides* SeITE01 and the Gram-negative *S. maltophilia* SeITE02) were used to produce the biogenic Bm-SeNPs(+) and Sm-SeNPs(-) respectively (Di Gregorio *et al.*, 2005; Lampis *et al.*, 2014). Sterile nutrient broth supplemented with 2 mM Na<sub>2</sub>SeO<sub>3</sub> was inoculated to achieve final concentrations of 10<sup>5</sup> and 10<sup>7</sup> CFU ml<sup>-1</sup> for *B. mycoides* SeITE01 and *S. maltophilia* SeITE02 respectively. The cultures were incubated aerobically at 27°C in a rotary shaker (150 r.p.m.) for 6 h (*B. mycoides* SeITE01) or 24 h (*S. maltophilia* SeITE02). Bacterial cells and nanoparticles were removed from the culture medium by centrifugation at 10 000 g for 10 min. The pellets were washed twice with 0.9% NaCl, suspended in TrisHCl buffer (pH 8.2) and the cells were disrupted by ultrasonication at 100 W for 5 min. The suspension was then centrifuged at 10 000 g for 30 min to separate disrupted cells (pellet) from nanoparticles (supernatant). The nanoparticles were recovered after centrifugation at 40 000 g for 30 min, washed twice and suspended in deionized sterile water. Ch-SeNPs were produced as described by Lin and Wang (2005), while Ch2-SeNPs were produced as described by Li *et al.* (2010).

#### Cell free extracts and CFX-SeNPs preparation

*Stenotrophomonas maltophilia* SeITE02 and *B. mycoides* SeITE01 cells were grown for 24 h until stationary phase. They were then centrifuged at 3000 g for 15 min and washed twice with phosphate buffer saline. The pellet was resuspended in 100 mM Tris-HCl pH 7.4 and sonicated at 100 W five times for 5 min. Finally, unbroken cells were separated by centrifugation at 16 000 g for 30 min and the supernatant was recovered.

CFX-SeNPs were then prepared by exposing Ch-SeNPs to CFX of *S. maltophilia* SeITE02 or *B. mycoides* SeITE01 overnight in agitation. CFX-SeNPs were recovered through centrifugation and washed twice with 100 mM Tris-HCl pH 7.4, as described by Dobias and coworkers (Dobias *et al.*, 2011).

#### Scanning electron microscopy

Both the biogenic and synthetic SeNPs were analysed by SEM. The nanoparticles were fixed, dehydrated

through an increasing ethanol concentration series and dried in liquid CO<sub>2</sub> using the critical point method. The particles were mounted on metallic specimen stubs and directly observed using an XL30 ESEM (FEI, Hillsboro, OR, USA) equipped with an EDAX micro-analytical system, which was used to determine the elemental composition of the analysed nanoparticles.

#### Dynamic light scattering

Dynamic light scattering analysis was carried out using a Zen 3600 Zetasizer Nano ZS (Malvern Instruments, Malvern, UK) equipped with a 633 nm helium-neon laser light source (4.0 mW), detecting scattering information at a fixed angle of 173°. Samples (300 µl) were transferred to a quartz cuvette (10 mm path length), and the mean size distribution and zeta potential were recorded at 25°C using the software provided by Malvern Instruments.

#### Microbial strains and growth conditions

We used five *P. aeruginosa* clinical strains (INT, CFC20, CFC21, CFCA and CFCB) and two reference strains (PAO1 and PYO27853). *P. aeruginosa* INT is a multidrug-resistant strain isolated from a urinary tract infection and it carries the class 1 integron containing multiple antibiotic-resistant gene cassettes. Strains CFC20, CFC21, CFCB and CFCA were isolated from the sputum of patients from the Cystic Fibrosis Center of Verona, following the provision of written informed consent from the subjects enrolled in the study.

The bacterial strains were grown in tryptic soy broth (TSB) (Difco Laboratories, Detroit, MI, USA) or TSB medium supplemented with 1% glucose (TSB-1% glucose).

Two yeast clinical strains, *Candida albicans* CVr-21 and *Candida parapsilosis* CPVr-5, isolated from vaginal swabs, were also included in the study and grown in Sabouraud medium. Cell growth was monitored with a LKB spectrophotometer at 640 nm (OD<sub>640nm</sub>).

#### Nanoparticle susceptibility assay

The MIC of the different types of SeNPs tested (Ch-SeNPs, Ch2-SeNP, Sm-SeNPs(-), Bm-SeNPs(+), CFX (Sm)-SeNPs, CFX(Bm)-SeNPs) and cell free extracts (CFX(Sm) and CFX(Bm)) was first measured against the reference strain *P. aeruginosa* PAO1.

Afterwards, MICs were determined by the broth microdilution method (National Committee for Clinical Laboratory Standards, 2010) and were used to evaluate the susceptibility of the microbial strains. The susceptibility of the strains was confirmed in an agar diffusion

assay by monitoring for the presence or absence of a bacterial growth inhibition halo surrounding wells containing different concentrations of SeNPs.

#### Biofilm formation assay

Bacterial cells were grown at 37°C in TSB-1% glucose and yeast cells were grown in Sabouraud medium until in each case they reached the exponential growth phase ( $OD_{650nm} = 0.4$ ). Cells were then diluted in TSB-1% glucose or Sabouraud medium to reach  $\sim 10^6$  CFU ml<sup>-1</sup>. We then inoculated sterile flat-bottomed polystyrene CytoOne microtiter plates (Starlab, Milan, Italy) with 200  $\mu$ l of each cell suspension or 200  $\mu$ l of the medium without cells as a negative control. The anti-biofilm properties of SeNPs were investigated by diluting them in growth medium to concentrations of 50, 100, 250 and 500  $\mu$ g ml<sup>-1</sup>, and adding them to the microtiter wells. The plates were incubated aerobically at 37°C without agitation for 48 h to allow biofilm formation. After incubation, the planktonic cells and the growth medium were aseptically aspirated and the biofilm matrix washed with sterile saline solution and dried. Biofilm quantification was carried out by adding 100  $\mu$ l of 1% methylene blue to each well and incubating for 15 min at room temperature. The wells were then slowly washed with sterile water and dried at 37°C. The methylene blue bound to the biofilm was extracted in 100  $\mu$ l 70% ethanol and the absorbance was measured at 570 nm using an A3 Plate Reader (DAS, Rome, Italy). All experiments were performed in triplicate. Optical densities greater than 2, between 1 and 2 or between 0.5 and 1 optical units were considered to correspond to strong (S), medium (M) or low (L) biofilm production respectively.

#### Biofilm disaggregation assay

Biofilm disaggregation triggered by SeNPs was measured by seeding the microbial suspensions into 96-well microplates and incubating at 37°C to allow biofilm formation. After 48 h, the medium was aseptically aspirated. SeNPs were diluted in growth medium to concentrations of 50, 100, 250 and 500  $\mu$ g ml<sup>-1</sup>, and were added to the wells. The prepared microplates were then incubated for 24 h at 37°C and the amount of biofilm was quantified as described above. All experiments were performed in triplicate.

#### Preparation and culture of dendritic cells

After written informed consent was received from donors, and approval by the Ethical Committee (Prot. no. 5626, February 2nd 2012, and Prot. no. 43318, September 4th 2013), buffy coats from the venous blood of normal

healthy volunteers were obtained from the Blood Transfusion Centre at the University Hospital of Verona. Peripheral blood mononuclear cells were isolated by Ficoll-Hypaque and Percoll density gradient centrifugation (GE Healthcare Life Sciences, Little Chalfont, UK) and used for the immunomagnetic isolation (Miltenyi Biotec) of CD14<sup>+</sup> cells as previously described (Zenaro *et al.*, 2009). DCs were isolated by incubating  $1 \times 10^6$  monocytes per ml at 37°C in 5% CO<sub>2</sub> for 5–6 days in six-well tissue culture plates (Greiner Bio-One, Nürtingen, Germany) in RPMI 1640 medium supplemented with heat-inactivated 10% low-endotoxin FBS, 2 mM L-glutamine, 50 ng ml<sup>-1</sup> GM-CSF and 20 ng ml<sup>-1</sup> IL-4. The final DC population was 98% CD1a<sup>+</sup>, as measured by FACS analysis.

#### Culture of fibroblasts

Human primary fibroblast CCD112Sk cells (ATCC® CRL-2429) were purchased from ATCC (Manassas, VA, USA) and cultured in DMEM supplemented with 10% heat-inactivated FBS plus 2 mM L-glutamine at 37°C in 5% CO<sub>2</sub>.

#### Quantification of cytokine production

Cytokine production in cell culture supernatants was determined by ELISA using Ready-Set-Go ELISA kits (eBioscience, San Diego, CA, USA) according to the manufacturer's instructions. We measured the levels of IL-12 (range 4–500 pg ml<sup>-1</sup>), TNF- $\alpha$  (range 4–500 pg ml<sup>-1</sup>) and IL-6 (range 2–200 pg ml<sup>-1</sup>). The ELISA development kit (Mabtech, Nacka Strand, Sweden) was used to determine the level of IL-8 (CXCL8 range 4–400 pg ml<sup>-1</sup>). Briefly, DCs were treated with different concentrations of SeNPs for 24 h, and then the supernatants were collected. DCs were also activated with 100 ng ml<sup>-1</sup> LPS as a positive control. The plates were read at 450 nm with Victor<sup>3</sup> 1420 Multilabel Counter (Perkin Elmer, Waltham, MA, USA).

#### Cell viability evaluation

Cell viability was assessed using the AlamarBlue® assay (Invitrogen, Thermo Fischer Scientific, Waltham, MA, USA) according to the manufacturer's instructions. After incubation for 24 h with SeNPs, the reagent was added to the culture medium a final concentration of 10% before measuring the absorbance at 570 and 600 nm.

#### Superoxide anion production

The release of O<sub>2</sub><sup>-</sup> was estimated by cytochrome c reduction as previously described (Vulcano *et al.*, 2004).



Briefly, after cell culture, the medium was replaced with HBSS (pH 7.4) containing 80  $\mu$ M ferricytochrome c (Sigma-Aldrich) and the required stimulus. Cytochrome c reduction was determined by measuring absorbance at 550 nm using a Perkin-Elmer Victor<sup>3</sup> 1420 Multilabel Counter.

#### Statistical analysis

Data are presented as means plus standard deviations. Statistical analysis, including two-way analysis of variance, was carried out using GraphPad Prism v6.0 (GraphPad Software Inc., La Jolla, CA, USA).

#### Conflict of interest

The authors have no conflict of interest to declare.

#### References

- Admyre, C., Axelsson, L.G., von Stein, O., and Zargari, A. (2015) Immunomodulatory oligonucleotides inhibit neutrophil migration by decreasing the surface expression of interleukin-8 and leukotriene B4 receptors. *Immunology* **144**: 206–217.
- Alexis, F., Pridgen, E., Molnar, L.K., and Farokhzad, O.C. (2008) Factors affecting the clearance and biodistribution of polymeric nanoparticles. *Mol Pharm* **5**: 505–515.
- Beyth, N., Hour-Haddad, Y., Domb, A., Khan, W., and Hazan, R. (2015) Alternative antimicrobial approach: nano-antimicrobial materials. *Evid Based Complement Alternat Med* **246012**: 1–16.
- Chang, C., and Gershwin, M.E. (2010) Drugs and autoimmunity—a contemporary review and mechanistic approach. *J Autoimmun* **34**: 266–275.
- Chudobova, D., Cihalova, K., Dostalova, S., Rutkay-Nedecky, B., Rodrigo, M.A., Tmejova, F., et al. (2014) Comparison of the effects of silver phosphate and selenium nanoparticles on *Staphylococcus aureus* growth reveals potential for selenium particles to prevent infection. *FEMS Microbiol Lett* **351**: 195–201.
- Ciofu, O., Tolker-Nielsen, T., Jensen, P.O., Wang, H., and Heiby, N. (2015) Antimicrobial resistance, respiratory tract infections and role of biofilms in lung infections in cystic fibrosis patients. *Adv Drug Deliv Rev* **85**: 7–23.
- Di Gioacchino, M., Tetrarca, C., Lazzarin, F., Di Giampaolo, L., Sabbioni, E., Boscolo, P., et al. (2011) Immunotoxicity of nanoparticles. *Int J Immunopath Pharmacol* **24**: 65S–71S.
- Di Gregorio, S., Lampis, S., and Vallini, G. (2005) Selenite precipitation by a rhizospheric strain of *Stenotrophomonas* sp. isolated from the root system of *Astragalus bisulcatus*: a biotechnological perspective. *Environ Int* **31**: 233–241.
- Dobias, J., Suvurova, E.J., and Bernier-Latmani, R. (2011) Role of proteins in controlling selenium nanoparticle size. *Nanotechnology* **22**: 195605.
- Donini, M., Zenaro, E., Tamassia, N., and Dusi, S. (2007) NADPH oxidase of human dendritic cells: role in *Candida albicans* killing and regulation by interferons, dectin-1 and CD206. *Eur J Immunol* **37**: 1194–1203.
- Elmqvist, J.K., Scammell, T.E., and Saper, C.B. (1997) Mechanisms of CNS response to systemic immune challenge: the febrile response. *Trends Neurosci* **20**: 565–570.
- Gadakh, B., and Van Aerschot, A. (2015) Renaissance in antibiotic discovery: some novel approaches for finding drugs to treat bad bugs. *Curr Med Chem* **22**: 2140–2158.
- Gantner, B.N., Simmons, R.M., Canavera, S.J., Akira, S., and Underhill, D.M. (2003) Collaborative induction of inflammatory responses by dectin-1 and Toll-like receptor 2. *J Exp Med* **197**: 1107–1117.
- Gill, E.E., Franco, O.L., and Hancock, R.E. (2015) Antibiotic adjuvants: diverse strategies for controlling drug-resistant pathogens. *Chem Biol Drug Des* **85**: 56–78.
- Grant, S.S., and Hung, D.T. (2013) Persistent bacterial infections, antibiotic tolerance, and the oxidative stress response. *Virulence* **4**: 273–283.
- Granucci, F., Zanoni, I., and Ricciardi-Castagnoli, P. (2008) Central role of dendritic cells in the regulation and deregulation of immune responses. *Cell Mol Life Sci* **65**: 1683–1697.
- Habash, M.B., Park, A.J., Vis, E.C., Harris, R.J., and Khursigara, C.M. (2014) Synergy of silver nanoparticles and aztreonam against *Pseudomonas aeruginosa* PAO1 biofilms. *Antimicrob Agents Chemother* **58**: 5818–5830.
- Jorgensen, J.H., and Ferraro, M.J. (2009) Antimicrobial susceptibility testing: a review of general principles and contemporary practices. *Clin Infect Dis* **49**: 1749–1755.
- Kazempour, Z.B., Yazdi, M.H., Rafii, F., and Shahverdi, A.R. (2013) Sub-inhibitory concentration of biogenic selenium nanoparticles lacks post antifungal effect for *Aspergillus niger* and *Candida albicans* and stimulates the growth of *Aspergillus niger*. *Iran J Microbiol* **5**: 81–85.
- Kostakiofi, M., Hadjirangiskou, M., and Hultgren, S.J. (2013) Bacterial biofilms: development, dispersal, and therapeutic strategies in the dawn of the postantibiotic era. *Cold Spring Harb Perspect Med* **3**: 1–23.
- Lampis, S., Zonaro, E., Bertolini, C., Bernardi, P., Butler, C.S., and Vallini, G. (2014) Delayed formation of zero-valent selenium nanoparticles by *Bacillus mycoides* SelTE01 as a consequence of selenite reduction under aerobic conditions. *Microb Cell Fact* **13**: 1–14.
- Lampis, S., Zonaro, E., Bertolini, C., Cecconi, D., Monti, F., Micaroni, M., et al. (2016) Selenite biotransformation and detoxification by *Stenotrophomonas maltophilia* SelTE02: novel clues on the route to bacterial biogenesis of selenium nanoparticles. *J Hazard Mater* in press. doi:10.1016/j.jhazmat.2016.02.035.
- Lara, H.H., Romero-Urbina, D.G., Pierce, C., Lopez-Ribot, J.L., Arellano-Jiménez, M.J., and Jose-Yacamán, M. (2015) Effect of silver nanoparticles on *Candida albicans* biofilms: an ultrastructural study. *J Nanobiotechnology* **13**: 1–12.
- Li, Q., Chen, T., Yang, F., Liu, J., and Zheng, W. (2010) Facile and controllable one-step fabrication of selenium nanoparticles assisted by L-cysteine. *Mater Lett* **64**: 614–617.
- Lin, Z.H., and Wang, C.R.C. (2005) Evidence on the size-dependent absorption spectral evolution of selenium nanoparticles. *Mat Chem Phys* **92**: 591–594.

- Loza, K., Diendorf, C., Sengstock, C., Ruiz-Gonzalez, L., Gonzalez-Calbet, J.M., Vallet-Regi, M., et al. (2014) The dissolution and biological effects of silver nanoparticles in biological media. *J Mater Chem B* 2: 1634–1643.
- Pelgrift, R.Y., and Friedman, A.J. (2013) Nanotechnology as a therapeutic tool to combat microbial resistance. *Adv Drug Deliv Rev* 65: 1803–1815.
- Penesyan, A., Gillings, M., and Paulsen, T.T. (2015) Antibiotic discovery: combating bacterial resistance in cells and in biofilm communities. *Molecules* 20: 5286–5298.
- Schäkel, K. (2009) Dendritic cells—why can they help and hurt us. *Exp Dermatol* 18: 264–273.
- Shakibaie, M., Forootanfar, H., Golkari, Y., Mohammadi-Khorsand, T., and Shakibaie, M.R. (2015) Anti-biofilm activity of biogenic selenium nanoparticles and selenium dioxide against clinical isolates of *Staphylococcus aureus*, *Pseudomonas aeruginosa*, and *Proteus mirabilis*. *J Trace Elem Med Biol* 29: 235–241.
- Suffredini, A.F., Fantuzzi, G., Badolato, R., Oppenheim, J.J., and O'Grady, N.P. (1999) New insights into the biology of the acute phase response. *J Clin Immunol* 19: 203–214.
- Sun, M., Yu, Q., Hu, M., Hao, Z., Zhang, C., and Li, M. (2014) Lead sulfide nanoparticles increase cell wall chitin content and induce apoptosis in *Saccharomyces cerevisiae*. *J Haz Mat* 273: 7–16.
- Tomita, R.J., de Matos, R.A., and Vallim, M.A. (2014) A simple and effective method to synthesize fluorescent nanoparticles using tryptophan and light and their lethal effect against bacteria. *J Photochem Photobiol, B* 140: 157–162.
- Tran, P.A., and Webster, T.J. (2011) Selenium nanoparticles inhibit *Staphylococcus aureus* growth. *Int J Nanomedicine* 6: 1553–1558.
- Vignali, D.A., and Kuchroo, V.R. (2012) IL-12 family cytokines: immunological playmakers. *Nat Immunol* 13: 722–728.
- Vulcano, M., Dusi, S., Lissandrini, D., Badolato, R., Mazzi, P., Riboldi, E., et al. (2004) Toll receptor-mediated regulation of NADPH oxidase in human dendritic cells. *J Immunol* 173: 5749–5756.
- Wang, T., Yang, L., Zhang, B., and Liu, J. (2010) Extracellular biosynthesis and transformation of selenium nanoparticles and application in H<sub>2</sub>O<sub>2</sub> biosensor. *Colloids Surf B Biointerfaces* 80: 94–102.
- Xiangqian, L., Huizhong, X., Zhe-Sheng, C., and Guofang, C. (2011) Biosynthesis of nanoparticles by microorganisms and their applications. *J Nanomater* 270974: 1–16. doi:10.1155/2014/359316.
- Zenaro, E., Donini, M., and Dusi, S. (2009) Induction of Th1/Th17 immune response by *Mycobacterium tuberculosis*: role of dectin-1, mannose receptor, and DC-SIGN. *J Leukocyte Biol* 86: 1393–1401.
- Zonaro, E., Lampis, S., Turner, R.J., Qazi, S.J., and Vallini, G. (2015) Biogenic selenium and tellurium nanoparticles synthesized by environmental microbial isolates efficaciously inhibit bacterial planktonic cultures and biofilm. *Front Microbiol* 6: 1–11.

**Biogenic selenium nanoparticles synthesized by *Stenotrophomonas maltophilia* SeITE02 loose anti-bacterial and anti-biofilm efficacy as a result of the progressive alteration of their organic coating layer**

Journal:	<i>Microbial Biotechnology</i>
Manuscript ID:	MICROBIO-2017-328-RA.R1
Manuscript Type:	Research Article
Date Submitted by the Author:	25-Jan-2018
Complete List of Authors:	Boaretti, Marzia; University of Verona, Department of Diagnostic and Public Health Leo, Maria; University of Verona, Department of Diagnostic and Public Health Cremonini, Eleonora; University of Verona, Department of Diagnostic and Public Health Lampis, Silvia; University of Verona, Department of Biotechnology Vallini, Giovanni; Department of Biotechnology
Keywords:	biogenic selenium nanoparticles, organic layer of nanoparticles, anti-microbial and anti-biofilm activity of nanoparticles

1 **Biogenic selenium nanoparticles synthesized by *Stenotrophomonas maltophilia***  
2 **SeITE02 loose anti-bacterial and anti-biofilm efficacy as a result of the**  
3 **progressive alteration of their organic coating layer**

4

5 Eleonora Cremonini<sup>1</sup>, Marzia Boaretti<sup>1\*</sup>, Ilse Vandecandelaere<sup>3</sup>, Emanuele Zonaro<sup>2</sup>, Tom Coenye<sup>3</sup>,  
6 Maria M. Lleo<sup>1</sup>, Silvia Lampis<sup>2\*</sup>, Giovanni Vallini<sup>2</sup>

7

8 <sup>1</sup>Department of Diagnostic and Public Health, University of Verona – Strada Le Grazie 8, 37134  
9 Verona, Italy

10 <sup>2</sup>Department of Biotechnology, University of Verona – Strada Le Grazie 15, 37134 Verona, Italy

11 <sup>3</sup>Laboratory of Pharmaceutical Microbiology, Ghent University – Ottergemsesteenweg 460, 9000  
12 Gent, Belgium

13

14 Running title: Anti-microbial activity of selenium nanoparticles

15

16 \* Corresponding authors:

17 Marzia Boaretti      Email: [marzia.boaretti@univr.it](mailto:marzia.boaretti@univr.it)

18 Silvia Lampis      Email: [silvia.lampis@univr.it](mailto:silvia.lampis@univr.it)

19

20

21

22 **Summary**

23 Increasing emergence of drug-resistant microorganisms poses a great concern to clinicians, thus  
24 new active products are urgently required to treat a number of infectious disease cases. Different  
25 metallic and metalloid nanoparticles have so far been reported as possessing anti-microbial  
26 properties and proposed as a possible alternative therapy against resistant pathogenic  
27 microorganisms.

28 In this study, selenium nanoparticles (SeNPs) synthesized by the environmental bacterial isolate  
29 *Stenotrophomonas maltophilia* SeITE02 were shown to exert a clear anti-microbial and anti-biofilm  
30 activity against different pathogenic bacteria, either reference strains or clinical isolates. Anti-  
31 microbial and anti-biofilm capacity seems to be strictly linked to the organic cap surrounding  
32 biogenic nanoparticles, although the actual role played by this coating layer in the biocidal action  
33 remains still undefined. Nevertheless, evidence has been gained that the progressive loss in protein  
34 and carbohydrate content of the organic cap determines a decrease of nanoparticle stability. This  
35 leads to an alteration of size and electrical properties of SeNPs along with a gradual attenuation of  
36 their anti-bacterial efficacy. Denaturation of the coating layer was proved even to have a negative  
37 effect on the anti-biofilm activity of these nanoparticles. The pronounced anti-microbial efficacy of  
38 biogenic SeNPs compared to the denaturated ones can – in first instance - be associated with their  
39 smaller dimensions. This study showed that the native organic coating layer of biogenic SeNPs  
40 functions in avoiding aggregation and maintaining electrostatic stability of the nanoparticles, thus  
41 allowing them to maintain efficient anti-microbial and anti-biofilm capabilities.

42  
43  
44  
45  
46



47 **Introduction**

48 In the last decades, widespread antibiotic treatment of clinical cases due to bacterial and fungal  
49 infections has become a threat because of increasing occurrence of antimicrobial resistance (AMR)  
50 within microorganisms that are often able to form fastidious biofilms on tissues and medical devices  
51 (Penesyan *et al.*, 2015). Both aspects represent a serious concern since available anti-microbial  
52 drugs have proved to be poorly active or inefficacious giving rise to the emergence of chronic  
53 infections and an increase in morbidity and death rate. This has led to a growing awareness that new  
54 approaches, including those based on the use of non-antibiotic anti-bacterial agents, need to be  
55 perfected to face the antibiotic resistance challenge (Beyth *et al.*, 2015).

56 In this perspective, tailored metal nanoparticles (NPs) have recently come to the forefront as  
57 promising anti-bacterial and anti-biofilm agents (Rizzello and Pompa, 2014; Shakibaie *et al.*, 2015).  
58 For instance, silver nanoparticles (AgNPs), one of the most studied classes of NPs, have been  
59 extensively considered in the last two decades as anti-microbial and anticancer agents drug delivery  
60 systems as well as in diagnostics and probing for the treatment of various diseases (Yuan *et al.*,  
61 2017). AgNPs are likely to exert their anti-bacterial effects in a dose- and time-dependent manner.  
62 Moreover, silver nanoparticles have been demonstrated able to perform their anti-bacterial activity  
63 through the generation of reactive oxygen species (ROS), production of malondialdehyde (MDA),  
64 and leakage induction of proteins and sugars from bacterial cells (Yuan *et al.*, 2017). Although the  
65 mechanisms underlying the anti-bacterial effect of metal NPs have not yet been elucidated, it is  
66 generally believed that induction of oxidative stress, release of metal ions and/or non-oxidative  
67 reactions are involved (Wang *et al.*, 2017). According to the information available from previous  
68 investigations, the major processes by which NPs exert anti-bacterial activity can be summarized as  
69 follows: 1) penetration into and disruption of bacterial cell membrane, 2) generation of ROS, and 3)  
70 induction of harmful intracellular reactions, including damages on DNA and proteins (Wang *et al.*,  
71 2017).

72 Recently, Cremonini *et al.* (2016) reported on comparative tests carried out with selenium  
73 nanoparticles (SeNPs) of biogenic nature, produced by two environmental bacterial strains (namely,  
74 *Bacillus mycoides* SeITE01 and *Stenotrophomonas maltophilia* SeITE02) and chemically  
75 synthesized selenium nanoparticles (Ch-SeNPs). Biogenic SeNPs showed a higher anti-bacterial  
76 activity against a number of clinical strains of *Pseudomonas aeruginosa* as well as a significant  
77 inhibition of biofilm formation along with disaggregation capacity toward already established  
78 bacterial biofilms. Furthermore, biogenic SeNPs showed no toxic effects in cell cultures of human  
79 dendritic cell (DCs) or fibroblasts and did not elicit production of pro-inflammatory and immune-  
80 stimulatory cytokines (Cremonini *et al.*, 2016).

81 By relying on these results, the aim of the present study was to investigate a possible wider anti-  
82 microbial activity of SeNPs from *S. maltophilia* SeITE02 against an extended list of bacterial  
83 species and strains, with attention to specific factors that could play a role in modulating the  
84 efficacy of such nanoparticles. In particular, we focused on the possible variations in anti-microbial  
85 and anti-biofilm capacity of SeNPs as a consequence of the denaturation of their organic coating  
86 layer.

87

## 88 Results

### 89 *Biosynthesis and structural features of selenium nanoparticles*

90 As reported in previous studies (Jain *et al.*, 2015; Lampis *et al.*, 2017; Cremonini *et al.*, 2016),  
91 biogenic SeNPs from the bacterial strain *Stenotrophomonas maltophilia* SeITE02 present a complex  
92 organic cap consisting of different biomolecules such as proteins, lipids and carbohydrates. In order  
93 to evaluate the possible influence of such an organic coating layer on the biological reactivity of  
94 these biogenic SeNPs (here called SeNPs-24 and also untreated SeNPs), different and progressively  
95 more aggressive denaturants were applied to the nanoparticles. Quantification of surface-associated

96 macromolecular matrix as well as measurement of physical and electrical properties were  
97 performed on untreated and differently treated SeNPs.

98 Figure 1(A) shows how the protein content associated with the organic coating layer of SeNPs  
99 decreases after exposure to the different denaturing agents. The concentration of proteins associated  
100 with untreated biogenic SeNPs is  $0.46 \pm 0.05$  mg/mg NPs; this value progressively decreases to  
101  $0.05 \pm 0.01$  mg/mg NPs after exposure to the most drastic denaturation by means of 10% sodium  
102 dodecyl sulphate (SDS) and 30 min boiling. A similar pattern was observed for carbohydrate  
103 concentration [Figure 1(B)] with untreated biogenic SeNPs showing a value of  $0.33 \pm 0.04$  mg/mg  
104 NPs that then fell to  $0.02 \pm 0.01$  mg/mg NPs after the strongest denaturing treatment.

105 Dynamic light scattering measurements (Table 1) showed an average size for untreated biogenic  
106 SeNPs of  $181 \pm 20$  nm with a Z-potential value of  $-32.01$  mV. Exposure to different denaturing  
107 treatments caused a progressive growth of nanoparticle dimensions, up to  $270 \pm 24$  nm after the  
108 treatment with 10% SDS and 30 min boiling. In particular, as shown in Figure S1, the progressively  
109 more denaturing treatment of biogenic NPs resulted in an increase of the number of SeNPs of  
110 larger size and more susceptible to aggregate each other. On the other hand, values of the Z-  
111 potential of SeNPs ranged within  $-17.40$  and  $-3.97$  mV after different denaturing procedures (Table  
112 1).

113 Another type of SeNPs (SeNPs-48) was also taken into consideration: these SeNPs were obtained  
114 from bacterial cultures after 48 hours of incubation with sodium selenite and showed a diameter of  
115  $276 \pm 26$  nm, with a Z-potential value of  $-29.27$  mV (Figure S2(A and B)). The protein concentration  
116 associated with these biogenic nanostructures was  $0.48 \pm 0.07$  mg/mg SeNPs, while the carbohydrate  
117 concentration was  $0.35 \pm 0.03$  mg/mg SeNPs (Figure S2(C)).

118

#### 119 *Anti-microbial activity of SeNPs in different conformational states*

120 A number of bacterial strains belonging to different species was screened for the susceptibility to  
121 untreated and treated SeNPs. These bacterial species/strains were selected on the basis of their

122 actual occurrence in biofilm-mediated infections. Therefore, *Pseudomonas aeruginosa* and  
123 *Burkholderia cenocepacia* as well as emerging harmful pathogens such as *Achromobacter*  
124 *xylooxidans* and *Stenotrophomonas maltophilia* causing chronic lung infections in cystic fibrosis  
125 and immunodepressed patients (Bjarnsholt, 2013) were taken into account. On the other hand, as far  
126 as gram-positive bacterial agents are concerned, staphylococci were considered important producers  
127 of biofilms associated with the implantation of biomedical devices or skin pathologies (Paharic and  
128 Horswill, 2016).

129 As shown in Table 2, MIC values of biogenic SeNPs varied widely among the different microbial  
130 species and even diverse strains belonging to the same species, ranging from 4 to 128 µg/ml.  
131 Nevertheless, an evaluation of the activity of SeNPs on the different bacterial strains tested (in term  
132 of susceptibility or resistance) turned out to be quite difficult since standard breakpoints do not exist  
133 and a comparison with the susceptibility to antibiotics is not predictable. Two groups of strains  
134 could be distinguished: one showing low values of MIC (4-16 µg/ml) while the other showing  
135 higher MIC values (32-128 µg/ml), although a strict association with specific bacterial species or  
136 even families cannot be done. For instance among *P. aeruginosa* strains, PAO1 and BR2 showed  
137 low values of MIC while in INT and BR1 higher MIC values were measured. The same was also  
138 demonstrated for *Staphylococcus aureus*, Mu50 strain showing the highest MIC value of 128 µg/ml.  
139 As a general rule, it seems that gram-positive strains responded to SeNPs with lower MIC values  
140 when compared to the gram-negative ones. Anyway, the number of bacterial strains studied so far is  
141 too restricted to confirm such a trend. To evaluate the influence by the whole organic cap of  
142 biogenic selenium nanoparticles on their anti-microbial efficacy, such an activity was tested with  
143 nanoparticles subjected to progressively stronger protocols for the denaturation of the external  
144 organic coating. Data reported in Table 2 show, for almost all the strains screened, a decrease in the  
145 anti-microbial activity of SeNPs which experienced the most intensive denaturation, as revealed by  
146 progressively higher MIC values.

147 In order to evaluate the bioactivity of SeNPs still surrounded by an intact organic cap with those of  
148 similar size but extensively denatured, SeNPs-48 were tested against those strains that had shown  
149 the highest MIC values against denatured SeNPs, namely *P. aeruginosa* PAO1, *P. aeruginosa* BR2,  
150 *S. maltophilia* VR20, and *S. aureus* UR1. As reported in Figure S2(D), the MIC values for SeNPs-  
151 48 were lower than those registered with most extensively denatured SeNPs, ranging between 16  
152 and 256 µg/ml with reference to the different bacterial strains tested.

153

#### 154 *Anti-biofilm activity of SeNPs in different conformational states*

155 Efficacy of both untreated and denatured SeNPs in preventing bacterial biofilm formation or  
156 promoting biofilm eradication was also evaluated. Tests were carried out on a selection of bacterial  
157 strains, namely PAO1, BR1, and BR2 of *P. aeruginosa*, *B. cenocepacia* and the *S. haemolyticus*.  
158 The choice was made on the basis of low MIC values for SeNPs shown by the respective planktonic  
159 cultures and the high capacity of biofilm formation of these strains. On the other hand, *S. aureus*  
160 Mu50 showing methicillin resistance as well as being known as moderately resistant to vancomycin  
161 was also taken into consideration as a bacterial strain able to withstand the presence of antibiotics  
162 and SeNPs. By relying on the results of preliminary tests (data not shown), anti-biofilm activity of  
163 SeNPs in different conformational states was measured at a nanoparticle concentration of 128  
164 µg/ml, found as the lowest concentration with a significant contrasting effect on biofilm formation.  
165 Quantification of the total biofilm biomass singularly formed by the six bacterial strains tested was  
166 obtained through crystal violet (CV) staining. Afterward, counts of viable cells (reported as  
167 CFU/ml) still present within biofilm matrices were determined by plating aliquots of biofilms on an  
168 agarized growth substrate. Exposure of biofilms produced by all *P. aeruginosa* strains tested to 128  
169 µg/ml of SeNPs in their different conformational states resulted in a clear decrease in the CV signal.  
170 This effect was more pronounced with untreated biogenic SeNPs rather than with most extensively  
171 denatured SeNPs (Figure 2A). Culturable cells of *P. aeruginosa* PAO1 decreased significantly after  
172 treatments with different types of SeNPs with the exception of those harshly denatured (Figure 2B).

173 On the other hand, the number of CFU/ml counted from biofilms of *P. aeruginosa* BR1 and BR2  
174 decreased significantly only in case of exposure to untreated SeNPs (Fig 2B). Moreover, it is worth  
175 noting that the biofilm generated by *B. cenocepacia* LMG 16656 was quite susceptible to  
176 degradation by all conformational types of SeNPs, including most extensively denatured  
177 nanoparticles. Numbers of culturable cells recovered from biofilms of this strain, exposed to all  
178 kind of SeNPs were significantly lower than those from control biofilms (Figure 3).

179 As far as strain Mu50 of *S. aureus* is concerned, despite the low susceptibility to the action of  
180 SeNPs in planktonic state (MIC of 128 µg/ml), its biofilm depositions were easily degradable by all  
181 forms of SeNPs tested. A decrease in the number of culturable cells associated with the biofilm  
182 matrix was observed after treatment with selenium nanoparticles. The lowest effects were however  
183 revealed when most denatured SeNPs were applied. Finally, *S. haemolyticus* UST1 that synthesizes  
184 a very SeNP-resistant biofilm did not show any decrease in the number of culturable cells after  
185 exposure to all the NPs tested (Figure 3).

186 The comparison of the effects on biofilm biomass and cell viability between the different types of  
187 SeNPs tested (Figure 2 and 3) showed a difference not only in term of the control but also among  
188 the various denaturing treatments applied to the NPs. In all the strains tested, except for the *S.*  
189 *haemolyticus* UST1 strain, the progressive denaturation of the surface biomolecular cap is related to  
190 a loss of their anti-biofilm activity shown by an increasing value of CV signal and increasing  
191 number of CFU/ml. The statistic analysis reported, indeed, points out a significant difference in  
192 particular between the anti-biofilm activity of the untreated NPs and the ones exposed to the harshly  
193 denaturing treatment.

194

#### 195 *Role of reactive oxygen species induced by SeNPs*

196 Reactive oxygen species (ROS) are important elements in the bacterial response to physical and  
197 chemical environmental stresses and have been associated with the killing action of a variety of  
198 anti-microbial agents (Van Acker and Coenye, 2017). The production of ROS in response to



199 treatment with biogenic SeNPs was analysed in *P. aeruginosa* PAO1, *S. aureus* Mu50 and *B.*  
200 *cenocepacia* LMG16656 strains. As shown in Figure 4, in all bacterial strains tested an increase in  
201 ROS produced after treatment with biogenic nanoparticles was observed compared to the untreated  
202 controls.

203

#### 204 **Discussion**

205 Over the last two decades, several authors have made increasing efforts to develop innovative anti-  
206 microbial agents based on metal/metalloid nanostructured particles as an alternative strategy to  
207 overcome the worrisome increase of antibiotic resistance. Antibiotic-resistant infections are in fact  
208 more and more widespread, particularly in nosocomial contexts. The emergence of such pathogenic  
209 conditions generates in turn further risks due to the recourse to higher doses of drugs or additional  
210 toxic therapeutic treatments which can be responsible for longer hospital stays and an increased  
211 death rate (Ferri *et al.*, 2015). Major concerns are associated in this respect with multidrug  
212 resistance (MDR) bacteria and biofilm forming microbial communities.

213 In this scenario, selenium nanoparticles either of biogenic origin or chemically synthesized have  
214 been proven to possess surprising anti-bacterial and anti-biofilm capabilities (Cihalova *et al.*, 2014;  
215 Cremonini *et al.*, 2016; Huang *et al.*, 2016).

216 The present study focused on the influence that the outer organic coating layer of biogenic SeNPs  
217 synthesized by the bacterial strain *S. maltophilia* SeITE02 (Zonaro *et al.*, 2015; Lampis *et al.*, 2017)  
218 plays in determining anti-microbial and anti-biofilm efficacy of such nanostructured particles.  
219 Actually, biogenic SeNPs produced by the strain SeITE02 are surrounded by an organic cap mainly  
220 consisting of proteins, lipids and carbohydrates (Lampis *et al.*, 2017; Cremonini *et al.*, 2016). Four  
221 different types of biogenic elemental selenium nanoparticles obtained as a result of 24 h incubation  
222 of *S. maltophilia* SeITE02 in the presence of selenite were considered according to the follow  
223 scheme : a) untreated SeNPs as well as the same biogenic nanoparticles subjected however to  
224 increasingly stronger denaturing procedures, namely b) denatured through a treatment with 10%

225 SDS; c) treated with 10% SDS and 10 min boiling, and d) strongly denatured with 10% SDS and 30  
226 min boiling. By increasing the strength of denaturing treatments, a progressive loss of proteins and  
227 carbohydrates from the organic coat surrounding SeNPs was shown along with an increment in  
228 nanoparticle size and a change in their Z potential.

229 Growth in size of biogenic selenium nanoparticles as a consequence of denaturation due to partial  
230 loss of the external coating layer was an expected result since this phenomenon is widely reported  
231 in the literature (Dobias *et al.*, 2011). Therefore, the presence of an organic cap surrounding  
232 biogenic SeNPs confirmed its pivotal role in preventing particle aggregation. Furthermore, the shift  
233 of Z potential measurements toward less negative values also reduced the stability of untreated  
234 SeNPs. It is in fact well known that NPs with charges close to a neutral value tend to coalesce  
235 (Hunter, 1981). Moreover, anti-microbial activity of each type of SeNPs tested against different  
236 bacterial pathogens was quantified by MIC value determination. Results showed a wide variability  
237 of bacterial response to distinct kind of SeNPs as regards this parameter not only among different  
238 species but also within strains belonging to the same species. Despite this variable anti-microbial  
239 efficacy of untreated SeNPs toward the different bacterial strains tested, as a general rule MIC  
240 values increased with the progressive denaturation of the organic coating layer. These findings  
241 suggest that anti-microbial activity of SeNPs is size-dependent, with higher inhibiting effects  
242 associated with the smallest ones, as already reported in previous studies (Lu *et al.*, 2013;  
243 Chudobova *et al.*, 2014; Zonaro *et al.*, 2015). Indeed, denaturation of the external organic cap  
244 which leads to a progressive increase of particle dimensions coincides with a gradual drop in anti-  
245 bacterial efficacy. Nevertheless, also variations in the quali-quantitative features of the organic  
246 coating seem to affect the anti-microbial properties of SeNPs biosynthesized by *S. maltophilia*  
247 SeITE02. To verify a direct influence of the organic layer surrounding these nanoparticles on their  
248 biocidal potential, SeNPs from strain SeITE02 cultures after a 48 h incubation (SeNPs-48), larger in  
249 size than those recovered from a 24 h culture (SeNPs-24) but with similar size to the strongly  
250 denaturated ones, were tested against the bacterial strains that have shown to withstand the highest



251 MIC values. Interestingly, these biogenic SeNPs-48 owning their native surrounding layer, showed  
252 MIC values significantly lower than those detected with more extensively denatured SeNPs.  
253 Therefore, on the basis of these observations, it can be argued that the organic cap surrounding  
254 biogenic SeNPs plays a direct role in the efficacious anti-microbial interaction with target bacterial  
255 planktonic cells and biofilms.

256 In conclusion, factors that are likely to concur in influencing the anti-microbial potential of biogenic  
257 metal/metalloid nanoparticles can be summarized as follows: i) the nature of constitutive elements  
258 (Natan and Banin, 2017); ii) the size (Lu *et al.*, 2013; Zonaro *et al.*, 2015), and iii) the surface  
259 architecture (Verma and Stellaci, 2009). Much is still to be clarified however in order to elucidate in  
260 detail the nature of the external organic coating of biogenic metal nanoparticles for an actual  
261 interpretation of the intimate biocidal mechanisms.

262 Finally, in order to investigate in depth the anti-biofilm activity of SeNPs already highlighted in  
263 previous findings by the authors (Cremonini *et al.*, 2016), the impact on either biofilm biomass or  
264 viability of bacterial cells embedded in biofilm extracellular polymeric substances (EPS) was  
265 evaluated. With reference to the induction of consistency loss of biofilm biomass, untreated SeNPs  
266 were able to significantly disrupt the EPS matrix produced by all bacterial strains tested. Moreover,  
267 quantification of culturable cells trapped inside bacterial biofilms confirmed the biocidal potential  
268 of untreated SeNPs, with a marked reduction of counts in five of the six strains tested, with the  
269 exception of *S. haemolyticus* UST1, which instead retained cell viability. Results from the tests  
270 carried out with differently denatured SeNPs, compared to the untreated nanoparticles, highlighted  
271 a progressively weaker effect on biofilm with a strength increase of denaturation treatments,  
272 confirming the key role played by the organic cap even in terms of anti-biofilm activity.

273 Although mechanisms through which metal/metalloid nanoparticles exert anti-microbial activity are  
274 not completely understood, a number of authors claim the production of reactive oxygen species  
275 (ROS) as one of the possible modes of action (Manke *et al.*, 2013; Yan *et al.*, 2013). In particular,  
276 anti-microbial effects of different selenium compounds have been attributed to the formation of free

277 radicals (Tran *et al.*, 2009). In this study, exposure of three bacterial strains (namely *P. aeruginosa*  
278 PAO1, *S. aureus* Mu50 and *B. cenocepacia* LMG16656) to untreated SeNPs actually caused an  
279 increase in ROS production compared to the controls. The amount of ROS observed in our  
280 experiments is in the same order of magnitude as those that were induced by some antibiotics (Van  
281 Acker *et al.*, 2016) or by selenite alone (Zonaro *et al.*, 2015).

282 In conclusion, with the present investigation, evidence has been found that biogenic SeNPs,  
283 synthesized by an eco-friendly process can reasonably be considered a reliable anti-microbial and  
284 anti-biofilm agent capable of efficaciously inhibiting fastidious biofilm-producing bacteria of  
285 medical concern. Despite the formation of ROS, which could contribute to the anti-microbial  
286 activity of SeNPs, features of the organic coat surrounding biogenic SeNPs were correlated to a  
287 marked influence on the anti-microbial properties of those nanoparticles. The external coating layer  
288 seems in fact to have a pivotal role in hindering particle aggregation, maintaining nanoparticles in a  
289 functional conformational state, and favouring their interaction with bacterial cells.

290 The information gained so far on biogenic SeNPs opens a realistic perspective for a possible use of  
291 these nanostructured particles as a novel non-antibiotic anti-microbial tool to treat challenging  
292 nosocomial infections, including biofilm-associated syndromes and diseased states caused by  
293 multidrug-resistant bacteria. Further investigations are however required to elucidate in detail the  
294 actual mechanisms of action of these nanoparticles as well to evaluate their whole biological  
295 compatibility with the human body.

296

## 297 **Experimental procedures**

### 298 *Biosynthesis of biogenic SeNPs*

299 Selenium nanoparticles were produced and purified from *Stenotrophomonas maltophilia* SeITE02  
300 culture after 24 h of growth in Nutrient Broth supplied with 0.5 mM Na<sub>2</sub>SeO<sub>3</sub>.

301 The microbial culture was incubated in the dark at 27°C on a rotary shaker at 200 rpm. Bacterial  
302 cells and SeNPs were removed from culture medium after 24 hours by centrifuging at 10,000 x g

303 for 10 min. The pellets were washed twice with 0.9% NaCl solution, re-suspended in Tris/HCl  
304 buffer (pH 8.2) and cells were then disrupted by ultrasonication at 100 W for 5 min. The suspension  
305 was centrifuged at 10,000 x g for 30 min to separate disrupted cells (pellet) from SeNPs  
306 (supernatant). SeNPs were recovered after centrifugation at 40,000 x g for 30 min, washed twice  
307 and re-suspended in deionized water (Zonaro *et al.*, 2015; Cremonini *et al.*, 2016). The SeNPs thus  
308 synthesized were indicated as SeNPs-24 and also as “untreated SeNPs”. The same experimental  
309 protocol of preparation was applied using a microbial culture incubated in the presence of 0.5mM  
310 sodium selenite for 48 hours. The SeNPs obtained were indicated as SeNPs-48.

311

#### 312 *Nanoparticle treatments and quantification of proteins and carbohydrates*

313 Biogenic SeNPs were collected through centrifugation at 16,000 rpm and subsequently exposed to  
314 three different treatments: 10% SDS (treatment 1); 10% SDS and boiling for 10 min (treatment 2);  
315 10% SDS and boiling for 30 min (treatment 3) (Dobias *et al.*, 2011). SeNPs were then centrifuged  
316 at 16,000 rpm and the supernatants were separated to quantify protein and carbohydrate content  
317 obtained after different treatments. The evaluation of proteins and carbohydrates was applied also  
318 on untreated SeNPs and SeNPs-48. Protein concentration was determined following the method of  
319 Lowry *et al.* (1951) using bovine serum albumin (BSA) as standard; carbohydrates were measured  
320 using the anthrone method (Roe, 1955) using glucose as standard. Differences between the protein  
321 and carbohydrate content after treatments were determined using One-Way analysis of variance  
322 (ANOVA) with GraphPad Prism 6.0 (GraphPad Software Inc., La Jolla, CA, USA). The level of  
323 significance was set at  $P < 0.05$ . All tests were carried out in triplicate ( $n = 3$ ) and the results were  
324 averaged.

325 SeNPs-24, SeNPs-48 and SeNPs obtained after different treatments were characterized by means of  
326 Dynamic Light Scattering (DLS) analysis. DLS was carried out using a Zen 3600 Zetasizer Nano  
327 ZS (Malvern Instruments, Malvern, UK) equipped with a 633 nm helium-neon laser light source  
328 (4.0 mW), detecting scattering information at a fixed angle of 173°. SeNP samples (300 µl) were

329 transferred to a quartz cuvette (10 mm path length), and the mean size distribution and zeta  
330 potential were recorded at 25°C using the software provided by Malvern Instruments.

331

#### 332 *Microbial strains and growth conditions*

333 Experiments were conducted with both reference and clinical strains. Specifically, we analysed four  
334 strains of *Pseudomonas aeruginosa*, namely *P. aeruginosa* PAO1 (reference strain), INT (multi-  
335 resistant clinical isolate) and BR1 and BR2 (both isolated from bronchial aspirates), two clinical  
336 strains of *Stenotrophomonas maltophilia* (*S. maltophilia* VR10 and VR20), *Achromobacter*  
337 *xyloxidans* strain C and *Burkholderia cenocepacia* strain LMG 16656. As far as Gram-positive  
338 bacterial strains we included in the study the methicillin-resistant *Staphylococcus aureus* Mu50  
339 strain (reference strain) and a clinical strain isolated from an urine sample (*S. aureus* UR1), as well  
340 as *Staphylococcus epidermidis* ET024, isolated from a biofilm on an endotracheal tube  
341 (Vandecastelaere *et al.*, 2014) and *Staphylococcus haemolyticus* UST1, a clinical isolate from a  
342 burn wound. All bacterial strains were grown in Tryptone Soy Broth (Oxoid, Basingstoke, England)  
343 at 37°C.

344

#### 345 *Determination of the minimum inhibitory concentration (MIC) of biogenic NPs*

346 The susceptibility of each strain to different types of SeNPs was determined in triplicate according  
347 to the National Committee for Clinical and Laboratory Standards (NCCLS) protocol using the broth  
348 microdilution method in flat-bottom 96 well microtiter plates. The microbial inoculum was  
349 standardized to approximately  $10^5$  CFU/ml. Plates were incubated at 37°C for 24 h and the optical  
350 density (O.D.) at 590 nm was determined using a multilabel microtiter plate reader (Envision,  
351 Perkin-Elmer LAS, Waltham, MA, USA). The MIC was recorded as the lowest SeNP concentration  
352 at which no significant O.D. increase was observed.

353

#### 354 *Biofilm formation and treatment*

355 Polystyrene round-bottomed 96-well microtiter plates were inoculated with 100  $\mu$ l of a bacterial  
356 suspension containing approximately  $5 \times 10^7$  CFU/ml and incubated at 37°C for 4 h. The biofilms  
357 formed were rinsed once with 100  $\mu$ l of physiological saline solution (PS) to remove all non-  
358 adherent cells and subsequently treated with 128  $\mu$ g/ml of the four different kinds of SeNPs diluted  
359 in PS. For every strain, untreated biofilms were included as controls. Then, 100  $\mu$ l of fresh medium  
360 was added to each well and the plates were incubated for an additional 20 hours at 37°C (Peeters *et*  
361 *al.*, 2008).

362

#### 363 *Quantification of the biofilm biomass (Crystal Violet (CV) assay)*

364 After 24 h of incubation, biofilms were rinsed with 100  $\mu$ l PS and were fixed by addition of 100  $\mu$ l  
365 99% methanol. After an incubation of 15 min at room temperature, the supernatant was removed  
366 and the plates were air-dried at 37°C. Then, 100  $\mu$ l of a 0.1% CV solution was added to each well  
367 (20 min incubation at room temperature). The dye-stained total biofilm mass included live, dead  
368 cells and extracellular polymeric substances (EPS) grown on the bottom and the walls of microtiter  
369 plate wells. The excess of CV was removed by washing the plate under running tap water. Finally,  
370 150  $\mu$ l of 33% acetic acid were added to resolubilize the stain and the plate was put on a vortex for  
371 at least 20 minutes (800 rpm). The attached bacterial biomass was measured by evaluation of  
372 absorbance at 590 nm (Peeters *et al.*, 2008).

373

#### 374 *Quantification of surviving cells*

375 After 24 h of incubation, cells were collected by two cycles of sonication and vortexing. The cell  
376 pellet obtained after centrifugation (5 min at 13,000 rpm) was suspended in 1 ml of PS and the  
377 number of colony forming units (CFU) was determined by plating on TSA (Tryptone Soy Agar,  
378 Oxoid) (Peeters *et al.*, 2008).

379

#### 380 *Measurement of ROS production*

381 ROS production by bacterial cultures after treatment with biogenic nanoparticles was investigated.  
382 The concentration of SeNPs used corresponded to the MIC for all strains tested.  
383 Overnight cultures of every strain were dispensed in tubes and 2-7-dichlorodihydrofluorescein  
384 diacetate (H<sub>2</sub>DCF-DA, Sigma-Aldrich, Bornem, Belgium) was added at a final concentration of 10  
385  $\mu$ M. All tubes were incubated for 1 hour at 37°C and then centrifuged for 5 min at 13,000 rpm.  
386 Biogenic NPs were added to two aliquots of cells (one with H<sub>2</sub>DCF-DA and one without).  
387 Appropriate controls, to which an equal volume of PS was added instead of NPs, were also  
388 included. All cell suspensions were transferred to a black microtiter plate. Six wells were filled per  
389 condition. The fluorescence ( $\lambda_{ex}$ = 485 nm and  $\lambda_{em}$ =535 nm) was measured every 30 min for  
390 approximately 24 hours with microtiter plate reader (Perkin-Elmer LAS). The net fluorescence  
391 emission by the NPs-treated and untreated cells was calculated and a corresponding graph was  
392 created. The results are only comparable within a plate and not between different plates (Wang and  
393 Joseph, 1999).

394

#### 395 *Statistical analysis*

396 The data are expressed as means plus Standard Error Meaning (SEM). Statistical analyses,  
397 including t-Test and One-Way analysis of variance (ANOVA), were performed using GraphPad  
398 Prism 6.0 (GraphPad Software Inc., La Jolla, CA, USA). All experiments were carried out in  
399 triplicate. The level of significance was set at *P* value < 0.05.

400

#### 401 **Conflict of interest statement**

402 The authors have no conflict of interest to declare.

403

404

405



406 **References**

- 407 Beyth, N., Hourri-Haddad, Y., Domb A., Khan, W., and Hazan, R. (2015) Alternative antimicrobial  
408 approach: nano-antimicrobial materials. *Evid Based Complement Alternat Med*  
409 doi:10.1155/2015/246012.
- 410 Bjarnsholt T. (2013) The role of bacterial biofilm in chronic infections. *APMIS* 136: 1-51.
- 411 Chudobova, D., Cihalova, K., Dostalova, S., Ruttkay-Nedecky, B., Rodrigo, M.A., Tmejova, F., *et*  
412 *al.* (2014) Comparison of the effects of silver phosphate and selenium nanoparticles on  
413 *Staphylococcus aureus* growth reveals potential for selenium particles to prevent infection. *FEMS*  
414 *Microbiol Lett* 351: 195-201.
- 415 Cihalova, K., Chudobova, D., Michalek, P., Moulick, A., Guran, R., Kopel, P., Adam, V., and  
416 Kizek, R. (2015) *Staphylococcus aureus* and MRSA growth and biofilm formation after treatment  
417 with antibiotics and SeNPs. *Int. J Mol Sci* 16: 24656-24672.
- 418 Cremonini, E., Zonaro, E., Donini, M., Lampis, S., Boaretti, M., Dusi, S., Melotti, P., Lleo, M.M.,  
419 and Vallini, G. (2016) Biogenic selenium nanoparticles: characterization, antimicrobial activity and  
420 effect on human dendritic cells and fibroblasts. *Microb Biotechnol* 9(6): 758-771.
- 421 Dobias, J., Suvurova, E.I., and Bernier-Latmani, R. (2011) Role of proteins in controlling selenium  
422 nanoparticle size. *Nanotechnology* 22: 195605.
- 423 Ferri, M., Ranucci, E., Romagnoli, P., and Giaccone, V. (2015) Antimicrobial resistance: a global  
424 emerging threat to public health systems. *Crit Rev Food Sci Nutr*  
425 doi:10.1080/10408398.2015.1077192.
- 426 Huang, X., Chen, X., Chen, Q., Yu, Q., Sun, D., and Liu, J. (2016) Investigation of functional  
427 selenium nanoparticles as potent antimicrobial agents against superbugs. *Acta Biomaterialia* 30:  
428 397-407.
- 429 Hunter, R.J. (1981) *Z Potential in Colloid Science: Principles and Applications*, Academic Press,  
430 Oxford.

431 Jain, R., Jordan, N., Weiss, S., Foerstendorf, H., Heim, K., Kacker, R., *et al.* (2015) Extracellular  
432 polymeric substances govern the surface charge of biogenic elemental selenium nanoparticles.  
433 *Environ Sci Technol* **49**: 1713-1720.

434 Lampis, S., Zonaro, E., Bertolini, C., Cecconi, D., Monti, F., Micaroni, M., *et al.* (2017) Selenite  
435 biotransformation and detoxification by *Stenotrophomonas maltophilia* SeITE02: novel clues on the  
436 route to bacterial biogenesis of selenium nanoparticles. *J Hazard Mater*  
437 doi:10.1016/j.jhazmat.2016.02.035.

438 Lowry O., Rosebrough N.J., Farr, A.L., and Randall, R.J. (1951) Protein measurement with the  
439 folin phenol reagent. *J Biol Chem* 265-75.

440 Lu, Z., Rong, K.L.J., Yang, H., and Chen, R. (2013) Size-dependent antibacterial activities of silver  
441 nanoparticles against oral anaerobic pathogenic bacteria. *J Mater Sci Mater Med* **24**: 1465-1471.

442 Manke, A., Wang, L., Rojanasakul, Y. (2013) Mechanisms of nanoparticle-induced oxidative stress  
443 and toxicity. *Biomed Res Int* 2013:942916.

444 Natan, M., and Banin, E. (2017) From Nano to Micro: using nanotechnology to combat  
445 microorganisms and their multidrug resistance. *FEMS Microbiol Rev* **41**(3): 302-322. doi:  
446 10.1093/femsre/fox003.

447 Paharik, A.E., and Horswill, A.R. (2016) The staphylococcal biofilm: adhesins, regulation, and host  
448 response. *Microbiol Spectr* doi:10.1128/microbiolspec.VMBF-0022-201.

449 Peeters, E., Hans, J., Nelis, H.J., and Coenye, T. (2008) Comparison of multiple methods for  
450 quantification of microbial biofilms grown in microtiter plates. *J Microbiol Methods* **72**(2): 157-65.

451 Penesyan, A., Gillings, M., and Paulsen, T.T. (2015) Antibiotic discovery: combating bacterial  
452 resistance in cells and in biofilm communities. *Molecules* **20**: 5286-5298.

453 Rizzello, L., and Pompa, P.P. (2014) Nanosilver-based antibacterial drugs and devices:  
454 mechanisms, methodological drawbacks, and guidelines. *Chem Soc Rev* **43**(5): 1501-1518.

455 Roe, J.H. (1955) The determination of sugar in blood and spinal fluid with anthrone reagent. *J Biol*  
456 *Chem* **212**: 335-343.



457 Shakibaie, M., Forootanfar, H., Golkari, Y., Mohammadi-Khorsand, T., and Shakibaie, M.R. (2015)  
458 Anti-biofilm activity of biogenic selenium nanoparticles and seleniumdioxide against clinical  
459 isolates of *Staphylococcus aureus*, *Pseudomonas aeruginosa*, and *Proteus mirabilis*. *J Trace Elem*  
460 *Med Biol* **29**: 235–241.

461 Tran, P.L., Hammond, A.A., Mosley, T., Cortez, J., Gray, T., Colmer-Hamood, J.A. *et al.* (2009)  
462 Organo selenium coating on cellulose inhibits the formation of biofilms by *Pseudomonas*  
463 *aeruginosa* and *Staphylococcus aureus*. *Appl Environ Microbiol* **75**: 3586–3592.

464 Van Acker, H., and Coenye, T. (2017) The role of reactive oxygen species in antibiotic-mediated  
465 killing of bacteria. *Trends Microbiol* doi: 10.1016/j.tim.2016.12.008

466 Van Acker, H., Gielis, J., Acke, M., Cools, F., Cos, P., and Coenye, T. (2016) The role of reactive  
467 oxygen species in antibiotic-induced cell death in Burkholderia cepacia Complex Bacteria. *PLoS*  
468 *One* **11**(7):e0159837. doi:10.1371/journal.pone.0159837.

469 Vandecandelaere, I., Van Nieuwerburgh, F., Deforce, D., Nelis, H.J., and Coenye, T. (2014) Draft  
470 genome sequence of methicillin-resistant *Staphylococcus epidermidis* strain et-024, isolated from an  
471 endotracheal tube biofilm of a mechanically ventilated patient. *Genome Announc* **2**(3). pii: e00527-  
472 14. doi:10.1128/genomeA.00527-14.

473 Verma, A., and Stellacci, F. (2010) Effect of surface properties on nanoparticle-cell  
474 interactions. **6**(1):12-21. doi: 10.1002/sml.200901158.

475 Wang, H., and Joseph, J.A. (1999) Quantifying cellular oxidative stress by dichloro fluorescein  
476 assay using microplate reader. *FreeRad Bio Med* **27**: 612–616.

477 Wang, L., Hu, C., and Shao, L. (2017) The antimicrobial activity of nanoparticles: present situation  
478 and prospects for the future. *Int J Nanomedicine*. **12**: 1227-1249.

479 Yan, L., Gu, Z., and Zhao, Y. (2013) Chemical mechanisms of the toxicological properties of  
480 nanomaterials: generation of intracellular reactive oxygen species. *Chem Asian J* **8**(10): 2342-53.

481 Yuan, Y.G., Peng, Q.L., and Gurunathan, S. (2017) Effects of Silver Nanoparticles on Multiple  
482 Drug-Resistant Strains of *Staphylococcus aureus* and *Pseudomonas aeruginosa* from Mastitis-  
483 Infected Goats: An Alternative Approach for Antimicrobial Therapy. *Int J Mol Sci*. **6**: 18.  
484 Zonaro, E., Lampis, S., Turner, R.J., Qazi, S.J. and Vallini, G. (2015) Biogenic selenium and  
485 tellurium nanoparticles synthesized by environmental microbial isolates efficaciously inhibit  
486 bacterial planktonic cultures and biofilm, *Front Microbiol* **6**: 584.

487  
488  
489  
490  
491  
492  
493  
494  
495  
496  
497  
498  
499  
500  
501  
502  
503  
504  
505  
506  
507

For Review Only

508 **Table and Figure legends**

509

510 **Table 1:** Dynamic light scattering analysis and zeta potential of SeNPs as biogenic product and  
511 after different treatments (n=3; average±SD). Untreated: biogenic SeNPs; Treatment 1: 10% SDS;  
512 Treatment 2: 10% SDS+10 min boiling; Treatment 3: 10% SDS+30 min boiling.

513

514 **Table 2.** MIC (Minimum Inhibitory Concentration) of different types of SeNPs against various  
515 bacterial strains. Untreated: biogenic SeNPs; Treatment 1: 10% SDS; Treatment 2: 10% SDS+10  
516 min boiling; Treatment 3: 10% SDS+30 min boiling. Data are expressed as the average of 3  
517 biological replicates.

518

519 **Figure 1:** Protein (A) and carbohydrate (B) content of SeNPs as biogenic product and after  
520 different treatments (n=3; p<0.05). Untreated: biogenic SeNPs; Treatment 1: 10% SDS; Treatment  
521 2: 10% SDS+10 min boiling; Treatment 3: 10% SDS+30 min boiling.

522

523

524 **Figure 2.** Anti-biofilm activity of different types of SeNPs measured by CV staining (effect on  
525 biofilm biomass) (A) and colony counting (effect on cell viability) (B), as regards *P.aeruginosa*  
526 strains PAO1, BR1 and BR2 (n=3, Average ±SEM). # p<0.05 compared to a biofilm grown in the  
527 absence of SeNPs (Control); \* p<0.05 compared to a biofilm treated with "Untreated SeNPs".  
528 Untreated: biogenic SeNPs, Treatment 1: 10% SDS, Treatment 2: 10% SDS+ 10 min boiling,  
529 Treatment 3: 10% SDS+30 min boiling.

530

531 **Figure 3.** Anti-biofilm activity of different types of SeNPs measured by CV staining (effect on  
532 biofilm biomass) (A) and colony counting (effect on cell viability) (B), as regards *B. cenocepacia*  
533 LMG 16656, *S.aureus* Mu50 and *S.haemoliticus* UST1 (n=3, Average ±SEM). # p<0.05 compared

534 to a biofilm grown in the absence of SeNPs (Control); \*  $p < 0.05$  compared to a biofilm treated with  
535 "Untreated SeNPs". Untreated: biogenic SeNPs, Treatment 1: 10% SDS, Treatment 2: 10% SDS+  
536 10 min boiling, Treatment 3: 10% SDS+30 min boiling.

537

538 **Figure 4.** Formation of ROS in *P. aeruginosa*, *B. cenocepacia*, *S. aureus* cells exposed to SeNPs  
539 for 24 hours (SeNPs) normalized to cells not exposed to NPs (Control) ( $n=3$ ; Average $\pm$ SEM;  
540  $p < 0.05$ ).

541

For Review Only

	Diameter (nm)	Z-potential (mV)
Untreated SeNPs	181±20	-32.01±2.67
Treatment 1	209±25	-17.40±3.45
Treatment 2	233±19	-8.11±2.36
Treatment 3	270±24	-3.97±1.34

Table 1

For Review Only

Bacterial species	Strain Name	MIC $\mu\text{g/ml}$			
		Untreated SeNPs	Treatment 1	Treatment 2	Treatment 3
<i>P. aeruginosa</i>	PAO1	8	16	128	64
<i>P. aeruginosa</i>	INT	64	512	>512	>512
<i>P. aeruginosa</i>	BR1	32	64	32	64
<i>P. aeruginosa</i>	BR2	8	16	32	128
<i>S. maltophilia</i>	VR10	32	16	32	64
<i>S. maltophilia</i>	VR20	64	256	512	>512
<i>A. xylooxidans</i>	C	64	>512	>512	>512
<i>B. cenocepacia</i>	LMG16656	16	16	32	32
<i>S. aureus</i>	Mu50	128	128	256	512
<i>S. aureus</i>	UR1	4	16	32	64
<i>S. haemolyticus</i>	UST1	16	8	32	64
<i>S. epidermidis</i>	ET024	4	8	16	64

**Table 2**

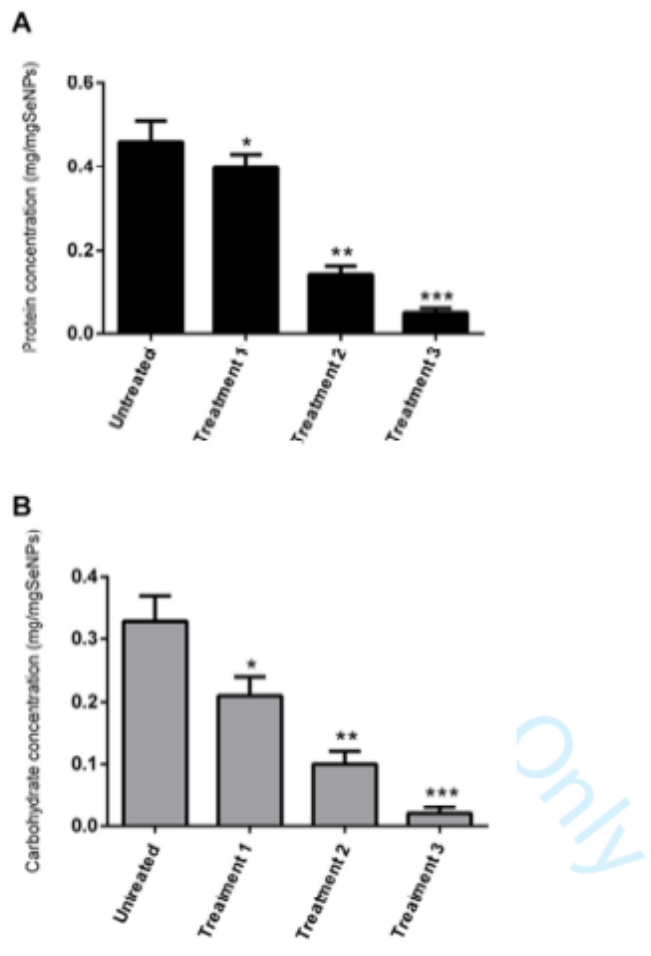
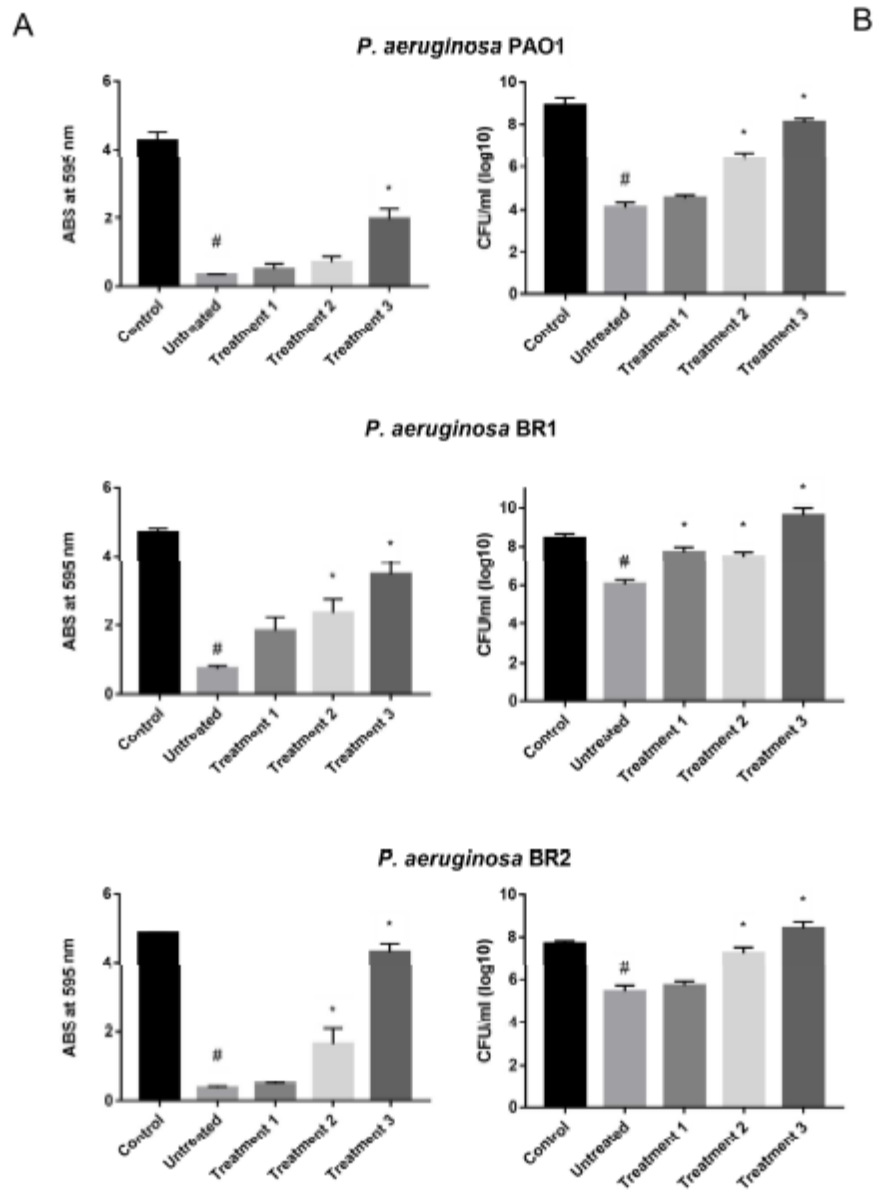
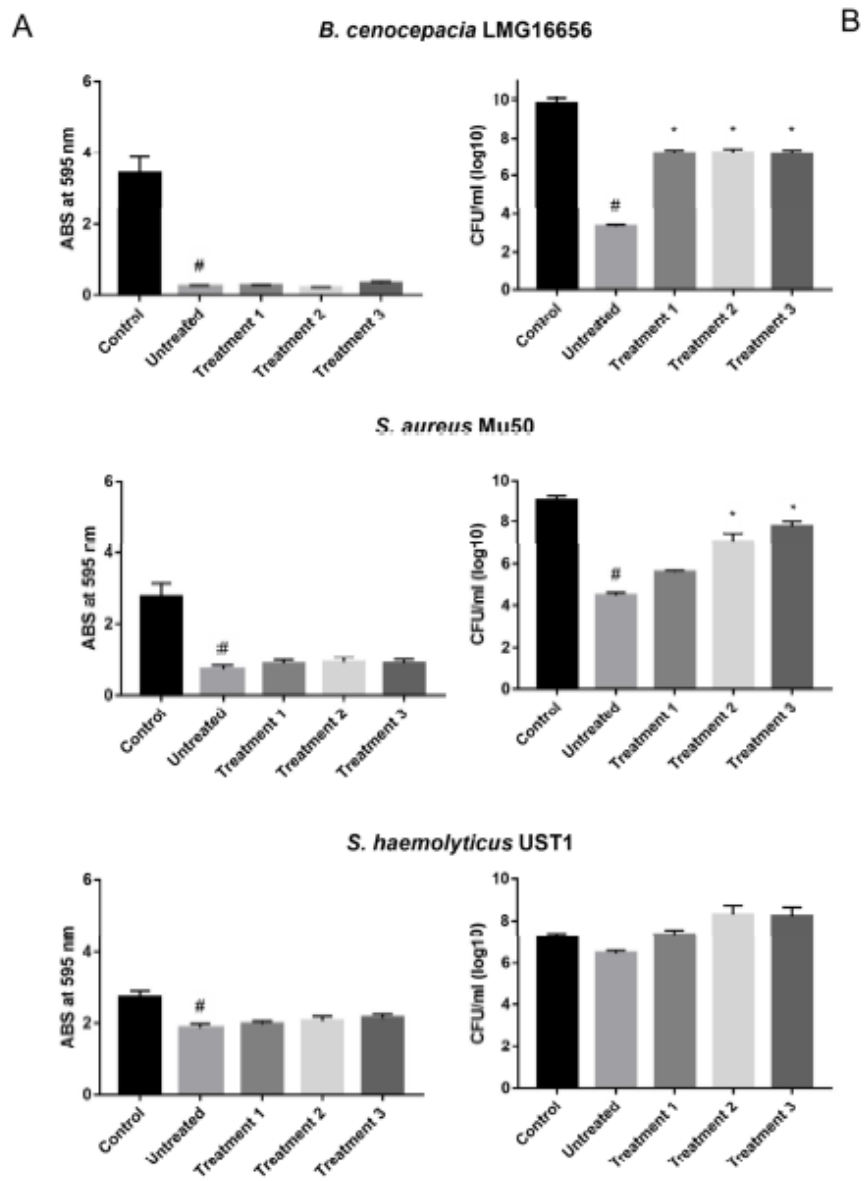


Figure 1



**Figure 2**





**Figure 3**

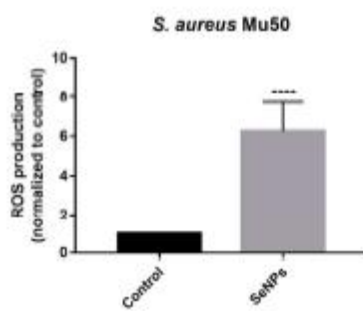
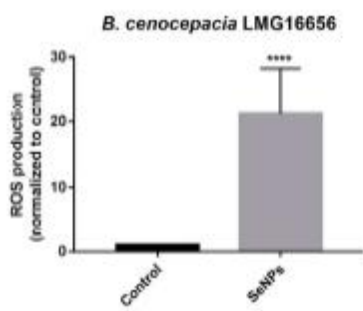
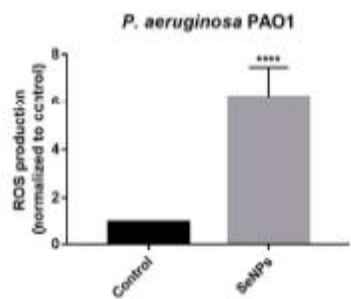


Figure 4